Canonical Wnt signaling activation enhances cardiac tissue repair by arteriole formation and attenuation of fibrosis

By

David Tohyun Paik

Dissertation

Submitted to the Faculty of the

Graduate School of Vanderbilt University

in partial fulfillment of the requirements

for the degree of

DOCTOR OF PHILOSOPHY

in

Cell and Developmental Biology

December, 2015

Nashville, Tennessee

Approved:

Antonis K. Hatzopoulos, Ph.D.

H. Scott Baldwin, M.D.

Mark P. deCaestecker, M.B., B.S., Ph.D.

Stephen R. Hann, Ph.D.

David M. Miller, III, Ph.D.

To my parents, Joonki and Sunjoo

and

To all of my teachers and mentors who believed in me and supported me

You made this work possible.

ACKNOWLEDGEMENTS

My graduate training at Vanderbilt University has been supported by the Vanderbilt University Interdisciplinary Graduate Program (IGP), T32 Training Grant in Cardiovascular Research (NIH NHLBI T32HL007411), HHMI/VUMC Certificate Program in Molecular Medicine (CPMM), and NIH grants to Antonis K. Hatzopoulos (U01HL100398 and R01HL083958).

Dr. Antonis Hatzopoulos has been the best mentor I could ask for. He has been tremendously supportive, fair, and fun to work with. He has been patient and understanding with me, even in my low moments. Most importantly, he taught me how to think and work as a scientist. Dr. Hatzopoulos provided all of the necessary tools and resources to develop and train me as a young scientist and to allow me to expand on my career goals and dreams. I am truly grateful for his support, mentorship, and friendship.

I am grateful to Dr. Douglas Sawyer for being my clinical mentor, as part of my HHMI/VUMC CPMM training. Dr. Sawyer allowed me to shadow him during his clinical duties at Vanderbilt Heart and Vascular Institute for many days and hours. During the shadowing, I was able to build relationships with the patients and to engage hands-on in diagnosing and evaluating the patients. He was willing to spend his valuable time and effort to teach me and answer my questions. Most importantly, shadowing Dr. Sawyer allowed me to recognize the assets that make a successful physician-scientist.

I thank all of my committee members for their role in my Ph. D. training. Dr. H. Scott Baldwin’s advice and support have been invaluable in developing this project from the start to finish. Dr. Mark deCaestecker supported my participation in the CPMM, one

of the most important parts of my training at Vanderbilt. Dr. Stephen Hann and Dr. David Miller maintained my perspective on the importance of basic science research. All members of the committee have been greatly supportive in all phases of my Ph.D. training as well as with my career development.

I cannot thank Dr. Sergey Ryzhov enough for not only making significant contributions to this work, but also for spending his valuable time and effort in teaching me the extensive details of performing *in vitro* cell culture experiments.

The Hatzopoulos laboratory has been a great place to work in. I cannot recall a single moment during my four years in the lab, where any sort of conflict among the members had surfaced, something that cannot be said for most work environments. It is a tribute to the unselfish and collaborative efforts of all members of the lab and also to the leadership of Dr. Hatzopoulos. I thank Dr. Meena Rai for her contributions to this work and her mentorship. I thank Bryan Fioret for being the best lab-mate and a wonderful friend, and for having me as part of his fabulous project. I appreciate Mitchell Funke for his contributions to this work, his friendship, and the times we spent together outside the lab. I especially thank Jeff Bylund for being a wonderful colleague who was always willing to engage in discussions of any topic and to help me with my concerns and issues to his fullest ability. Lastly I want to acknowledge Amy Zhu and Matthew Park for being superb mentees.

My life in Nashville has been an unforgettable one, thanks to many friends and families I had the opportunity to build relationships with. I will never forget the times I spent with friends from Nashville Korean United Methodist Church, with friends I met through the Korean Students and Scholars Association, and with numerous colleagues

and friends at Vanderbilt University.

I am grateful to Dr. Edward Loechler, Dr. Kwang Young Seo, and Dr. Sushil Chandani at Boston University for giving me an opportunity to engage in biomedical research as an undergraduate student and to recognize the importance of basic science research in advancing the field of medicine. The experience I was able to gain at the Loechler laboratory has been invaluable in my development as a young scientist.

I want to acknowledge my best friends, from Seoul, Boston, and Nashville, from past and present, for being there for me and for your love and support. I am who I am now because of you. Thank you.

I am most indebted to my loving family. To my dear parents, Joonki and Sunjoo, my sister, Sejin, and my grandparents, I dedicate this work to you.

TABLE OF CONTENTS

LIST OF FIGURES

Figure **Page**

Chapter I

Chapter II

Chapter III

Chapter IV

Chapter V

LIST OF TABLES

Table **Page**

LIST OF ABBREVIATIONS

Ang-1	Angiopoietin-1
BMP	Bone Morphogenetic Protein
JNK	c-Jun N-terminal Kinase
DAPI	4’,6-diamidino-2-phenylindole
Dsh	Dishevelled
ECG	Electrocardiogram
ESC	Embryonic stem cell
EMT	Epithelial to mesenchymal transition
EndMT	Endothelial to mesenchymal transition
ERG	ETS Related Gene
Fzd	Frizzled
Gapdh	Glyceraldehyde-3-phosphate dehydrogenase
GFR	Growth factor reduced
GSK-3β	Glycogen Synthase Kinase-3 beta
H&E	Hematoxylin and eosin
IL	Interleukin
I/R	Ischemia/reperfusion
ICM	Ischemic cardiomyopathy
LCA	Left coronary artery
LRP	Low-density lipoprotein receptor-related protein
LV	Left ventricle
LVIDd	Left ventricular internal dimension, dystolic
LVIDs	Left ventricular internal dimension, systolic
MCEC	Murine cardiac microvascular endothelial cell
mg	Milligram
mL	Milliliter
mM	Millimolar
µg	Microgram

µl	Microliter
µM	Micromolar
Mo-MLV	Moloney-Murine Leukemia Virus
MSC	Mesenchymal stem cell
MI	Myocardial infarction
αMHC	Alpha-Myosin Heavy Chain (Myh6)
NF-κB	Nuclear Factor-κB
OCT	Optimal cutting temperature
PBS	Phosphate buffered saline
PCR	Polymerase chain reaction
Pdgf-b	Platelet-derived growth factor subunit B
Pdgfr-β	Platelet-derived growth factor receptor, β polypeptide
SDS-PAGE	Sodium dodecyl sulfate-polacrylamide
SHF	Secondary heart field
αSMA	Alpha Smooth Muscle Actin
TCF/LEF	T-cell factor/lymphoid enhancer factor
Tie2	Tyrosine kinase with immunoglobulin-like and EGF-like domains 2
TNF-α	Tumor Necrotic Factor-alpha
TG	Transgenic (αMHC-Wnt10b)
Vegfr-2	Vascular endothelial growth factor receptor 2 (Flk-1)
vSMC	Vascular smooth muscle cell
WT	Wild-type

CHAPTER I

INTRODUCTION

Wnt signaling in stem cells and disease

Wnt signaling is a developmental pathway that regulates differentiation and fate decision of stem cells (Clevers and Nusse, 2012). During development, Wnt signaling has important functions in proliferation and pluripotency of embryonic stem cells (ESCs), as well as in specification and differentiation of mesoderm into muscle cells, endothelial cells, and blood cells. It also plays a role in differentiation of mesenchymal stem cells (MSCs). In addition, Wnt signaling has been found to regulate adult stem and progenitor cell niches in various mammalian tissue types (Paik and Hatzopoulos, 2014).

Wnt signaling pathway is classically divided in so-called canonical and non-canonical branches based on activation of specific intracellular components (Gessert and Kühl, 2010) (**Figure 1**). Canonical Wnt signaling is activated when Wnt ligands bind to Frizzled (Fzd) family of 7-transmembrane domain receptors and co-receptors such as low-density lipoprotein receptor-related protein (LRP) 5/6, Ryk, or Ror2 (Nusse, 2008; MacDonald *et al.,* 2009; van Amerongen and Nusse, 2009; Rao and Kühl, 2010). This disrupts the formation of the β-catenin destruction complex, consisting of scaffolding protein Axin, Adenomatous polyposis coli protein, Dishevelled (Dsh), Casein Kinase-Iα and Glycogen Synthase Kinase-3β (GSK-3β). The destruction complex dissociation leads to stabilization of cytoplasmic β-catenin that trans-locates to the nucleus to interact with T-cell factor/lymphoid enhancer factor (TCF/LEF) transcription factors and initiate

transcription of canonical Wnt signaling target genes, such as *c-Myc, Axin2* and *Snail* (He *et al.,* 1998; Jho *et al.,* 2002; ten Berge *et al.,* 2011). When canonical Wnt signaling is turned off, the destruction complex phosphorylates β-catenin for ubiquitin-mediated proteosomal degradation (Liu *et al.,* 2002).

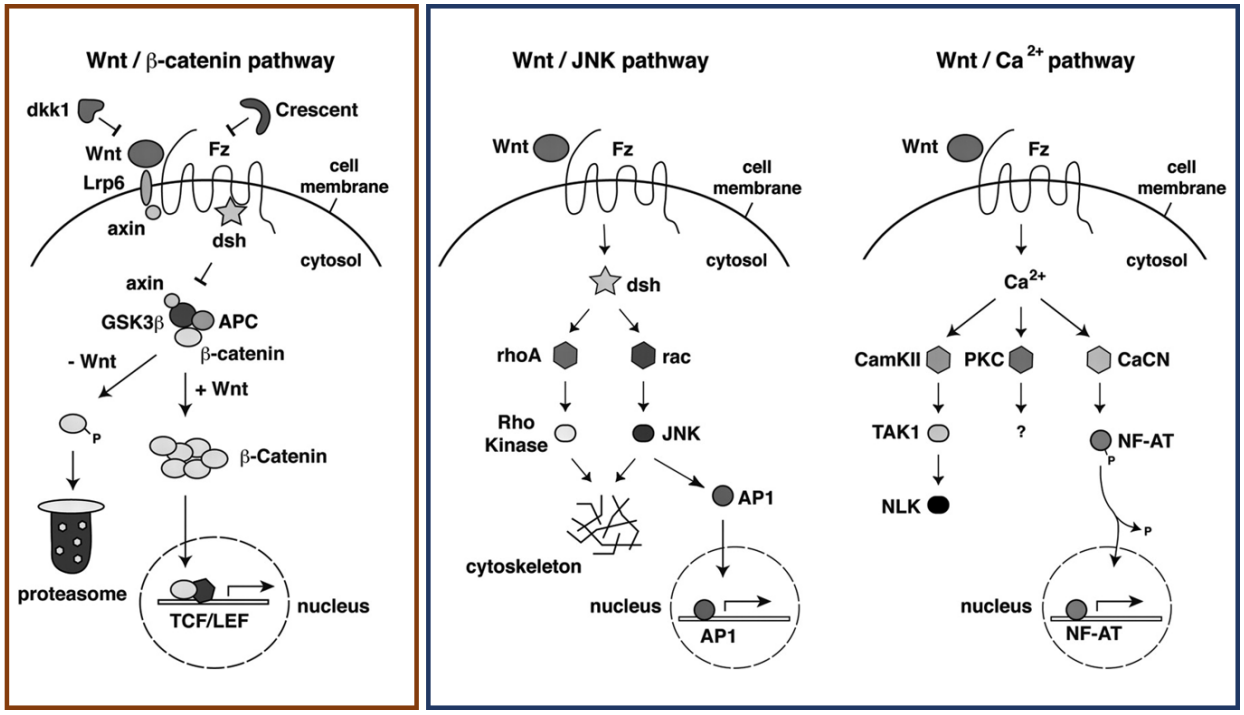

Figure 1. The Wnt signaling pathway. The Wnt pathway is divided into two branches of signaling. The canonical Wnt pathway is mediated by stabilization of β-catenin, which translocates into nucleus to activate transcription of canonical Wnt-responsive genes. In the absence of Wnt ligands, however, the destruction complex will target β-catenin for ubiquitin-proteosomal degradation. The non-canonical Wnt pathways, such as the planar cell polarity pathway, AP1/JNK pathway, and calcineurin/NFAT pathway, are mediated in β-catenin-independent manner. Adapted from Gessert and Kühl, 2010.

Non-canonical Wnt signaling pathways are β-catenin-independent and are mediated through other intracellular proteins (Veeman *et al.,* 2003). In the Wnt/JNK pathway, binding of Wnt to Fzd receptors activates small-GTPases, RhoA and Rac through recruitment of Dsh, which thereby activate Rho kinase and c-Jun N-terminal

kinases (JNK). In the Wnt/Ca^{+2} pathway, binding of Wnt to Fzd receptors increases intracellular Ca^{2+} levels, activating calcium/calmodulin-dependent kinase (CaMK) II, protein kinase C, and the protein phosphatase Calcineurin to trigger de-phosphorylation of NF-AT transcription factors. Thus activated NF-AT transcription factors translocate to the nucleus to stimulate transcription of their target genes, such as IL-2, IL-8, TNF-α, and Cox2 (Macián *et al.,* 2001; Gessert and Kühl, 2010). Intriguingly, non-canonical Wnt signaling has been shown to inhibit canonical Wnt signaling by varying mechanisms (Pandur *et al.,* 2002; Maye *et al.,* 2004; Cohen *et al.,* 2008).

To date, 19 Wnt ligands and 10 Fzd receptors have been identified. The 19 Wnt genes fall into 12 conserved Wnt subfamilies, which exist in most mammalian genomes including the human genome (Kusserow *et al.,* 2005). Different combinations of individual Wnt ligands, receptors, and co-receptors allow differential activation of β-catenin-dependent/canonical Wnt, non-canonical Wnt, or both in a cellular context-dependent manner.

Myocardial infarction and cellular events of cardiac tissue repair

Coronary heart disease leading to myocardial infarction (MI) is the major cause of death in the United States. Each year approximately 735,000 people in the U.S. have an MI and tissue damage that lead to ventricular remodeling, hypertrophy, dilatation, and heart failure (HF) (Mozaffarian *et al.,* 2015; Braunwald, 2015). HF is a progressive and lethal disease with few therapeutic options. It has annual costs close to $40 billion and has not decreased in incidence in two decades (Mozaffarian *et al.,* 2015). Few new pharmacological agents or devices have emerged in the last decade to improve outcomes

(McAlister *et al.,* 2007; Hunt *et al.,* 2009; Merlo *et al.,* 2011) and stem-cell based approaches have not yet matched the promise of pre-clinical and early clinical studies (Smith *et al.,* 2007; Rota *et al.,* 2008; Ellison *et al.,* 2013). Thus, there is an urgent and unmet need for new therapeutic directions to treat HF.

The cellular events that occur after an MI in adult murine heart are well understood (Boudoulas and Hatzopoulos, 2009) (**Figure 2**). During MI, a large number of cardiomyocytes in the ischemic zone die by both apoptosis and necrosis over the first 6 to 24 hours (Konstantinidis *et al.,* 2012). Toxic products and alarm signals released from dying cells induce cell adhesion proteins, cytokines, and chemokines to recruit inflammatory cells, which remove cellular debris and degrade extracellular matrix (Timmers *et al.,* 2012; Boudoulas and Hatzopoulos, 2009; Frangiogiannis, 2014). After debris is cleared, the gap is filled with granulation tissue composed of proliferating myofibroblasts that secrete extracellular matrix (ECM) proteins and endothelial cells that form new capillaries, but without regenerating functional cardiomyocytes (Boudoulas and Hatzopoulos 2009; Frangogiannis, 2014). Instead, two to three weeks after MI, ECM deposits from myofibroblasts begin to mature into a dense scar, leading to disruption in electro-mechanical coupling of surviving myocytes and to HF (Virag and Murry, 2003). As such, the ischemic heart suffers from excessive fibrotic scar formation while lacking sufficient cardiac and vascular regeneration.

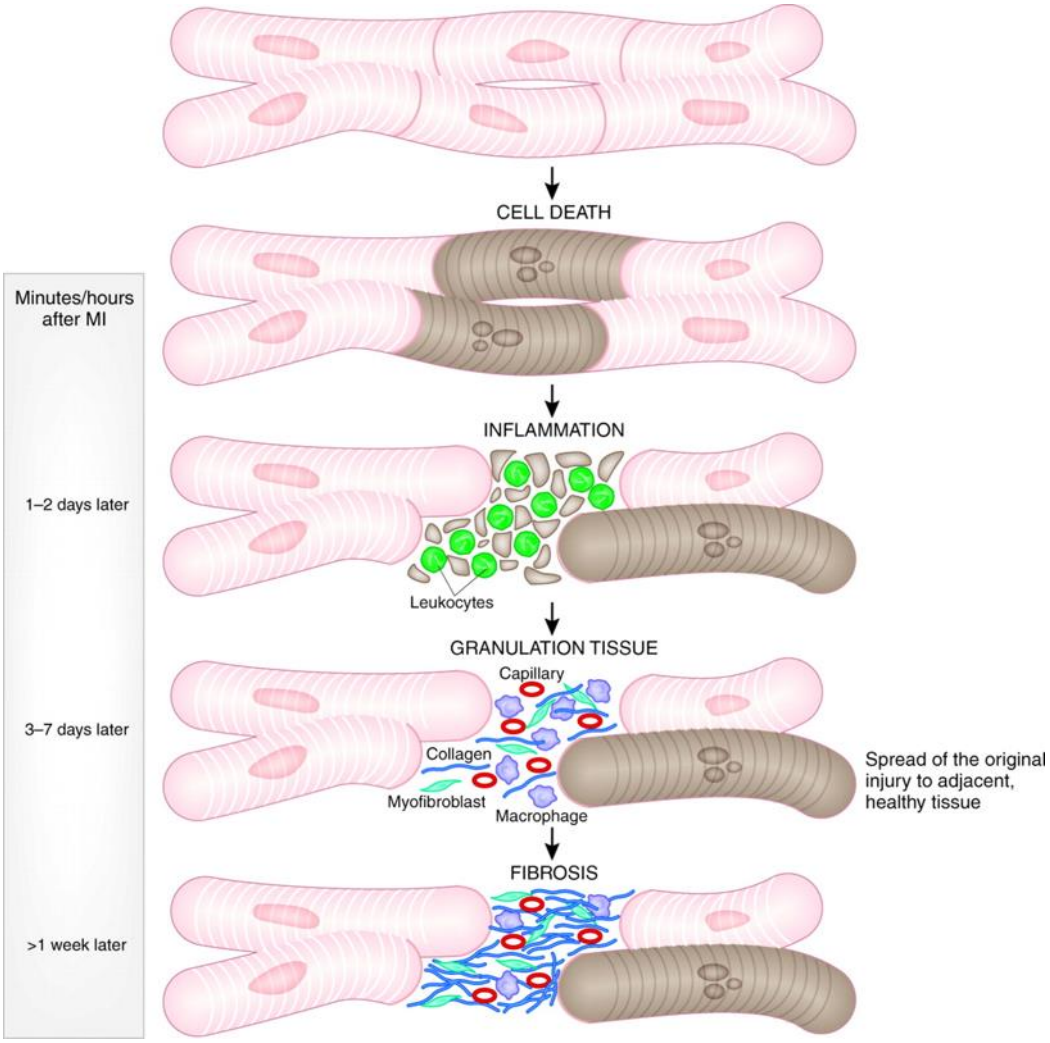

Figure 2. Cellular events of cardiac tissue repair. Following permanent occlusion of left coronary artery in a mouse heart, massive cell death occurs within minutes. The necrotic debris released from the rupture of the cardiac cells induces an inflammatory phase, where neutrophils, monocytes, and macrophages begin to populate the injured tissue. Inflammatory phase is followed by a proliferative phase consisting of neovascularization and fibrotic scar formation, which occurs most intensely from 3 to 7 days after injury. Afterwards, the heart will enter a remodeling phase, where maturing scar tissue will lead the heart to undergo adverse remodeling. Adapted from Boudoulas and Hatzopoulos, 2009.

Understanding the molecular mechanisms that govern these cellular events of cardiac tissue repair may lead to new approaches to induce regeneration of functional cell types and to moderate scar tissue formation.

Wnt signaling in cardiac development

Understanding cardiac development is necessary in optimizing the cellular and molecular mechanisms of adult cardiac repair. Damaged adult heart lacks the ability to regenerate the lost cardiomyocytes and vascular cells, whereas during development, the functional cell types and the structures of the heart are formed efficiently and in a well-organized manner. It is therefore important to identify the signaling pathways that govern these processes, to effectively translate the mechanisms of development to adult tissue repair.

Wnt signaling is a major cardiac developmental signaling pathway, playing multiple roles in cardiac differentiation and development (Brade *et al.,* 2006; Cohen *et al.,* 2008; van Amerongen and Nusse, 2009; Gessert and Kühl, 2010). Canonical Wnt signaling is required for formation of mesodermal germ layer during early development, which gives rise to cardiac progenitor cells. Genetic inactivation of β-catenin by homologous recombination failed to generate mesoderm and loss of Wnt3a function led to absence of mesoderm-specific genes (Liu *et al.,* 1999; Huelskin *et al.,* 2000). Moreover, canonical Wnt signaling is necessary for T-box transcription factor Brachyury, a pan-mesodermal marker gene (Yamaguchi *et al.,* 1999; Vonica *et al.,* 2002), which carries a binding site for TCF in its gene promoter (Gessert and Kühl, 2010).

Canonical Wnt signaling however plays an inhibitory role in cardiac specification of mesoderm to cardiac progenitor cells. Notch mediated suppression of inhibition of canonical Wnt signaling promotes cardiac differentiation (Chen *et al.,* 2008; Kwon *et al.,* 2009) and β-catenin, a key canonical Wnt molecule, has been shown to negatively regulate expression of GATA6, a major early cardiac transcription factor (Afouda *et al.,*

2008). In accordance with these findings, the canonical Wnt inhibitor Dkk1 has been shown to promote Mesp1-induced cardiomyogenesis (Lindsley *et al.,* 2008; David *et al.,* 2008). Mesp1 is the earliest marker gene for cardiovascular lineage (Saga *et al.,* 1999; Saga *et al.,* 2000). Dkk1 not only suppresses canonical Wnt signaling, but also activates non-canonical Wnt pathways such as the JNK signaling (Pandur *et al.,* 2002; Caneparo *et al.,* 2007).

Non-canonical Wnt pathways in fact are shown to promote cardiac specification of mesoderm. Wnt11, classically categorized as a non-canonical Wnt ligand, is expressed in the presumptive dorsal mesoderm and in the dorsal marginal zone during gastrulation in *Xenopus.* Loss-of-function of Wnt11 studies demonstrated Wnt11 is required for heart development and cardiac marker gene expression, while Wnt11 overexpression in *Xenopus* explants is sufficient to induce contractile tissue formation (Pandur *et al.,* 2002). Canonical Wnt signaling, on the other hand, plays a specific role in the secondary heart field (SHF) lineage and SHF-derived structures. Loss-of-function in β-catenin resulted in loss of SHF-derived outflow tract (OFT) and right ventricle (Ai *et al.,* 2007; Klaus *et al.,* 2007; Cohen *et al.,* 2007; Kwon *et al.,* 2007; Lin *et al.,* 2007) and β-catenin overexpression led to expansion of SHF-derived structures in the mature heart (Ai *et al.,* 2007; Kwon *et al.,* 2007).

Interestingly, canonical and non-canonical Wnt pathways appear to recapitulate their roles again during terminal differentiation of cardiomyocytes. Late addition of canonical Wnt ligand Wnt3a during mouse embryoid body differentiation resulted in a reduced number of cardiomyocytes (Nakamura *et al.,* 2003; Ueno *et al.,* 2007), as Wnt3a appear to inhibit differentiation of $Isl1^{+}$ cardiac progenitor cells (Qyang *et al.,* 2007). Non-

canonical Wnt signaling however promotes terminal differentiation of cardiomyocytes, shown in mouse ES cells and in *Xenopus* by the stimulatory role of Wnt11 on the process (Ueno *et al.,* 2007; Garriock *et al.,* 2005; Gessert *et al.,* 2008).

Taken together, Wnt signaling is described to be involved in four phases of cardiac specification and differentiation (Gessert and Kuhl, 2010). Canonical Wnt signaling is required for mesoderm formation, but needs to be suppressed for specification and generation of multipotent cardiac progenitor cells, accompanied by activation of non-canonical signaling. Canonical Wnt signaling is then required for proliferation and expansion of specified cardiac progenitor cells for formation of SHF-derived structures. For terminal differentiation, suppression of the canonical and activation of the non-canonical Wnt pathway is necessary.

In addition, Wnt signaling plays an important role in valve formation. Activation of canonical Wnt signaling by loss of APC resulted in excessive endocardial cushion formation from increased proliferation and epithelial-to-mesenchymal transition (EMT) of endocardial cells (Gitler *et al.,* 2003), while overexpression of APC or Dkk1 inhibited cardiac cushion formation in zebrafish (Hurlstone *et al.,* 2003; Liebner *et al.,* 2004). Cardiac cushions give rise to the cardiac valves, the tricuspid valve, and the mitral valve. Similarly in chicken, Wnt9a was found to promote proliferation of endocardial cells by canonical Wnt activation (Person *et al.,* 2005).

As such, both the canonical and the non-canonical branches of Wnt signaling play a dynamic role in heart development and formation. This presents an opportunity for us to translate the role of Wnt signaling in cardiac development to the mechanisms of adult tissue repair.

Activation of Wnt signaling during cardiac repair

Using the canonical Wnt reporter TOPGAL transgenic mice, our laboratory has previously shown that canonical Wnt signaling activity is present primarily in the media and intima layers of the aorta and pulmonary vessels as well in coronary vessels and subepicardial microvasculature in normal adult mouse heart (Aisagbonhi *et al.,* 2011). After experimental MI by ligation of left coronary artery (LCA), we detected canonical Wnt activation at 4 to 7 days post MI, localizing to a large number of cells within the infarct and the peri-infarct tissue (Aisagbonhi *et al.,* 2011) (**Figure 3**). Interestingly, activation of the signaling pathway was not observed during the early phase of repair (*i.e*. cell death and inflammation within 24 hour post MI) nor in the late phase of repair (*i.e*. scar maturation at 3 weeks post MI). This indicates that canonical Wnt activation during cardiac tissue repair is transient and specific to the granulation tissue formation phase, highlighted by the proliferative activity of endothelial cells and mesenchymal cells that contribute to neovascularization and fibrotic scar formation respectively. In support of this notion, our laboratory detected canonical Wnt signaling activation at 7 days post MI in mesenchymal cells and endothelial cells in the infarcted tissue (Aisagbonhi *et al.,* 2011).

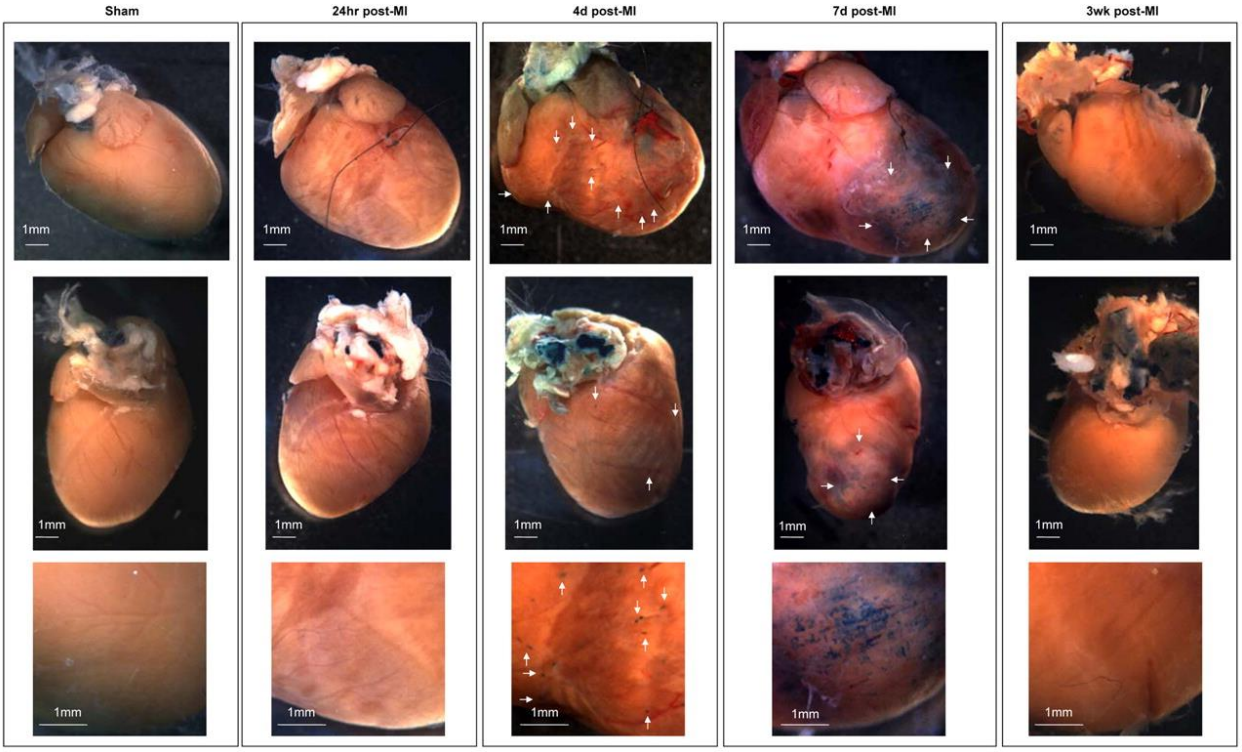

Figure 2. Canonical Wnt activation in adult mouse heart post MI. TOPGAL mouse hearts at 24 hours, 4 days, 7 days, and 3 weeks post MI stained with X-gal to assess canonical Wnt activity. Upper panels: front views with visible sutures; middle panels: rear views; lower panels: higher-magnification images of interest areas and infarct sites. In sham-operated control hearts, β-galactosidase activity staining is indistinguishable from normal (i.e. non-operated) hearts at all time points after surgery. The displayed sham examples are from 7 days after surgery. Similarly, there are no visible changes in β-galactosidase staining 24 hours after LAD occlusion, compared with non-operated heart. By contrast, starting at day-4 post-MI, numerous X-gal-positive cells (arrows) appear throughout the heart around blood vessels. By 7-days post-MI, X-gal-positive cells are present around the infarct and peri-infarct areas (arrows). Canonical Wnt pathway activity is undetectable in the injury area 3 weeks after experimental MI. Figure adapted from Aisagbonhi *et al.,* 2011.

We then analyzed the expression levels of Wnt signaling proteins during this window of canonical Wnt activation in hearts after MI, and compared to those of hearts with sham operation. Among the 19 Wnt ligands, we detected up-regulation of four ligands, Wnt2, Wnt4, Wnt10b, and Wnt11 (Aisagbonhi *et al.,* 2011). Wnt2 and Wnt10b are classically categorized as canonical Wnt signaling activators, while Wnt4 and Wnt11 are

known to activate the non-canonical branches. Induction of Wnt2 and Wnt10b expression in heart post MI has been reported in independent investigations (Barandon *et al.,* 2003; Abdul-Ghani *et al.,* 2011).

These observations demonstrate that canonical Wnt signaling is strongly activated in the heart following ischemic injury. However, at present, it is not known 1) what role canonical Wnt signaling plays in granulation tissue formation, and 2) whether modulation of the individual components that activate the signaling would be beneficial or detrimental to the endogenous tissue repair process.

Mixed results of Wnt modulation in heart after myocardial injury

Previous studies that modulated Wnt signaling in mammalian heart show mixed results on the effects of Wnt modulation on cardiac repair after injury. Overexpression of sFRP1, an endogenous Wnt antagonist, was shown to reduce infarct size and prevent cardiac rupture after experimental MI in mice (Barandon *et al.,* 2003). These effects were supported by decreased apoptosis and early leukocyte infiltration, with increased collagen deposition and capillary density in the scar tissue (Barandon *et al.,* 2003). Transplantation of bone marrow derived cells overexpressing sFRP1 was shown to diminish leukocyte infiltration after MI, by modulating the pro- and anti-inflammatory cytokine balance to reduce scar formation and to improve cardiac hemodynamic parameters (Barandon *et al.,* 2011). Such effects, however, were not observed in mice overexpressing sFRP1 in endothelial cells or cardiomyocytes, indicating that sFRP1 has a specific, autocrine role on BMCs during the inflammatory phase of repair (Barandon *et al.,* 2011). Mesenchymal stem cells (MSCs) overexpressing Akt gene reduced the infarct size after MI in sFRP2-

dependent manner (Mirotsou *et al.,* 2007). Similarly, implantation of MSCs overexpressing sFRP2 to ischemic mouse hearts resulted in enhanced engraftment, vascular density, and cardiac function (*Alfaro et al*., 2008). Injection of sFRP2 protein in the infarcted rat myocardium was shown to attenuate fibrotic scar formation by inhibiting Collagen I deposition (He *et al.,* 2010), and sFRP4 administration was shown to be beneficial after MI or ischemia/reperfusion (I/R) models in rat hearts (Matsushima *et al.,* 2010). Another study, however, demonstrated that sFRP2 knockout mice had improved cardiac function after MI with reduced fibrosis (Kobayashi *et al.,* 2009). These conflicting reports may be attributed to the unique inhibitory effects of sFRP2 on BMP1 that plays a key role in collagen synthesis and maturation, which are not observed by sFRP1 or sFRP3 (He *et al.,* 2010, Hermans and Blankesteijn, 2015).

Injection of another known Wnt antagonist Dkk2 was shown to moderate infarct size in rat myocardium after I/R injury, by reducing the number of apoptotic cells and increasing neovascularization of scar tissue (Min *et al.,* 2011). Dkk2 is an endogenous antagonist that binds directly to the membrane co-receptor LRP5/6 to inhibit canonical Wnt signaling. Administration of canonical Wnt ligand Wnt3a to the infarcted tissue was reported to be detrimental to cardiac repair by limiting proliferation of cardiac progenitor cells, with increased infarct size and left ventricular volume one week after MI (Oikonomopoulos *et al.,* 2011). Administration of UM206, a synthetic peptide fragment of Wnt3a/Wnt5a, for five weeks post MI was shown to reduce infarct size and improve cardiac function, though its exact mechanism remains unclear (Laeremans *et al.,* 2011).

Modulation of β-catenin, a key intracellular molecule of canonical Wnt pathway, has also yielded puzzling results. Inactivation of the β-catenin gene in epicardial cells

decreased epicardial expansion and further impaired cardiac function after I/R injury, by failing to generate myofibroblasts through EMT (Duan *et al.,* 2012). Adenoviral overexpression of a constitutively active form of β-catenin led to improved post-infarct remodeling by inducing differentiation of fibroblasts to myofibroblasts and by having anti-apoptotic effects on cardiomyocytes (Hahn *et al.,* 2006). Taken together, activation of canonical Wnt signaling by stabilization of β-catenin seems to be beneficial for remodeling of ischemic heart. However, another study reported loss of β-catenin function led to reduced mortality and infarct size by enhancing resident progenitor cell differentiation, while mice with the constitutively active form of β-catenin displayed the opposite phenotype (Zelarayan *et al.,* 2008).

The conflicting reports on Wnt modulation in rodent models after ischemic injury indicate the need to test stage-, ligand-, and cell-specific manipulation of Wnt signaling, as the modulation of the pathway affects nearly all cell types in all phases of cardiac tissue repair in varying degree and manner. It is also important to note that, to our knowledge, no study has yet investigated the effects of gain- or loss-of-function of endogenous canonical Wnt ligands. The plethora of published work has thus far focused on modulating the antagonists and intracellular members of the pathway, which calls for a need to study the effects of naturally induced canonical Wnt agonists in the heart tissue post ischemic injury.

Summary and hypothesis

Wnt signaling is a major cardiac developmental pathway, regulating proliferation, specification, and differentiation of stem/progenitor cells of cardiovascular lineage.

Though canonical Wnt signaling is mostly silent under physiological conditions in the adult heart, it is strongly induced in the ischemic heart, during the proliferative phase of tissue repair. While we and others have previously reported the role of canonical Wnt signaling in endothelial-to-mesenchymal transition (EndMT) in governing the processes of neovascularization and fibrosis, we lack understanding in whether modulation of endogenous Wnt activating molecules can optimize tissue repair and improve the heart function after an injury event. Wnt10b is one of such endogenous canonical Wnt activating ligand, whose expression is highly up-regulated in the heart tissue after MI (Aisagbonhi *et al.,* 2011).

Based on previous reports that Wnt10b regulates cell fate decisions of stem/progenitor cells and its induction after MI, we hypothesize that Wnt10b overexpression modulates the processes of neovascularization and fibrosis during cardiac repair to regulate injury outcomes.

CHAPTER II

WNT10B EXPRESSION IS INDUCED IN HEART TISSUE AFTER MYOCARDIAL INJURY

INTRODUCTION

Wnt10b is one of the two canonical Wnt ligands found to be up-regulated in the adult heart tissue after MI (Aisagbonhi *et al.,* 2011). Wnt10b has shown to regulate cell fate decisions in a number of tissue or organ systems (Wend *et al.,* 2012), but its role in the heart has yet to be investigated.

To address this question, we first analyzed the spatio-temporal patterns of Wnt10b RNA and protein levels in the heart before and after injury, in adult mouse and human hearts. Understanding the cell type(s) responsible for Wnt10b expression during homeostasis and induction after injury will allow us to create a model to explore its function in cardiac tissue repair.

EXPERIMENTAL METHODS

Human heart tissue

The human heart tissue samples were obtained from Vanderbilt Cardiology Main Heart Registry/Biorepository. The study was approved by the Vanderbilt Institutional Review Board, where written informed consent was obtained from all heart tissue donors or organ donor families. Explanted heart from patients with ischemic cardiomyopathy or organ donors whose heart were unmatched for transplantation was collected into the

Biorepository. At the time of explantation, a section of left ventricular (LV) free wall tissue was immediately frozen in liquid nitrogen, and a small piece of LV tissue from the same section was embedded in Optimal Cutting Temperature (OCT) compound and stored at -80ºC for immunofluorescence analysis.

Experimental Myocardial Infarction

Experimental myocardial infarction (MI) in adult mouse heart is created by permanent ligation of the left coronary artery (LCA). Under anesthesia, a 10-0 nylon suture is placed through the myocardium into the anterolateral left ventricular wall around the LCA, ligating the vessel. After surgery, the chest is closed and the animals are allowed to recover. Mice are administered with analgesics such as ketoprofen in the first 48 hours after surgery. Sham-operated animals undergo the same procedure, but without the coronary artery ligation. Surgeries were performed in the Vanderbilt Mouse Cardiovascular Pathophysiology and Complications Core.

Western blot analysis

Freshly isolated mouse hearts were thoroughly perfused with PBS and homogenized in 3% protease inhibitor, 1% phosphatase inhibitor II, 1% phosphatase inhibitor III in NP40 lysis buffer (Sigma) using tissue homogenizer. Tissue homogenate was spun at 14,000 rpm for 10 minutes and supernatants were collected as total protein samples. Proteins were separated by SDS-PAGE gel and transferred to nitrocellulose membranes. 10 ng of total protein was loaded per well. Primary antibodies recognizing β-Actin (Sigma A1978, 1:40,000) and Wnt10b (Santa Cruz sc-25524, 1:1000) were used.

Infrared secondary antibodies (LI-COR) were applied for 1 hour at room temperature at a dilution of 1:10,000. Signal was detected using the Odyssey infrared imaging system (LI-COR).

Immunofluorescence

Freshly isolated hearts were thoroughly perfused with Phosphate Buffered Saline (PBS) and embedded in OCT compound (Tissue-Tek). 5 µm cryo-sections were fixed in 1:1 acetone:methanol for 5 min at 4°C. Sections were blocked in 1% bovine serum albumin (BSA), 0.05% saponin in PBS for 1 hour at room temperature. Sections were incubated with primary antibodies overnight at 4°C, washed with 1X PBS, then incubated with Alexa-Fluor 488 and Cy3-conjugated secondary antibodies (Life Technologies, Jackson ImmunoResearch) and fluorescent dye DAPI (1:5,000) for 1 hour at room temperature. Slides were mounted with VECTASHIELD fluorescent mounting medium (Vector Laboratories). Images were taken on Olympus FV-1000 inverted confocal microscope and processed using the FV10-ASW 1.6 Viewer software (Olympus).

Gene expression analysis

Total RNA was isolated from mouse hearts using the TRIzol Reagent (Invitrogen) and from cultured cells using the RNeasy Mini Kits (Qiagen) following the manufacturers' instructions. 3 µg of RNA was reverse-transcribed to cDNA by incubation with 100 U Mo-MLV reverse transcriptase (Invitrogen) for 55 minutes at 37°C. Quantitative PCR was performed using the iQ SYBR Green Supermix (Bio-Rad) on an C1000 Thermal Cycler (Bio-Rad). Expression of Gapdh and β-Actin were used as internal controls to normalize

the expression of genes of interest. Primer sets were tested to have amplification efficiency of 90-110%, calculated via standard curve of log (DNA copy number) vs. relative fluorescence unit. Relative gene expression was calculated using the $2^{(-DDCt)}$ method (Livak and Schmittgen, 2001). Primers sets used are included in Appendix A.

Statistical Analysis

One-way ANOVA with Dunnett's multiple comparisons test was used to compare multiple groups against a single sham or control group. * $P < 0.05$, ** $P < 0.01$, *** $P < 0.001$ were considered significant. Results are reported as mean ± SEM.

RESULTS

Wnt10b is expressed in cardiomyocytes and stored in the intercalated discs

To determine the localization pattern of Wnt10b protein in the adult heart tissue, we immuno-stained human and mouse ventricle tissue sections. Immunofluorescence analysis with an antibody recognizing the N-terminal domain of WNT10B showed the protein expression in the intercalated discs of cardiomyocytes, which co-localizes with β-catenin (CTNNB1) and Connexin 43 (GJA1) in the human ventricular tissue (**Figure 4A**). β-catenin and Connexin 43 are cell junction proteins present in the intercalated discs of myocytes. Using a distinct antibody against the C-terminal domain of Wnt10b, we found similar accumulation of the protein in the intercalated discs of the mouse ventricular tissue. Wnt10b co-localizes with plakoglobin (Jup), a catenin molecule found in desmosomes and adherens junctions structures of intercalated discs of cardiomyocytes (**Figure 4B**). Western blot analysis of freshly isolated neonatal rat cardiomyocytes confirmed the

myocyte-specific Wnt10b expression (**Figure 4C**).

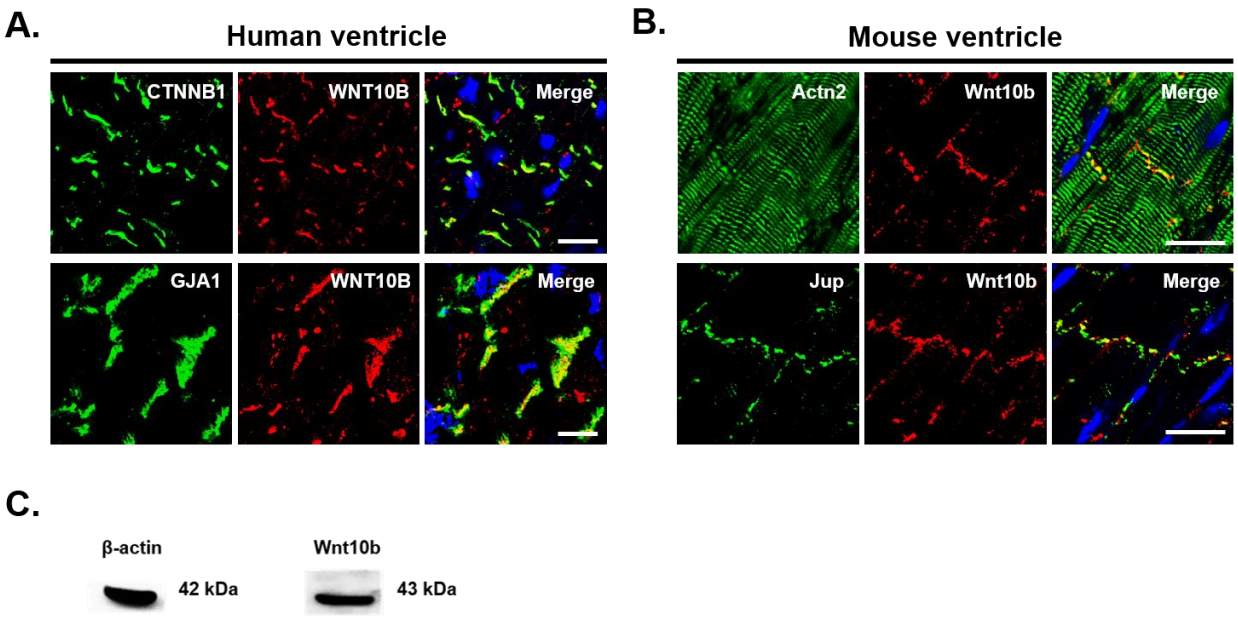

Figure 4. Localization of Wnt10b in human and adult heart. A. Localization of WNT10B protein in the normal adult human ventricular tissue. IF for WNT10B (red), β-catenin (CTNNB1, top, green) and connexin-43 (GJA1, bottom, green) illustrates localization of WNT10B in the intercalated discs of cardiomyocytes. Scale bars, 20 µm. **B.** Localization of Wnt10b in cardiomyocytes of normal adult mouse ventricular tissue. IF for α-Actinin (Actn2, top, green) and plakoglobin (Jup, bottom, green) shows localization of Wnt10b (red) in the intercalated discs. Scale bars, 20 µm. **C.** Wnt10b (43 kDa) in neonatal rat ventricular myocytes by Western blot. β-Actin (42 kDa) used as loading control.

Wnt10b expression is induced after myocardial injury

Previous studies have shown canonical Wnt signaling is activated in the myocardium after MI. Our laboratory has previously reported that Wnt10b is one of four Wnt ligands whose expression is induced in mouse hearts after MI (Aisagbonhi *et al.,* 2011). In order to better understand the temporal expression pattern of Wnt10b during the process of cardiac repair, we induced MI in C57Bl/6 adult mice and analyzed the ventricular tissue RNA at various time points after MI. Specifically, we quantified the

Wnt10b levels in the inflammatory response phase (day 1-3 post MI), the proliferative phase of neovascularization and fibrosis (day 5 and 7 post MI), and the scar tissue maturation phase (day 21 post MI). Our results showed *Wnt10b* RNA levels began to rise at day 3 post MI, peaked at day 7 by 6-8 fold, but returned to baseline levels during scar maturation (**Figure 5**). *Wnt10b* peak levels followed the induction of TGF-β1, an endogenous factor known to drive the fibrotic response during cardiac tissue repair.

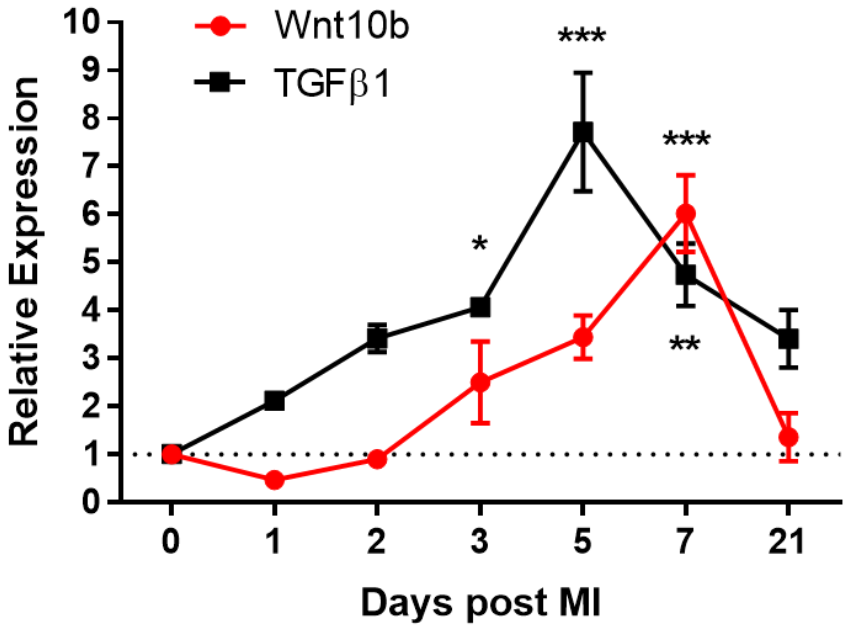

Figure 5. Wnt10b expression in adult heart post MI. *Wnt10b* and *Tgf-β1* mRNA expression by qPCR analysis at sequential time points post experimental myocardial infarction (MI) in mouse hearts. *Wnt10b* levels peak at day 7 after MI, during granulation tissue formation. * $P < 0.05$; ** $P < 0.01$; *** $P < 0.001$. One-way ANOVA with Dunnett's multiple comparisons test. N≥3 for all time points. All data are means ± SEM.

Wnt10b is induced in border zone cardiomyocytes

To identify the location of Wnt10b induction in the heart after injury, we analyzed adult human and mouse heart tissue after ischemic injury. We obtained ventricular tissue

samples of ischemic cardiomyopathy (ICM) patients from the Vanderbilt Cardiology Main Heart Registry/Biorepository and stained them for WNT10B and COL4A1, which marks the basement membrane of cells. DAPI counter-stain was used to visualize the nuclei. We detected abundant cytoplasmic staining of WNT10B that accumulated along the lateral borders of the cardiomyocytes in ventricular tissue of ICM patients, in addition to the intercalated disc localization normally observed in healthy tissue (**Figure 6A**).

We then induced experimental MI in C57Bl/6 adult mice and stained the ventricular tissue sections on day 2 and 7 post MI. While little to no changes in Wnt10b protein localization was observed at day 2 post MI (**Figure 6B**), we detected strong induction of Wnt10b protein in the myocytes of the infarct border zone at day 7 post MI (**Figure 6C-D**). In addition to the intercalated disc localization observed in normal hearts or in cardiomyocytes remote from the infarct, Wnt10b accumulated in the cytoplasm of border zone cardiomyocytes, similarly as observed in the ICM patient hearts.

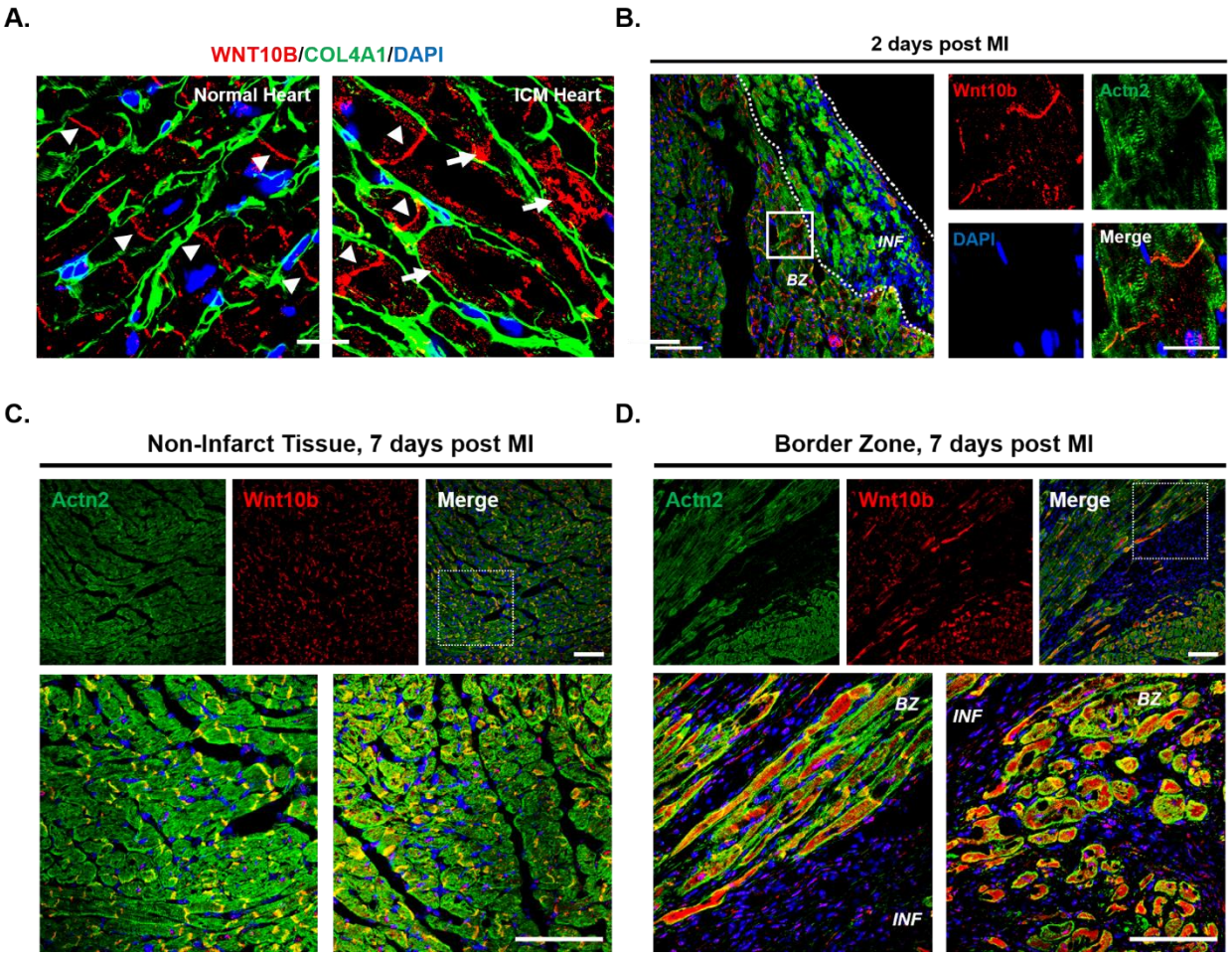

Figure 6. Wnt10b localization in adult human and mouse hearts before and after ischemic injury. A. Aberrant accumulation of WNT10B (red) in the cytoplasm of cardiomyocytes (arrows) in ischemic cardiomyopathy (ICM) patients (right), in addition to its localization in the intercalated discs (arrowheads). Normal human heart (left) shown as control. Collagen IV (COL4AI, green) antibody staining of basal membranes outlines borders between cardiomyocytes. Scale bars, 20 µm. **B.** Localization of Wnt10b in WT ventricle 2 days post MI. INF=infarct tissue, BZ=border zone. Scale bar, 100 µm; inset, 30 µm. **C.** Wnt10b remains associated with cardiomyocyte junctions in distal, non-infarcted, areas of mouse ventricle 7 days post MI. **D.** Wnt10b expression (red) is induced and becomes pervasive in the cytoplasm of cardiomyocytes (stained in green for Actn2) in the border zone of mouse hearts 7 days post MI. Low (top) and high (bottom) magnification of cardiac tissue is shown. Left bottom panels depict boxed areas on top. Scale bars, 100 µm. BZ=border zone, INF=infarct tissue. All tissue sections were counter-stained with DAPI (blue) to mark cellular nuclei.

DISCUSSION

In the homeostatic adult heart, activation of canonical Wnt signaling is confined and limited to subpopulations of endothelial cells and pericytes that reside in coronary arteries and subepicardial microvasculature (Aisagbonhi *et al.,* 2011). In response to MI, canonical Wnt signaling is highly induced in the damaged myocardial tissue. In the mouse heart, we observed activation of the canonical Wnt signaling pathway begins at day 4 post MI, peaks at day 7 post MI, then disappears by day 21 post MI (Aisagbonhi *et al.,* 2011). We identified Wnt2 and Wnt10b, the Wnt ligands classically known to activate canonical Wnt signaling, to be up-regulated in the cardiac tissue in this particular time window of cardiac repair (Aisagbonhi *et al.,* 2011). Knowing that Wnt10b regulates cell fate decisions in non-cardiac stem/progenitor cell types, we further delved into the spatio-temporal expression pattern of Wnt10b in the heart during the tissue repair process after an ischemic injury.

It is an intriguing observation that, under physiological conditions, Wnt10b protein is expressed in cardiomyocytes and localized in the intercalated discs in human and mouse hearts (**Figure 4**). It is noteworthy that there exists a number of proteins that localize to the intercalated disc structures, whose expressions change in heart failure conditions (Perriard *et al.,* 2003; Kaplan *et al.,* 2004; Estigoy *et al.,* 2009). Such proteins identified encompass various protein categories: adhesion, anchoring or binding proteins, channel proteins, enzymes, ligand and ligand receptors, structural proteins, and mechanoreceptors (Estigoy *et al.,* 2009). The expression changes of such proteins are regarded to be either a cause or a consequence of mammalian heart failure (Estigoy *et al.,* 2009). This notion raises the possibility that the adult heart possesses an innate

mechanism to store the injury-responding genes in the junctions of the cardiomyocytes and to release them upon an injury event. This makes sense, because under disease conditions, the myocyte-to-myocyte interaction is disrupted and the intercalated disc structures loosen and expand (Perriard *et al.,* 2003). Our observations of Wnt10b would support this theory, where Wnt10b is maintained in this particular cellular structure during homeostasis but is released to the extracellular space in response to injury (**Figure 4 & 6**).

In parallel to the temporal pattern of canonical Wnt activation we previously observed in TOPGAL mouse hearts post MI, we detected Wnt10b gene expression began to rise at day 5 post MI, peaked at day 7 post MI, and regressed to baseline levels by day 21 post MI (**Figure 5**). This suggests 1) induction of Wnt10b follows the canonical Wnt activation in response to injury, and 2) Wnt10b is involved in Wnt signaling activation in different cell types during the proliferative phase of cardiac repair. These observations also point towards a role of Wnt10b in cardiac tissue repair after the end of the inflammatory phase and debris clearance. We speculate that the members of the molecular pathways activated during the inflammatory phase, such as the Bone Morphogenetic Protein (BMP), NF-κB, TNF-α, and/or c-Myc signaling, are factors that likely trigger Wnt10b induction in the ensuing proliferative phase. For example, in mammalian cardiac development, BMP4 has been shown to couple with Hopx gene to modulate Wnt signaling during differentiation of cardiomyoblasts to cardiomyocytes (Jain *et al.* 2015). In adipose cells with an activated state of inflammation, TNF-α and IL-6 together were shown to activate canonical Wnt signaling. TNF-α was found to activate Wnt10b expression in the preadipocytes, while IL-6 increased the levels of Dvl but not

Wnt10b (Gustafson and Smith, 2006).

It would be of interest to explore whether a similar pattern of Wnt10b induction occurs in other tissue types, such as skin, liver, or kidney, during the wound healing process following an acute or an ischemic injury. If so, the induction of Wnt10b gene during proliferative phase of tissue repair may be an evolutionarily conserved mechanism in regulating the cellular process of scar formation.

We found Wnt10b to localize in the intercalated discs, the cellular junctions of cardiomyocytes under physiological conditions. In both ICM human patients and wild-type mice subjected to MI by LCA ligation, however, we detected Wnt10b to also accumulate in the cytoplasm of the myocytes (**Figure 6A**). Analysis of mouse hearts at 7 days post MI revealed that the peri-infarct cardiomyocytes displayed such phenotype while the myocytes remote from the injury did not, suggesting that induction of Wnt10b in response to injury is local (**Figure 6C-D**). This would indicate that canonical Wnt activation by Wnt10b during the proliferative phase is confined to the peri-infarct and infarcted tissue, where induced expression of Wnt10b affects the cells involved in wound healing, but not the cells of uninjured regions of the heart.

We have not tested ourselves the specificity of the antibodies used to target Wnt10b (**Figure 4 & 6**). Given the similarities in the conserved domains of the Wnt proteins, it is possible that the antibodies generated to target Wnt10b may inadvertently bind to other similar Wnt ligands. However, we believe this is unlikely because 1) at least two independent studies showed the antibody's specificity to Wnt10b (Armstrong and Esser, 2005; Chen *et al.,* 2008), and 2) we used two antibodies that target distinct amino acid sequences of Wnt10b and observed identical staining pattern from both in two

difference species.

CHAPTER III

WNT10B OVEREXPRESSION IMPROVES VENTRICULAR SYSTOLIC FUNCTION AFTER INJURY BY ATTENUATION OF FIBROSIS AND ENHANCED MYOCYTE REGENERATION

INTRODUCTION

A number of previous studies have elucidated the effects of Wnt modulation on cardiac repair after injury in rodent models, by gain- or loss-of-function studies of Wnt antagonists such as Dkk and sFRP proteins or of intracellular components of canonical Wnt pathway such as Dvl and β-catenin. As discussed in Chapter II, however, the results have been inconsistent. Moreover, no study to our knowledge has studied the effects of overexpressing an endogenous canonical Wnt agonist, such as Wnt10b.

Based on our understanding of the spatial expression of Wnt10b in the heart before and after an ischemic injury, we created a transgenic mouse model that overexpresses Wnt10b in cardiomyocytes, its natural location of expression. Using this model, we compared the differences in the cellular and molecular events of cardiac tissue repair between the transgenic hearts and their control counterparts. We also investigated the effects of Wnt10b overexpression in cardiac function after injury to test our hypothesis that canonical Wnt activation by Wnt10b gain-of-function would be beneficial for heart repair.

EXPERIMENTAL METHODS

Animals

The αMHC-Wnt10b plasmid was generated by inserting the full-length *Wnt10b* cDNA into the *αMHC* (*Myh6*) gene promoter-polyA hGH cloning vector (Subramaniam *et al.,* 1991). The *αMHC-Wnt10b* transgenic (TG) mouse was generated by pronuclear microinjection of the construct into fertilized oocytes at the Vanderbilt Transgenic Mouse/Embryonic Stem Cell Shared Resource (TMESCSR). Two independent lines that displayed identical phenotypes in response to injury were maintained and used in this work. TG mice were raised in C57Bl/6 background and wild-type littermates were used as controls. All analyses were performed using mice at 12-32 weeks of age fed with a normal chow diet. All experiments were performed in accordance with the Institutional Animal Care and Use Committee (IACUC) at Vanderbilt University Medical Center.

Cryoinjury

Mice were anesthetized with 50 mg/kg pentobarbital sodium via intraperitoneal injection. Following aseptic preparation, an incision on the anterolateral left ventricle wall was performed. The left coronary artery was explored and a round 3-mm diameter metal probe cooled to -196^{o}C with liquid nitrogen was applied to the left ventricle wall for 10 seconds. The cryoinjured area was macroscopically identified as a firm white disk-like region. Continuous Electrocardiograms (ECGs) were obtained during the procedure. At the conclusion of the myocardial injury procedure, the intercostal space and skin were closed and the mice were recovered on a water-circulated heating pad (van den Bos *et al.,* 2005).

Echocardiography

Mice were rested and calmed before echocardiography was performed. All mice were conscious and unsedated during the procedure. VEVO 2100 machine and transducer MS-400 (VisualSonics) were used to measure and calculate various cardiac parameters. The left ventricle was located in B-Mode and traced over five consecutive beats in M-Mode. Left ventricular internal dimension in diastole and systole (LVIDd and LVIDs) were measured from M-Mode using the short axis. Final values were averaged from three independent measurements. The following equations were used to calculate the LV EF and FS:

LV Vol;d = [(7.0 / (2.4 + LVIDd)] * (LVIDd ^ 3)

LV Vol;s = [(7.0 / (2.4 + LVIDs)] * (LVIDs ^ 3)

LV EF (%) = 100 * [(LV Vol;d - LV Vol;s) / LV Vol;d]

LV FS (%) = 100 * [(LVIDd - LVIDs) / LVIDd]

Western blot analysis

Preparation of protein samples from mouse heart tissue and Western blot analysis were performed as described in the previous chapter.

Gene expression analysis

Gene expression analysis was performed as described in the previous chapter.

Trichrome Masson staining

5 µm of transverse ventricular cryo-sections were stained with Trichrome Masson

blue using the manufacturer's instructions. Slides were imaged on AZ100M widefield microscope (Nikon). Scar area ratio was calculated as (scar area) / (total ventricular area) of a given transverse ventricle section. Scar area and total ventricular area were calculated using the NIH ImageJ software.

Immunohistochemistry

Standard procedure for hematoxylin and eosin (H&E) staining following manufacturer's instructions was performed with the assistance of Translational Pathology Shared Resource of Vanderbilt University Medical Center.

Immunofluorescence

Immunofluorescence was performed as described in the previous chapter. Relative fibrotic density of injured tissue was calculated from Col1A immuno-stained transverse ventricular sections using ImageJ software (NIH), where images were RGB-stacked with identical maximum threshold value and their mean gray values were measured.

Electron microscopy

Mouse heart tissue was fixed in 2.5 % glutaraldehyde, 0.1 M sodium cacodylate solution for 1 hour in room temperature, then for 24 hours at 4°C. Electron micrograms were taken on Philips/FEI T-12 transmission electron microscope in the Cell Imaging Shared Resource at Vanderbilt University Medical Center.

Flow cytometry

To prepare primary non-myocyte cardiac cells, mice were first injected intraperitoneally with 50 U heparin for 10 minutes, then euthanized. Hearts were isolated and washed with 2% FBS, 10,000 U/ml heparin, 1X PBS solution. Ventricular tissue was then minced and digested with 10 mg/ml Collagenase type II, 2.4 U/ml Dispase II, 0.3 µg/ml DNAse IV, 2.5 mM $CaCl_2$ solution for 20 minutes at 37°C. Digested tissue is filtered through 100 µm filter and again with 70 µm filter. Flow cytometry analysis were performed using BD LSR II with the aid of Flow Cytometry Shared Resource at Vanderbilt University Medical Center (Ryzhov *et al.,* 2012). Live cells were distinguished by LIVE/DEAD Fixable Blue Dead Cell Stain Kit (Life Technologies). Antibodies used were biotin anti-Col1A (Rockland immunochemicals), anti-α-smooth muscle actin-FITC (Sigma), Leukocyte Common Antigen Ly-5 (CD45)-V450 (BD Bioscience), CD11b-V450 (BD Bioscience), PE/Cy7 anti-mouse Ly-6G (Biolegend), anti-mouse/rat Ki-67-PE (eBiosciences) and APC anti-mouse CD31 (Biolegend).

Statistical Analysis

Unpaired two-tailed *t* test was used to compare differences between two unpaired groups. * $P < 0.05$, ** $P < 0.01$, *** $P < 0.001$ were considered significant. Results are reported as mean ± SEM.

RESULTS

αMHC-Wnt10b transgenic mouse overexpresses Wnt10b in the heart

To determine whether Wnt10b gain-of-function is beneficial or detrimental to cardiac repair, we genetically enhanced the natural Wnt10b expression cardiomyocytes by generating a transgenic (TG) mouse that expresses the Wnt10b gene under the adult cardiomyocyte-specific alpha-myosin heavy chain (αMHC) gene promoter (**Figure 7A**). Because Wnt10b is normally expressed in cardiomyocytes in the adult heart, the TG mouse effectively overexpresses the gene at its natural location of expression.

To confirm this notion, we compared the RNA and protein levels of Wnt10b of TG ventricles to those of wild-type (WT) counterparts. Wnt10b RNA levels in TG hearts were approximately 5000-fold higher than those of the WT hearts (**Figure 7B**), and Western blot showed that Wnt10b protein was increased in the TG hearts by approximately 2-fold (**Figure 6C**). Immunofluorescence of the transverse ventricle sections showed the localization of Wnt10b protein in the TG hearts remained in the intercalated discs of cardiomyocytes, as observed in the WT hearts (**Figure 7D**).

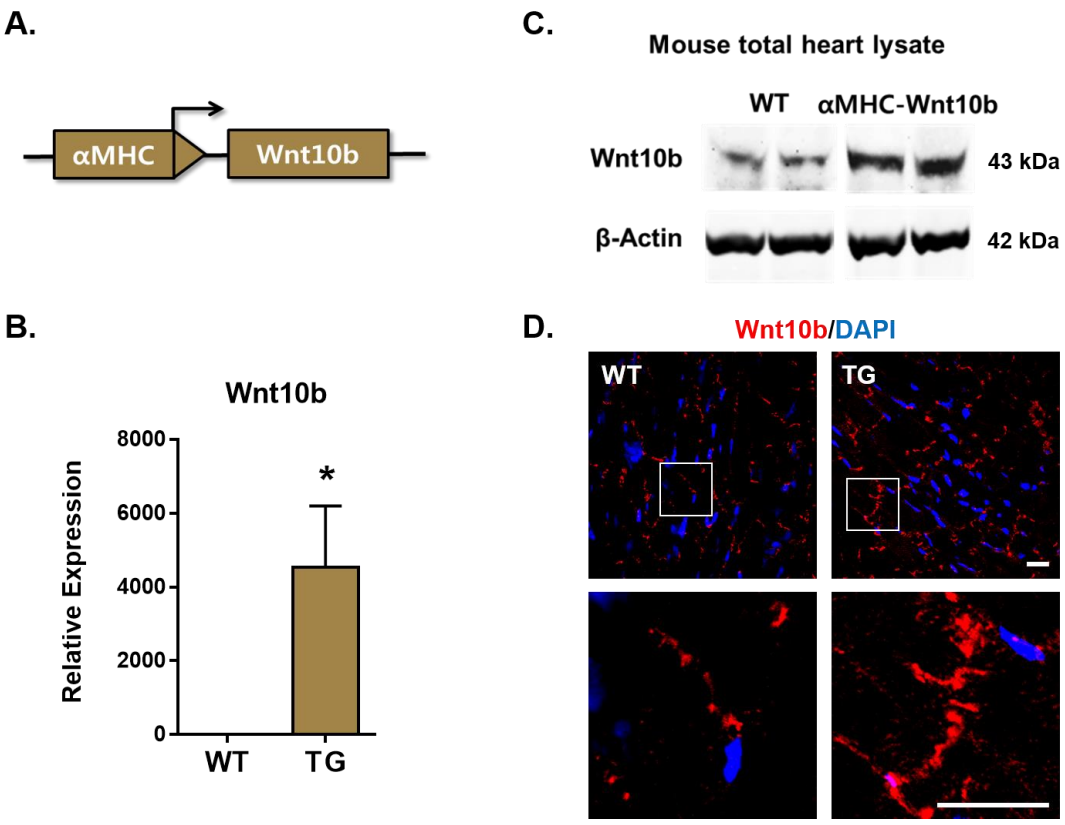

Figure 7. αMHC-Wnt10b transgenic mouse overexpresses Wnt10b in cardiomyocytes. **A.** Schematic drawing of the *αMHC-Wnt10b* transgene (TG). **B.** mRNA expression of Wnt10b gene in WT And TG ventricles. N=4/group. Unpaired *t* test. * *P*< 0.05. **C.** Western blot analysis of protein samples isolated from total cardiac tissue shows higher Wnt10b protein levels in TG hearts compared to wild types (WT). β-actin served as loading control. Molecular weights are indicated in kilodaltons (kDa). **D.** Localization of Wnt10b in WT and TG ventricle. Low magnification (top) and high magnification (bottom) images shown. Scale bar 20 μm.

Wnt10b overexpression did not cause changes in the ventricles of TG mice at the macroscopic or ultrastructural level. H&E staining of WT and TG ventricular tissue showed no difference in the morphology and size of cardiomyocytes (**Figure 8A**). Electron microscopy also confirmed no significant difference exists in the width or the shape of intercalated discs of WT and TG cardiomyocytes (**Figure 8B**).

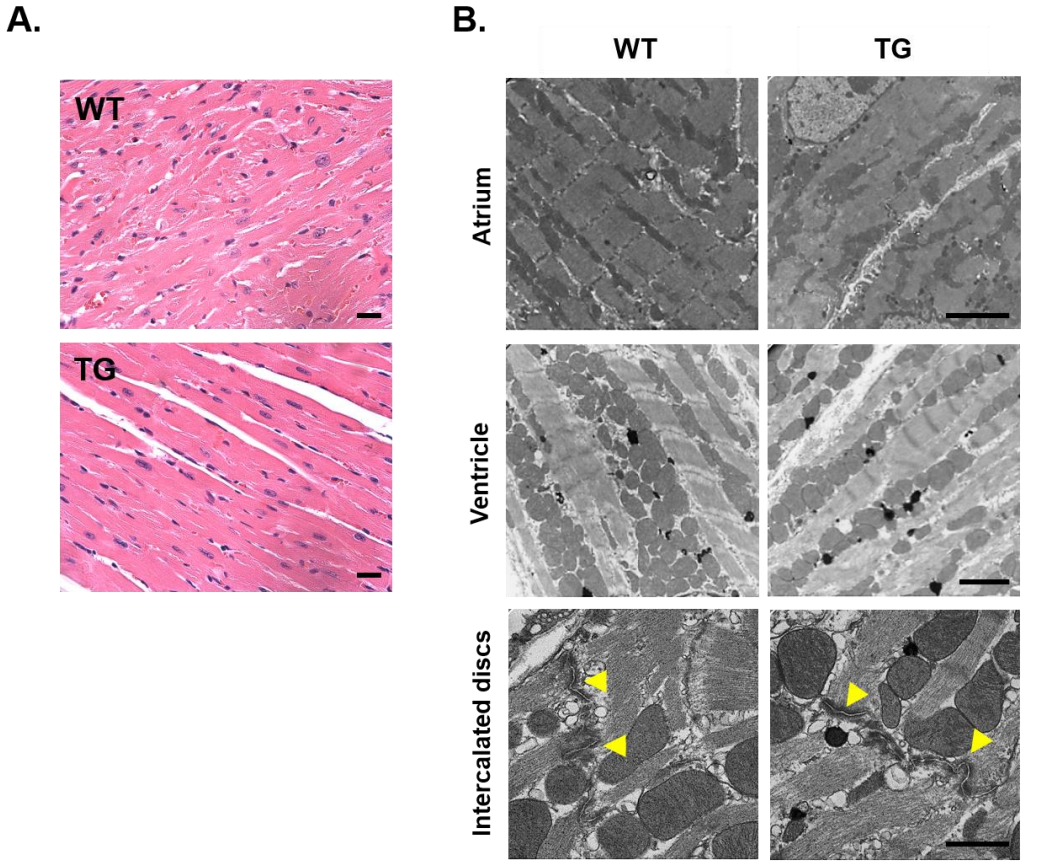
A.
WT
TG
B.
WT
TG
Atrium
Ventricle
Intercalated discs

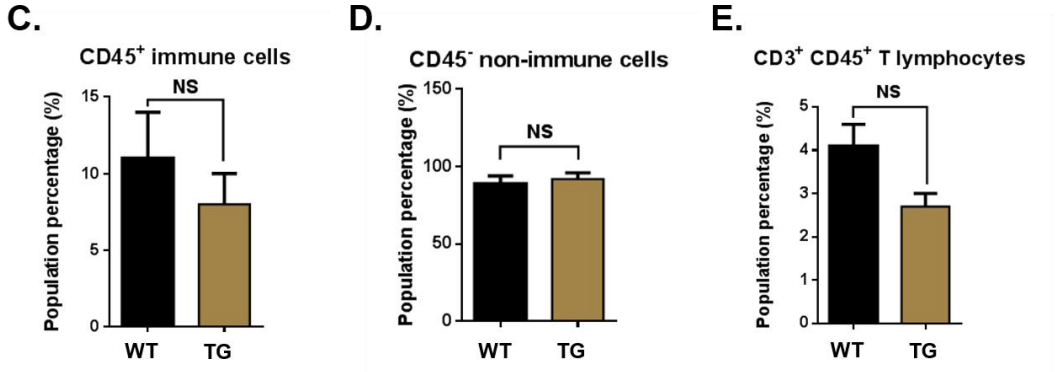
C.
CD45+ immune cells
NS
Population percentage (%)
15
10
5
0
WT
TG
D.
CD45- non-immune cells
NS
Population percentage (%)
150
100
50
0
WT
TG
E.
CD3+ CD45+ T lymphocytes
NS
Population percentage (%)
5
4
3
2
1
0
WT
TG

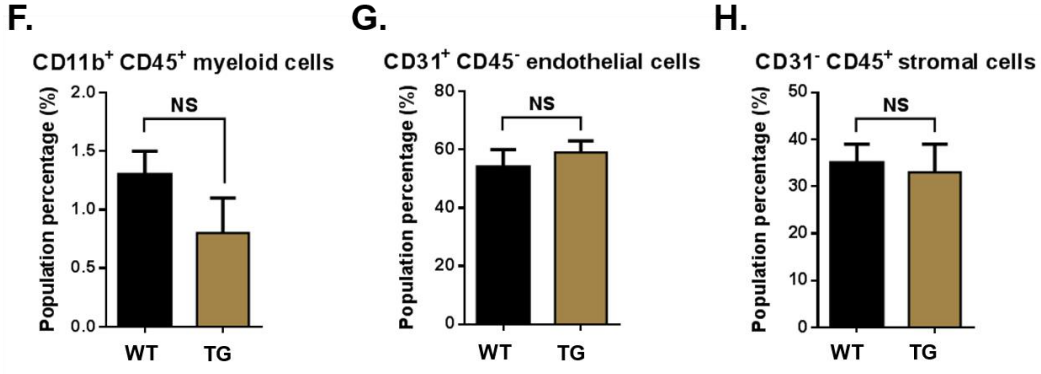
F.
CD11b+ CD45+ myeloid cells
NS
Population percentage (%)
2.0
1.5
1.0
0.5
0.0
WT
TG
G.
CD31+ CD45- endothelial cells
NS
Population percentage (%)
80
60
40
20
0
WT
TG
H.
CD31- CD45+ stromal cells
NS
Population percentage (%)
50
40
30
20
10
0
WT
TG

Figure 8. TG ventricles show no abnormalities in cardiomyocyte morphology and in other cell types of the heart. A. mRNA expression of Wnt10b gene in WT and TG ventricles. N=4/group. Unpaired *t* test. * *P*< 0.05. **B.** Electron micrographs of atrial myocytes (top), ventricular myocytes (middle), and intercalated discs in ventricular cardiomyocytes (bottom) of adult WT and TG hearts. Scale bar, 2 μm. Percentage population of **C.** CD45+ immune cells, **D.** CD45- non-immune cells, **E.** CD3+ CD45+ T lymphocytes, **F.** CD11b+ CD45+ myeloid cells, **G.** CD31+ CD45- endothelial cells, and **H.** CD31-CD45- stromal cells in uninjured adult WT and TG ventricles. Data presented as Mean±SEM. Unpaired *t* test. Mean values of total cell number were 0.86±0.13 and 0.78±0.21 x 10^6 cell per WT and TG ventricles respectively. N=4 per group. NS, not significant.

Echocardiographic measurements showed normal ventricular dimensions and functional parameters in the TG hearts compared with WT controls (**Table 1**). Flow cytometry of primary non-myocyte cells isolated from adult WT and TG ventricles also showed comparable numbers of immune, endothelial, and stromal cells, indicating overexpression of Wnt10b does not alter the morphology, function, and cellular composition of adult ventricular tissue (**Figure 8C**).

	Body Weight (g)	**LV Mass (mg)**	**HR (bpm)**	
WT	24.74 ± 0.58	61.61 ± 4.53	692.2 ± 12.36	
TG	24.78 ± 0.61	60.81 ± 3.90	651.1 ± 12.53	
P value	NS	NS	* (P=0.03)	
		Wall Dimensions		
	IVS;d (mm)	**IVS;s (mm)**	**LVPW;d (mm)**	**LVPW;s (mm)**
WT	0.764 ± 0.034	0.931 ± 0.039	0.722 ± 0.029	0.974 ± 0.037
TG	0.765 ± 0.024	0.951 ± 0.037	0.695 ± 0.024	0.958 ± 0.038
P value	NS	NS	NS	NS
		Cavity Dimensions		
	LVID;d (mm)	**LVID;s (mm)**	**LV Vol;d (ul)**	**LV Vol;s (ul)**
WT	3.256 ± 0.067	1.731 ± 0.059	42.99 ± 2.12	8.958 ± 0.77
TG	3.288 ± 0.082	1.775 ± 0.050	44.15 ± 2.78	9.520 ± 0.70
P value	NS	NS	NS	NS
		Systolic Function		
	EF (%)	**FS (%)**	**SV (ul)**	**CO (ml/min)**
WT	79.41 ± 1.04	46.95 ± 1.00	33.74 ± 1.51	23.28 ± 0.95
TG	78.52 ± 0.62	46.01 ± 0.61	34.02 ± 2.04	22.13 ± 1.38
P value	NS	NS	NS	NS

Table 1. Echocardiographic parameters of WT and TG ventricle. Wall and cavity dimensions and calculated functional parameters of left ventricle in WT and TG adult mouse hearts measured by echocardiography. WT N=10, TG N=11. Unpaired *t* test. * *P* = 0.03. NS, not significant.

Wnt10b overexpression, however, led to enlargement of both atria (**Figure 9A-C**). Atrial enlargement in TG hearts is suspected to be due to hyperplasia of the atrial myocytes, though this notion is not yet confirmed. It is also to be determined whether the change in tissue morphology is due to the direct or indirect effects of Wnt10b overexpression.

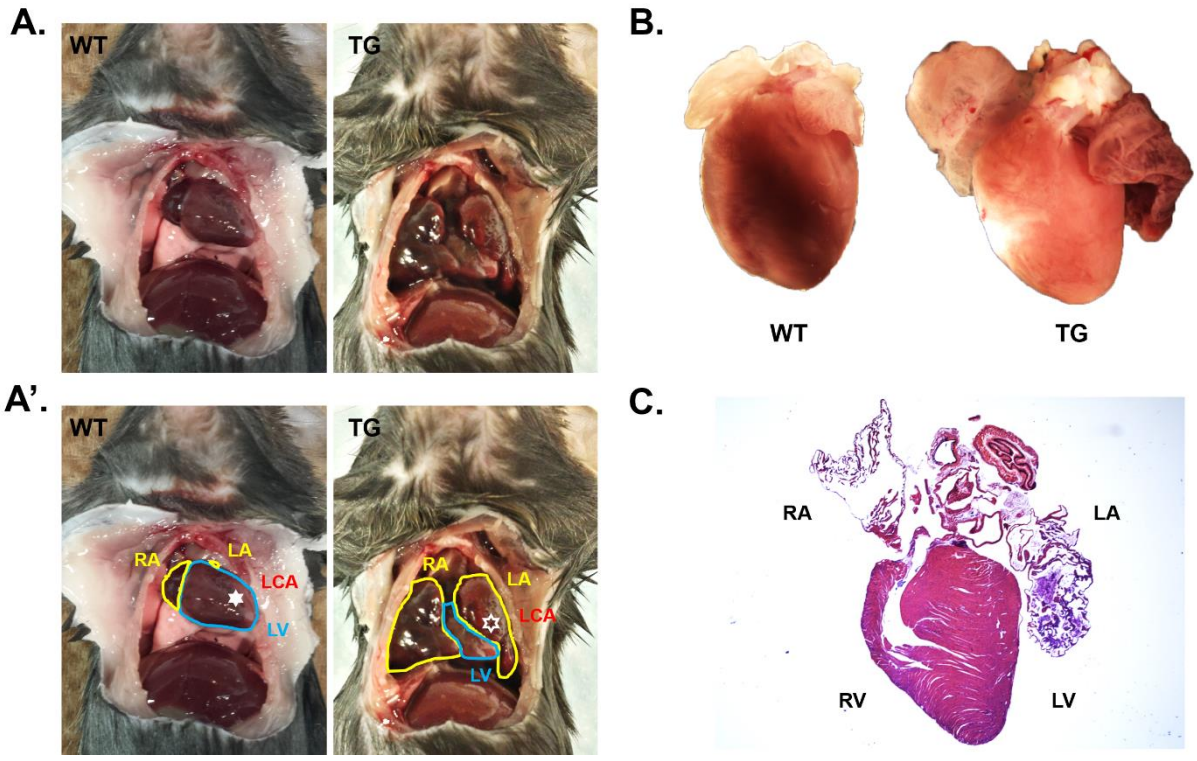

Figure 9. Enlarged atrial phenotype of adult TG hearts. A. Images of opened chest cavity of adult WT (left) and TG (right) mice. **A'.** Yellow lines outline the visible parts of the atria and blue lines outline the ventricles. The solid white star indicates the position of the left coronary artery (LCA) and the approximate site of ligation in WT mice. In TG mice, the open star marks the corresponding LCA site, which is hidden below the enlarged left atrium. **B.** Whole mount images of WT and TG hearts after isolation. **C.** H&E image of the TG mouse heart in sagittal position. The left atrial tissue of the TG heart overhangs the left ventricle. LA=left atrium, RA=right atrium, LV=left ventricle.

Ventricular systolic function is improved in αMHC-Wnt10b mouse hearts after cryoinjury

Because the enlarged atria of TG mice hindered ligation of LCA, we assessed the effects of Wnt10b overexpression on cardiac tissue repair using the cryoinjury model (van den Bos *et al.,* 2005; van Amerongen *et al.,* 2008). Cryoinjury generated comparably-sized and sharply-outlined transmural injury, allowing straightforward and consistent evaluation of tissue repair among different experimental groups. By triggering instant

tissue ablation and necrotic cell death, the cryoinjury model also highlights the direct effects of Wnt10b gain-of-function on repair mechanisms and eliminates effects on cardiomyocyte survival under hypoxic conditions.

Histological and molecular analyses of Wnt10b expression after cryoinjury showed induction at day 7 after injury that was confined to cardiomyocytes in the injury border zone, as observed in the MI model, suggesting both spatial and temporal Wnt10b expression patterns are comparable in the two injury models (**Figure 10A-B**).

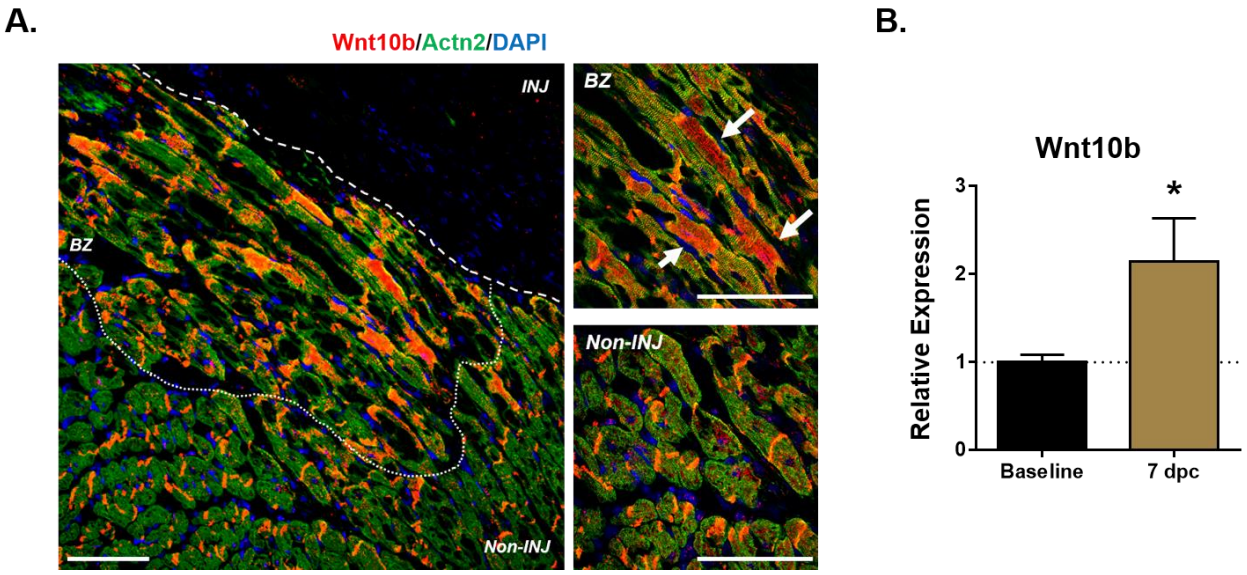

Figure 10. Wnt10b induction pattern after cryoinjury mimics that after MI. A. Induced expression of Wnt10b in cardiomyocytes of border zone in WT ventricle 7 days post cryoinjury, which mimics the expression pattern observed in WT ventricles 7 days post MI. Low magnification image (left) and high magnification images (right) shown. INJ=Injured tissue, BZ=border zone, Non-INJ: Non-injured tissue. Scale bar, 100 μm. **B.** mRNA expression level of Wnt10b in WT ventricles, at baseline and at 7 days post cryoinjury (dpc). N=3-4 mice/group. Unpaired two-tailed t test. * *P*<0.05.

Cardiac functional parameters were measured by echocardiography at baseline before injury, and at 1 day, 1 week, and 3 weeks after injury (**Figure 11A**). The results showed the extent of the initial injury was similar in WT and TG mice as demonstrated by similar drops in fractional shortening 1 day after injury. However, whereas the function of WT hearts continued to deteriorate over time, left ventricular functional output of TG hearts improved 3 weeks after injury (**Figure 11A**). Functional recovery in TG mice was attributed to preservation of systolic function, suggested by the mitigated increase in the systolic left ventricle internal dimension at 3 weeks after injury (**Figure 11B**). M-mode echocardiogram also noted preserved left ventricular chamber size and contractility of TG hearts, whereas the WT left ventricle chamber was significantly dilated at systole (**Figure 11C**).

Improved cardiac function in TG mice matched attenuated induction of prognostic markers of heart failure and hypertrophy, such as matrix metalloproteinase-9 (Mmp9) and natriuretic peptide A and B (Nppa, Nppb) when compared to WT counterparts (Omland *et al.,* 1996; Spinale *et al.,* 2000; Chan and Ng, 2013) (**Figure 11D**).

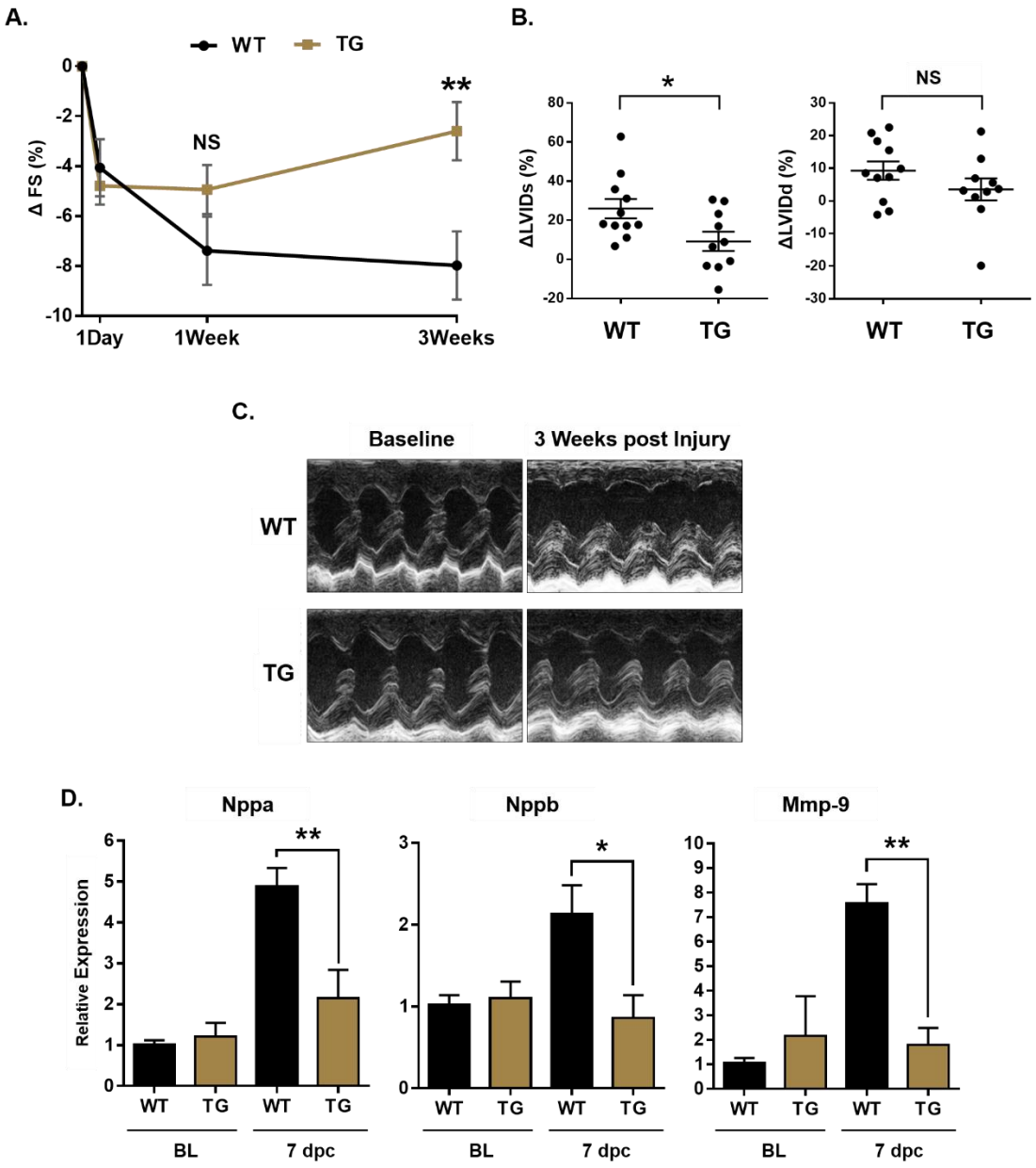

Figure 11. Wnt10b overexpression improves systolic ventricular function. A. Fractional shortening percentage changes at 1 day, 1 week and 3 weeks after cryoinjury show that cardiac function recovers over time in TG mice, whereas it deteriorates in WT controls. WT N=10, TG N=11. **B.** Percentage changes in left ventricular internal dimension in systole (LVIDs) and diastole (LVIDd) 3 weeks post cryoinjury, relative to baseline values, indicate functional recovery in TG mice is primarily due to improved systolic function. WT N=10, TG N=11. **C.** Representative M-mode echocardiograms at baseline and 3 weeks after cryoinjury demonstrate improved ventricular function in TG mice compared to WT counterparts 3 weeks after injury. **D.** mRNA analysis by qPCR at baseline (arbitrarily set as value 1 in WT) and 7 days post cryoinjury shows that expression of heart failure predictor genes is attenuated in TG mouse hearts compared to WT. BL=baseline, dpc=days post cryoinjury. N=3-6 mice/group. * $P < 0.05$; ** $P < 0.01$; NS, not significant, unpaired *t* test. All data are means ± SEM.

Wnt10b overexpression limits pathological cardiac fibrosis

One of the major causes for deterioration in cardiac function after an injury event is excessive formation of fibrotic scar tissue. The fibrotic tissue prevents electro-mechanical coupling of healthy, contracting myocytes, which leads the heart to undergo hypertrophy and adverse remodeling. We therefore assessed the level of pathological fibrosis that occurred in WT and TG hearts after cryoinjury through histological analysis.

Trichrome Masson staining is a useful tool in visualizing fibrotic tissue on tissue sections because it labels collagen fibers as blue, muscle fibers as red, and cell nuclei as dark brown. We stained WT and TG transverse ventricle sections 4 day and 3 weeks after cryoinjury and measured the area of fibrotic scar tissue. At 4 day after injury, the original transmural injury area was comparable in WT and TG mice, covering approximately 25-30% of the ventricles in both groups (**Figure 12A**). By 3 weeks after injury, however, the TG ventricles displayed reduced scar tissue size than WT counterparts. The WT ventricles displayed approximately 15% of the ventricular area to be scar tissue, while approximately 10% of the TG ventricular area was calculated to be fibrotic (**Figure 12A**).

Immunohistochemistry with Collagen IA antibody of transverse ventricular sections 3 weeks post cryoinjury also revealed that the relative fibrotic density by Collagen I deposition is significantly reduced in TG hearts (**Figure 12B**).

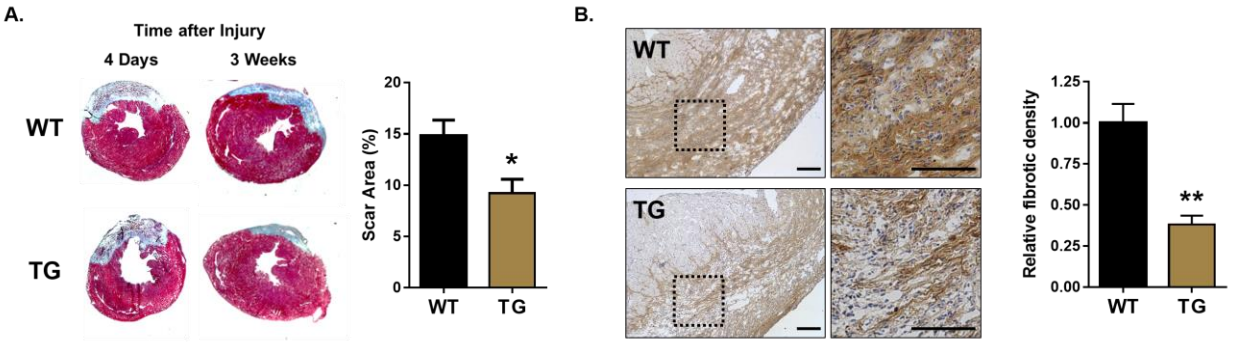

Figure 12. Reduced scar formation in TG ventricles after cryoinjury. A. Trichrome Masson staining of ventricle sections 4 days and 3 weeks after cryoinjury (left) and quantification of scar size as percentage of horizontal ventricle area (right). TG and WT mice display similar size of original injury. 3 weeks later, scar size in TG hearts is reduced by approximately 2-fold compared to WTs. N=4 mice per group. **B.** Immunohistochemistry of Col1A in injured tissue of WT and TG ventricles 3 weeks post cryoinjury shows reduced collagen deposits in TG (left). Boxed areas are shown at higher magnification. Scale bars, 200 μm. Quantification of relative fibrotic density (arbitrarily set as value 1 in WT) based on Col1A staining (right). N=4 mice per group. * $P < 0.05$; ** $P < 0.01$; NS, not significant, unpaired *t* test. All data are means ± SEM.

Consistent with the histological analysis, we found Wnt10b overexpression reduced the number of myofibroblasts generated after injury, the cell type primarily responsible for production and deposition of Collagen I fibers in the scar tissue. By flow cytometry analysis of non-myocyte, non-immune cells isolated from ventricular tissue, we observed no difference in the number of total fibroblasts ($CD31^{-}CD140a^{+}$) after injury between the two groups (**Figure 13A**). Number of activated myofibroblasts ($\alpha SMA^{+}CD31^{-}$ and $\alpha SMA^{+}Col1A^{+}$) after injury, however, was significantly reduced in the TG ventricles compared to the WT counterparts (**Figure 13B-C**).

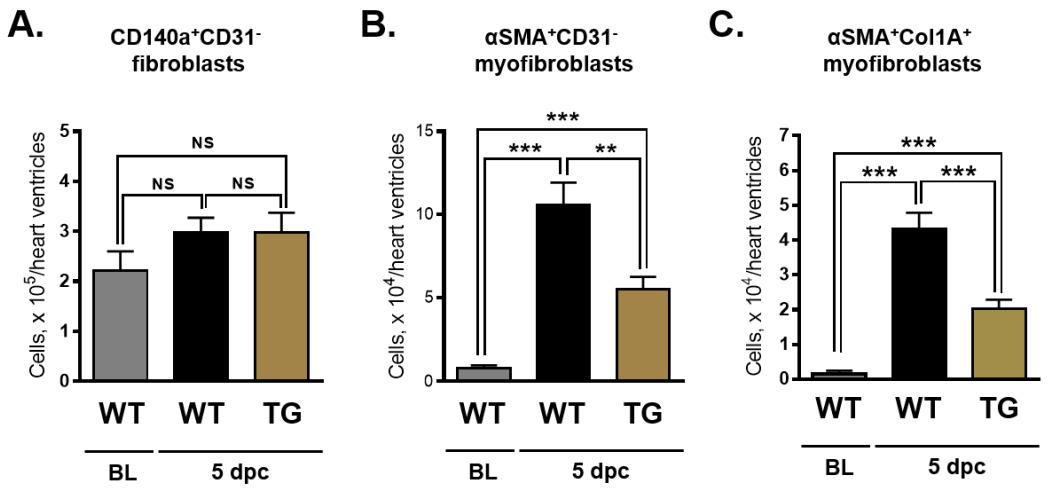

Figure 13. Wnt10b overexpression reduces generation of myofibroblasts. Number of **A.** CD140a^{+}CD31^{-} fibroblasts, **B.** αSMA^{+}CD31^{-} myofibroblasts, and **C.** αSMA^{+}Col1A^{+} myofibroblasts among non-cardiomyocyte CD45^{-} primary cells isolated from WT and TG ventricles, determined by flow cytometry. Cell population numbers from WT ventricles at baseline shown as reference. TG hearts contain higher endothelial cell, equal fibroblast and lower myofibroblast numbers compared to WT 5 days after cryoinjury. BL=baseline, dpc=days post cryoinjury. N=6 mice per group. ** $P < 0.01$; *** $P < 0.001$; NS, not significant, unpaired *t* test. All data are means ± SEM.

Wnt10b overexpression promotes myocyte regeneration

Because the Collagen content in the scar tissue was significantly attenuated in TG hearts, we explored whether the fibrotic tissue was replaced by other cell types, such as cardiomyocytes. Staining the WT and TG ventricular sections at 7 days post injury with α-Actinin (Actn2) surprisingly revealed the scar tissue in TG hearts contained numerous patches of α-Actinin^{+} cells (**Figure 14A-B**). These cells displayed sarcomeric structures, though not organized or aligned as a mature myocyte would show. While the cells appeared in groups or patches, only few formed cellular junctions with one another and the size and the morphology of the cells were highly variable. Nevertheless, the number of the α-Actinin^{+} cells found in TG scar tissue was noteworthy, as no such cells were found in the WT scar tissue (**Figure 14A-B**).

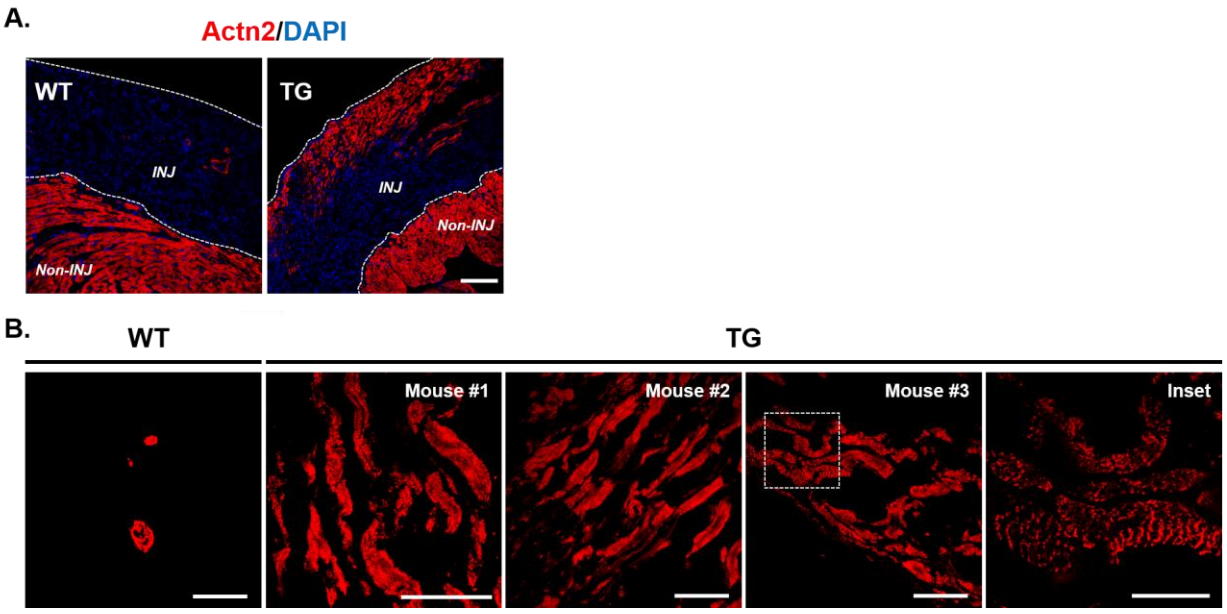

Figure 14. Wnt10b overexpression generates myocytes in the scar tissue. A. Comparison of α-Actinin staining for cardiomyocytes in WT and TG ventricles 7 days post cryoinjury in low magnification shows the appearance of cardiomyocyte patches in TG. Injury areas between epicardium and healthy tissue are delineated with dashed lines. **B.** Actn2 staining in WT and TG ventricles 7 days post cryoinjury in high magnification. Images from three distinct TG mice display abundant Actn2 staining within scar tissue. Inset (far right) shows sarcomeric structures in Actn2^{+} cells. Scale bar, 200 μm; inset, 50 μm. INJ=injured tissue, Non-INJ=non-injured tissue.

DISCUSSION

To assess the effects of Wnt10b gain-of-function on cardiac tissue repair, we genetically engineered αMHC-Wnt10b transgenic (TG) mice to overexpress the Wnt10b gene in adult cardiomyocytes, its natural location of expression. We confirmed RNA and protein levels of Wnt10b to be significantly increased in the TG hearts (**Figure 7**).

No obvious abnormalities in the TG ventricles were observed at cellular or subcellular level (**Figure 8**). Echocardiography measurements indicated adult TG hearts maintained normal left ventricular function, comparable to that of WT counterparts (**Table 1**). This allowed us to subsequently compare WT and TG ventricles on their molecular, cellular, and physiological response to injury.

TG hearts did however display enlargement of both atria (**Figure 9**). At this point, we do not fully understand the role of Wnt10b overexpression plays on creating such phenotype. The differential effects of Wnt10b overexpression on atria and ventricles may be due to a number of reasons. First, the expression of αMHC promoter in adult cardiomyocytes in the atria and ventricles may differ, which would affect the expression of the Wnt10b transgene in different chambers of the TG heart. If the expression of αMHC promoter in adult cardiomyocytes is otherwise uniform in the two sets of chambers, the observed phenotype may be an indication that cardiomyocyte biology of adult atria and ventricles are innately dissimilar, in ways to which they respond to activation or inhibition of signaling pathways.

It is noteworthy that despite the atrial enlargement, the systolic and diastolic ventricular functions of TG mouse hearts under physiological conditions were not significantly altered (**Table 1**). Similar phenotype is apparently observed in human

patients as well, where patients with left atrial enlargement had normal left ventricular systolic function (Katayama *et al.,* 2010). This particular clinical study attributed the left atrial enlargement to decreased hemoglobin levels, a factor that may or may not be influenced by cardiomyocyte-specific overexpression of Wnt10b in the case of the TG mouse hearts. At the same time, an association of left atrial enlargement with left ventricular hypertrophy and diastolic dysfunction was reported in human subjects, where atrial enlargement phenotype may be a long-term predictor for ventricular dysfunction (Cuspidi *et al.,* 2012; Bombelli *et al.,* 2014). Our data suggest that ventricular dysfunction-caused atrial enlargement could be due to an aberrant activation of canonical Wnt signaling in atrial cardiomyocytes.

Following cryoinjury, the TG ventricles showed improved functional recovery in comparison to their WT counterparts (**Figure 11A-C**). Wnt10b overexpression led to left ventricular systolic function improvement by preservation of the chamber size and contractility, accompanied by attenuated fibrotic response and regeneration of α-Actinin^{+} cardiomyocytes in the scar tissue after cryoinjury (**Figure 12-14**). This observed phenotype, in particular, requires further attention because no other study to our knowledge has reported a possible regeneration of myocytes in the scar tissue of a damaged mammalian heart. Our observation is consistent with the findings from development, which showed canonical Wnt signaling activation promotes cardiomyocyte proliferation in the embryonic heart (Heallen *et al.,* 2011), and in mouse ESCs, αMHC-driven overexpression of Wnt proteins enhanced cardiomyocyte growth (Rai *et al.,* 2012). In zebrafish, activation of myocardial NF-κB was shown to be essential for myocyte generation in a ventricular resection model (Karra *et al.,* 2015). This will be explored

empirically and discussed in the later chapters. At present, it is not known whether the observed cellular responses reflect direct effects of Wnt10b on myofibroblast or cardiomyocyte proliferation, expansion and differentiation of cardiac progenitor cells, or regulation of cell fates during EndMT or mesenchymal-to-endothelial transition (MEndT) (Boudoulas and Hatzopoulos, 2009; Aisagbonhi *et al.,* 2011; Senyo *et al.,* 2013; Fioret *et al.,* 2014; Ubil *et al.,* 2014).

Taken together, these data suggest Wnt10b overexpression in the adult heart is beneficial for cardiac tissue repair. Expression induction of markers of heart failure and/or hypertrophy such as Mmp-9, Nppa, and Nppb were moderated in the TG ventricles, indicating that Wnt10b-overexpressing hearts are more likely to preserve their systolic function long-term (**Figure 11D**).

It is worth mentioning that the nature of myocardial injury triggered by the cryoinjury model is inherently different from that by the permanent artery ligation performed in Chapter II, or by the I/R model discussed in Chapter I. Cryoinjury ablates the cells upon contact of chilled metal probe to the heart tissue, causing massive and instant cell death by necrosis. On the other hand, the ischemic injury models triggers cell death by necrosis and apoptosis (Konstantinidis *et al.,* 2012). Differences in the mechanisms of cell death likely causes different types of an inflammatory response in the two injury models. After I/R, there are also hypoxic elements and reactive oxygen species that linger in the infarcted tissue, which are known to affect cell survival and death. To that end, it is necessary to administer I/R injury models, where possible, to the TG mouse hearts and determine whether the myocyte regeneration observed from the cryoinjury model is reproducible in the ischemic models.

CHAPTER IV

WNT10B PROMOTES PROLIFERATION AND ANGIOGENIC POTENTIAL OF CARDIAC ENDOTHELIAL CELLS

INTRODUCTION

Ischemic heart suffers from loss of cardiomyocytes and blood vessels accompanied by excessive fibrotic scar formation. Cardiomyocytes require constant and efficient supply of oxygen- and nutrient-rich blood, due to the nature of the highly demanding contractile workload on the cardiac muscle cells. Blood flow by coronary vessels and microvasculature in the heart is thus critical in cardiac function. Therefore methods to increase neovascularization of injured myocardium may enhance cardiomyocyte survival and regeneration.

While coronary artery bypass grafting and percutaneous coronary interventions to restore the blood flow in ischemic heart disease patients have shown to reduce morbidity and mortality (Caines *et al.,* 2004), a large number of patients are ineligible for these procedures because of the presence of diffuse, complicated, or intractable lesions (Lavine and Ornitz, 2009). The improved blood flow on a macrovascular level also does not translate to restoration of myocardial perfusion, as significantly impaired microvasculature has not been rectified (Saraste *et al.,* 2008). This calls for a need to find therapeutics that can restore the lost vasculature during the endogenous wound healing process.

Over the past years, a number of factors that can promote blood vessel growth in animal models have been identified, such as FGF2, VEGF-A, and ANG-2 (Lavine and

Ornitz, 2009). Unfortunately, clinical trials using either protein or gene therapy with such factors have overall been disappointing (Henry *et al.,* 2000; Losordo *et al.,* 2002; Simons *et al.,* 2002; Syed *et al.,* 2004).

Based on the known angiogenic effects of canonical Wnt signaling during cardiac development and in adult tissue, we investigated the potential of Wnt10b in promoting growth and angiogenic potential of cardiac endothelial cells after injury.

EXPERIMENTAL METHODS

Cell culture

Primary cardiac endothelial cells were isolated using the immuno-magnetic sorting method by positive selection with the CD31 antibody. Mouse ventricles were excised and digested in DMEM with 10 mg/ml Collagenase type II, 2.4 U/ml Dispase II, 0.3 µg/ml DNAse IV, 2.5 mM $CaCl_2$ solution and non-myocyte cells were isolated through nylon filter. Leukocytes were removed by immuno-sorting against CD45 antibody by negative selection. Cardiac endothelial cells were isolated by immuno-sorting with the CD31 antibody using MS columns - MACS separator system by positive selection (Miltenyi Biotec Inc.).

Murine cardiac microvascular endothelial (MCEC-1) cells, generously provided by Dr. J. Mason (National Heart and Lung Institute, London, UK), were isolated from mice containing a gene encoding the thermo-labile SV40 T antigen and maintained in the presence of interferon-γ at 33°C (Lidington *et al.,* 2002). Six days prior to performing experiments, cells were re-plated and cultured in the absence of interferon-γ at 37°C (Ryzhov *et al.,* 2008).

Tube formation assay

Primary cardiac endothelial cells isolated from WT and TG ventricles were cultured for 5 days in EC medium at 37°C, then in DMEM with 10% FBS but no growth factors for 24 hours. Primary cardiac endothelial cells were then seeded on Growth Factor Reduced (GFR) Matrigel (BD Biosciences) at 40,000 cells per well on a 96-well plate. MCEC-1 cells at P0 at 37°C were treated with 300 ng/ml rmWnt10b and/or 10 ng/ml rmVEGF-165 (R&D Systems) for 24 hours in 10% FBS in DMEM without growth factors, then seeded on GFR Matrigel at 40,000 cells per well on a 96-well plate. Endothelial cell tubes were imaged using light microscope 6 hours after plating. Total number of branches was counted and averaged over three biological replicates per sample.

Flow cytometry

Flow cytometry was performed as described in the previous chapter.

Immunofluorescence

Immunofluorescence was performed as described in the previous chapter. To measure the vascular densities of injured and non-injured tissue, we calculated pixel density of fluorescence using the MetaMorph 7.6 software (Molecular Devices). 18 to 53 0.035 mm^2 frames were randomly selected and analyzed per mouse.

Gene expression analysis

Gene expression analysis was performed as previously described in Chapter II.

Statistical analysis

Unpaired two-tailed *t* test was used to compare differences between two unpaired groups. One-way ANOVA with Bonferroni's multiple comparisons test was used to compare multiple unpaired groups. * $P < 0.05$, ** $P < 0.01$, *** $P < 0.001$ were considered significant. Results are reported as mean ± SEM.

RESULTS

Wnt10b overexpression enhances neovascularization of injured tissue

Flow cytometry analysis showed ventricles of uninjured, adult WT and TG mouse hearts contained comparable numbers of endothelial cells (**Figure 8G**). Histological analysis also revealed no significant abnormalities in the coronary vasculature or the microvasculature of TG hearts (data not shown).

In contrast, we observed marked differences in the scar vasculature of injured WT and TG hearts. 3 weeks after cryoinjury, scar tissue of injured WT ventricles contained small and sparse micro-capillaries, as previously reported (van Amerongen *et al.,* 2008). The vascular density of the WT scar tissue was visibly lower than that of the adjacent uninjured tissue. On the other hand, the corresponding injured tissue in TG ventricles contained more vascular beds that were organized in dense vascular regions or as large-diameter blood vessels resembling coronary arteries (**Figure 15A**). Vascular density in the TG scar tissue, quantified by fluorescence intensity, was approximately 2-fold greater than that in the WT scar tissue (**Figure 15B**).

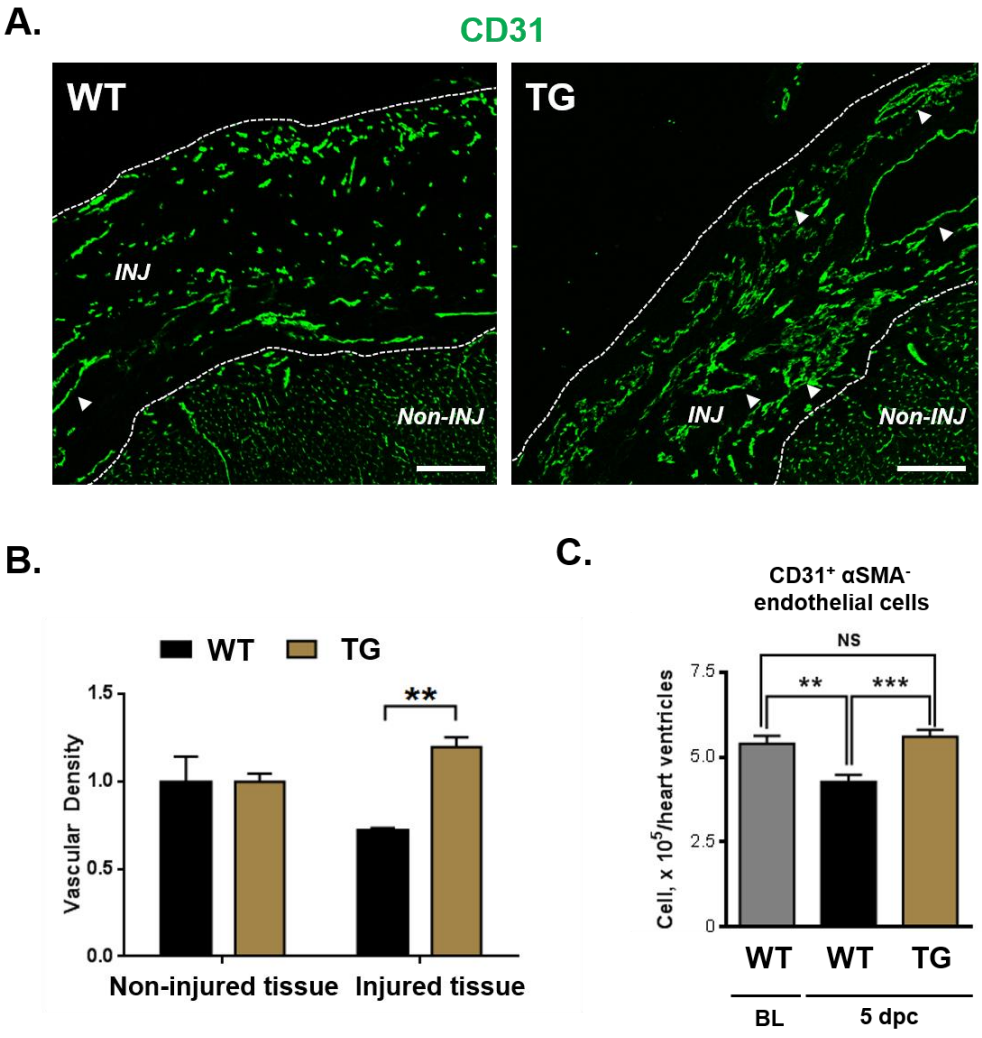

Figure 15. Increased vascular density in TG scar tissue. A. Immunofluorescence images of CD31 antibody staining (green) in the injury (INJ) and peri-injury (Non-INJ) zones of WT and TG mouse cardiac tissue sections 3 weeks after cryoinjury (left panels). Injury zones between epicardium and non-injured tissue are delineated with dashed lines. The injury zone in WT mice contains mostly micro-capillaries, whereas in TG mice it contains numerous large blood vessels (arrowheads). Scale bars, 200 µm. **B.** Quantification of vascular density in non-injury and injury cardiac sections (right) shows scar tissue in TG mice is approximately 2-fold more densely vascularized than WT controls (right). N=3 mice per group. **C.** Number of $CD31^{+}\alpha SMA^{-}$ endothelial cells among non-cardiomyocyte $CD45^{-}$ primary cells isolated from WT and TG ventricles, determined by flow cytometry. Cell population numbers from WT ventricles at baseline shown as reference. TG hearts contain higher endothelial cell, equal fibroblast and lower myofibroblast numbers compared to WT 5 days after cryoinjury. BL=baseline, dpc=days post cryoinjury. N=6 mice per group. ** $P < 0.01$; *** $P < 0.001$; NS, not significant, unpaired *t* test. All data are means ± SEM.

Consistent with the histology data, flow cytometry analysis of dissociated total ventricular tissues showed TG hearts contained approximately 30% more endothelial cells ($CD31^{+}\alpha SMA^{-}$) than WT hearts, indicating that Wnt10b overexpression led to greater number of endothelial cells in the injured tissue (**Figure 15C**).

Wnt10b activates canonical Wnt signaling in cardiac endothelial cells

To better understand the effects of Wnt10b gain-of-function on scar neovascularization, we tested whether Wnt10b activates the canonical Wnt signaling in cardiac endothelial cells. Immunofluorescence of transverse tissue sections of WT and TG ventricles with canonical Wnt signaling molecule β-catenin showed accumulation of the protein in endothelial cells of TG hearts, but not in WT hearts (**Figure 16A**).

We also isolated cardiac endothelial cells from WT and TG ventricles by immuno-magnetic sorting with endothelial cell-specific CD31 antibody, and transfected the cells with the canonical Wnt activity luciferase reporter plasmid SuperTOPFlash. Luciferase assays revealed two-fold induction in canonical Wnt activity in endothelial cells isolated from the TG ventricles when compared to those from the WT ventricles (**Figure 16B**).

Our data suggest that the endothelial cells of TG ventricles are canonical Wnt activated by the Wnt10b protein secreted from the cardiomyocytes. To determine whether Wnt10b directly activates the canonical Wnt signaling in the cells, we treated MCEC-1 cells with recombinant Wnt10b protein for 24 hours and performed SuperTOPFlash luciferase reporter assay. We detected that exogenous treatment of Wnt10b induced canonical Wnt activity in the MCEC-1 cells in a dose-dependent manner (**Figure 16C**).

These results together indicate Wnt10b overexpression in cardiomyocytes of the TG hearts directly activated canonical Wnt signaling in the endothelial cells.

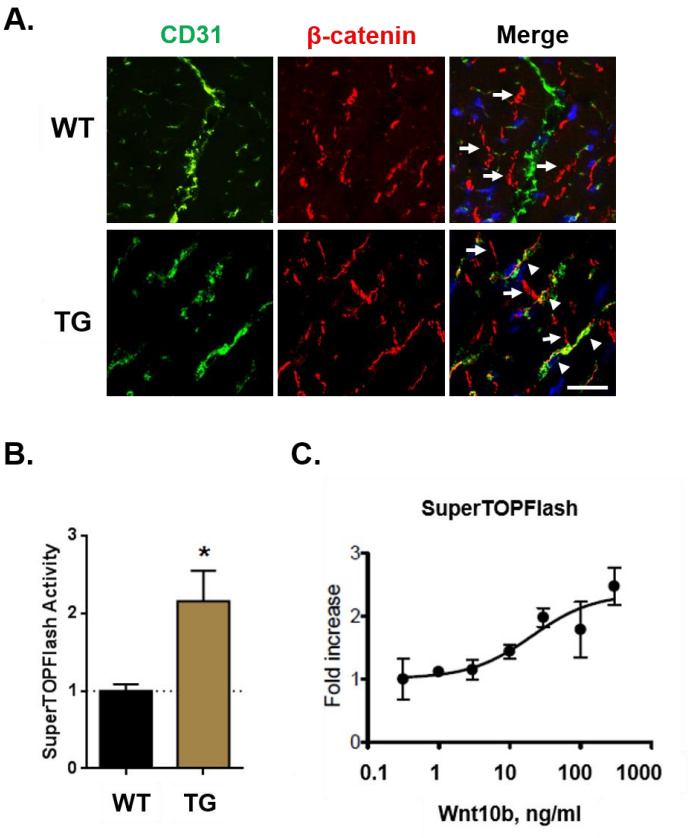

Figure 16. Wnt10b directly activates canonical Wnt signaling in endothelial cells. A. Immunofluorescence images of CD31 (green), β-catenin (red), and DAPI staining (blue) in cardiac tissue sections. β-catenin is present in the intercalated discs of WT and TG cardiomyocytes (arrows), but shows additional staining in endothelial cells (arrowheads) of TG mice. Scale bar, 20 μm. **B.** Luciferase reporter assay using the canonical Wnt reporter SuperTOPFlash in primary cardiac endothelial cells isolated from WT and TG ventricles shows TG endothelial cells have activated canonical Wnt signaling. Results obtained in independent cell isolation experiments from 3 mice per group. **C.** SuperTOPFlash luciferase reporter assays in MCEC-1 cells treated with varying concentration of Wnt10b. Increasing concentrations of Wnt10b directly induced canonical Wnt signaling in MCEC-1 cells. N=3/group.

Wnt10b promotes proliferation and tube formation of cardiac endothelial cells

To test whether canonical Wnt activation promotes the proliferative capacity of cardiac endothelial cells, we purified and cultured freshly isolated endothelial cells

(CD31^{+}CD45^{-}) from WT and TG ventricles using immuno-magnetic sorting technique. By day 5 of culture, we observed the endothelial cells from TG ventricles possessed higher growth potential than those from WT ventricles (**Figure 17A-C**). In addition, the endothelial cells from TG ventricles displayed greater potential to change their morphology to tube-like structures when seeded on growth factor reduced (GFR) Matrigel (**Figure 17D**). *In vitro* tube formation assay reflects the endothelial cells' potential to undergo anastomosis as tip cells during the process of angiogenesis.

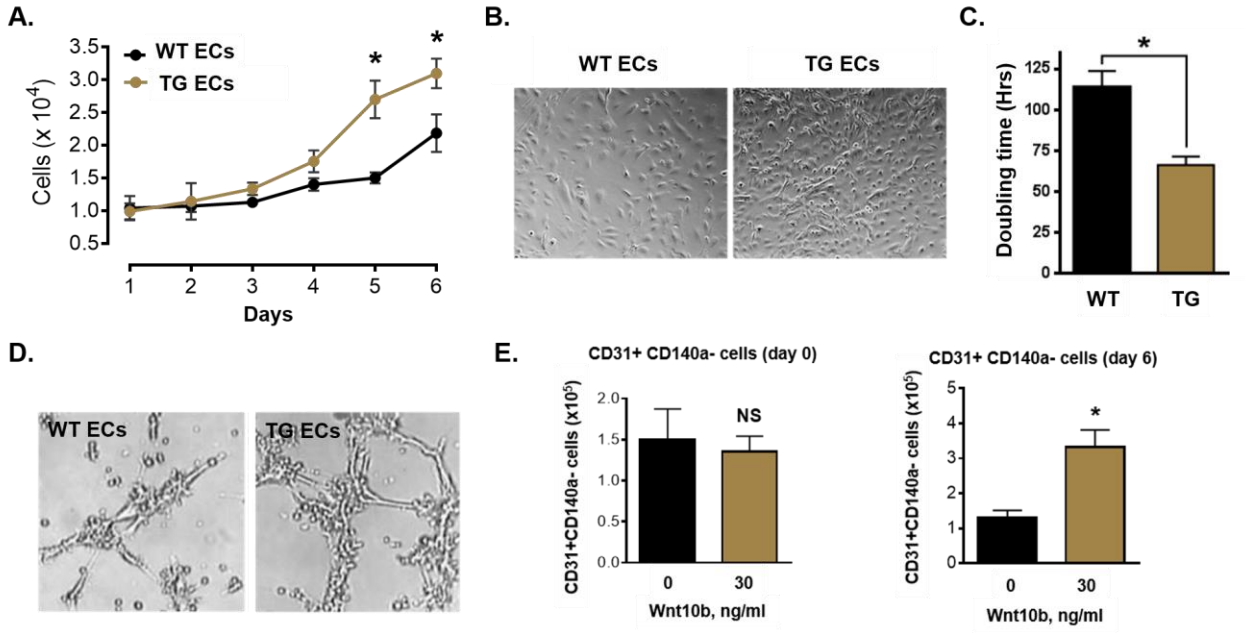

Figure 17. Wnt10b stimulates proliferation and branching morphogenesis of endothelial cells. A. Primary cardiac endothelial cells were isolated from WT and TG ventricles, seeded, grown in culture for 6 days and counted. Endothelial cells isolated from TG ventricles show higher growth than WT. Results obtained in independent cell isolation experiments from 3 mice per group. **B.** Images of isolated endothelial cells from WT and TG hearts at day 5 in culture. Endothelial cell cultures from TG mice are denser than those from WT controls. **C.** Doubling time of cardiac primary endothelial cells isolated from TG mice is 2-fold shorter than the corresponding WT controls. N=3 mice per group. **D.** Tube formation assay on GFR Matrigel shows cardiac endothelial cells from TG ventricles form more tubes than WT controls. **E.** primary cardiac endothelial cells isolated from 4 week-old C57Bl/6 mouse ventricles, grown on culture for 6 days in PBS or 30 ng/ml Wnt10b. Number of CD31+CD140a- endothelial cells is counted by flow cytometry (right). Unpaired two-tailed t test. * P<0.05, NS, not significant.

To test whether the high growth potential of endothelial cells isolated from TG ventricles was a direct effect of Wnt10b on endothelial cells, we isolated cardiac microvascular endothelial cells from WT mice and exposed them to increasing concentrations of recombinant Wnt10b protein, which induced canonical Wnt activity (**Figure 16C**). Wnt10b protein directly promoted endothelial cell proliferation in culture (**Figure 17E**), suggesting canonical Wnt activity induction and stimulation of endothelial cell proliferation was a direct effect of Wnt10b.

Furthermore, we determined that the increased proliferative potential of endothelial cells by Wnt10b is dependent on canonical Wnt activation. Treatment of endothelial cells from TG ventricles with a canonical Wnt inhibitor IWR-1-endo (Chen *et al.,* 2009) abolished the proliferation of cells, while an inhibitor for JNK, a non-canonical Wnt pathway, had no effect (**Figure 18A-B**).

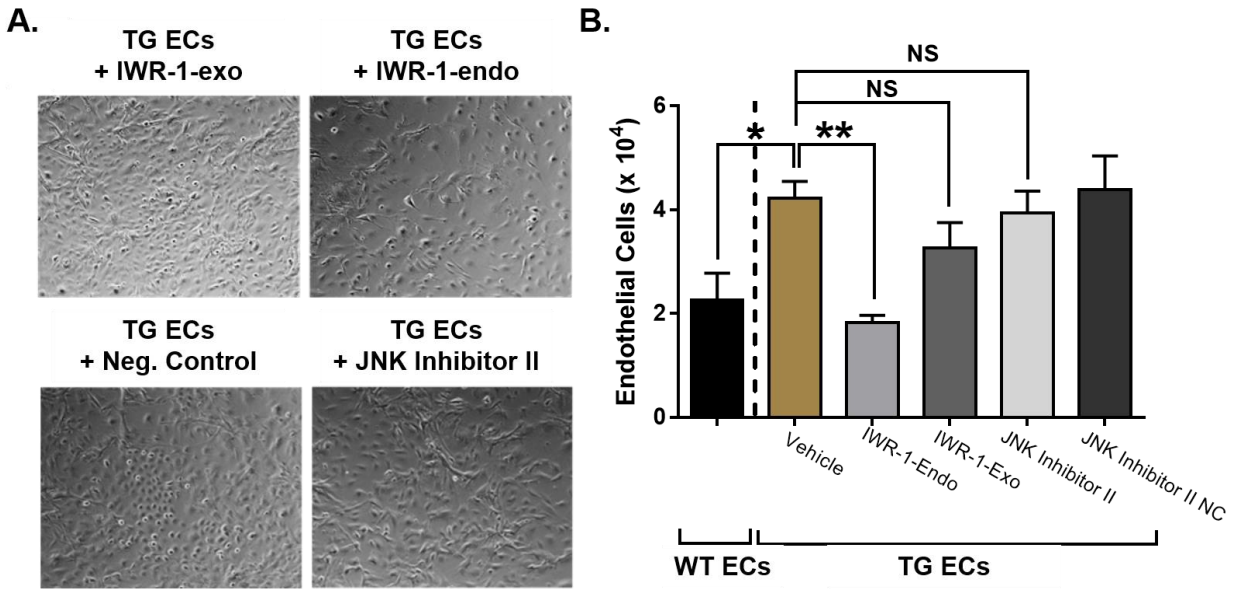

Figure 18. Stimulation of endothelial cell proliferation by Wnt10b is canonical Wnt-dependent. A. Cardiac endothelial cells from TG ventricles were cultured with canonical Wnt inhibitor (IWR-1-endo, 1 μM, top right) and its negative control counterpart (IWR-1-exo, 1 μM, top left) as well as with JNK inhibitor II (1 μM, bottom right) and its negative control counterpart (1 μM, bottom left) during the entire duration of culture. Canonical Wnt inhibition blocks endothelial cell growth, but JNK inhibition has no effect. **B.** Quantification of endothelial cells for each group counted at day 5 of culture. Cells isolated from WT ventricles served as baseline control. Results obtained in independent cell isolation experiments from 3 mice per group. * $P < 0.05$; ** $P < 0.01$; NS, not significant, unpaired *t* test. All data are means ± SEM.

Wnt10b induces Vegfr-2 expression to enhance angiogenic potential of endothelial cells

To understand the molecular mechanisms by which Wnt10b promotes proliferation and branching morphogenesis of endothelial cells, we performed gene expression analysis of various angiogenesis-related signaling pathways in MCEC-1 cells treated with recombinant Wnt10b protein.

RNA expression analysis showed Wnt10b induced expression of Axin2, a canonical Wnt-responsive gene (**Figure 19A**). We found Wnt10b to induce Vegfr-2 expression, but did not affect expression levels of the Vegf-a ligand or the antagonizing receptor Vegfr-1 (**Figure 19A**). This indicates Wnt10b can enhance the response of endothelial cells to Vegf-a by increasing levels of its receptor. The Vegf-a/Vegfr-2 ligand/receptor axis is known to promote endothelial cell proliferation and angiogenesis (de Vries *et al.,* 1002). We thus analyzed the effects of Vegf-a in vascular tube formation in presence or absence of Wnt10b. While Wnt10b or Vegf-a alone was sufficient to stimulate endothelial tube formation, Wnt10b and Vegf-a together were synergistic in further enhancing branching morphogenesis of the endothelial cells (**Figure 19B**). Taken together, our results indicate Wnt10b directly stimulates endothelial cell growth by

activation of canonical Wnt signaling and amplifies the pro-angiogenic effects of Vegf-a by inducing expression of its receptor Vegfr-2.

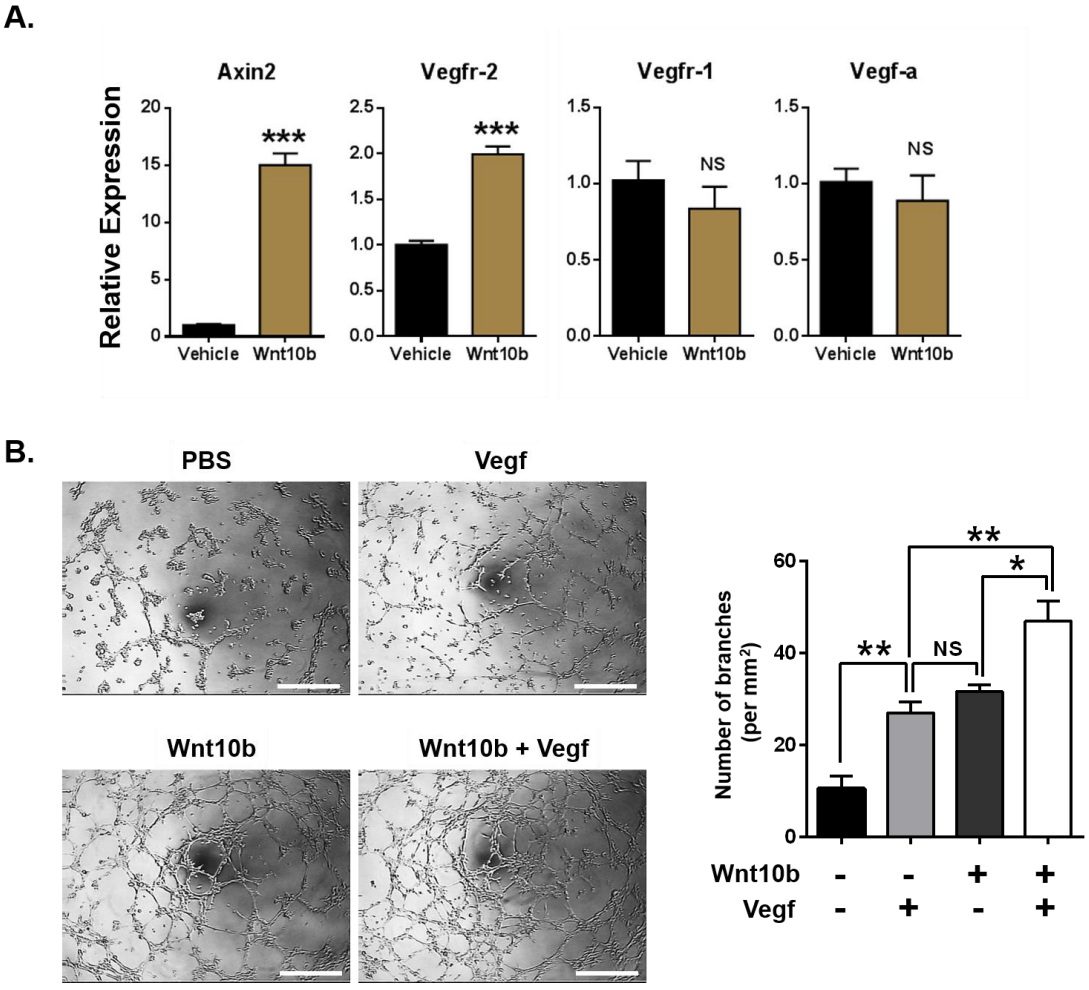

Figure 19. Wnt10b amplifies angiogenic effects of Vegf-a/Vegfr-2 signaling axis. A. qPCR analysis shows that Wnt10b induces *Axin2* and *Vegfr-2* in microvascular cardiac endothelial cells (MCEC-1), but it has no effect on *Vegfr-1* and *Vegf-a* expression. **B.** Wnt10b (300 ng/ml) promotes branching morphogenesis and synergizes with VEGF165 (10 ng/ml) in MCEC-1 cells on GFR Matrigel (left panels). Total number of branches per 1 mm^2 field (right). Results obtained in independent cell isolation experiments from 3 mice per group. * $P < 0.05$; ** $P < 0.01$; *** $P < 0.001$; NS, not significant, unpaired *t* test in panel A and one-way ANOVA with Bonferroni's multiple comparisons test in panel B. All data are means ± SEM.

DISCUSSION

Our data show that Wnt10b gain-of-function stimulates new blood vessel growth in two ways. First, Wnt10b activates canonical Wnt signaling in endothelial cells (**Figure 16**), a process known to promote angiogenesis after injury (Blankestejin *et al.,* 2000). Second, by inducing Vegfr-2 expression in endothelial cells, Wnt10b synergizes with Vegf-a to further enhance the proliferative and angiogenic potential of endothelial cells (**Figure 19**). This is consistent with previous results from development and in tumor cells, which identified a regulatory role of Wnt activation on VEGF signaling (Zhang *et al.,* 2001; Dejana, 2010).

We also found that these effects of Wnt10b on endothelial cells are direct. While we detected all ten Frizzled receptor genes to be expressed in the cardiac endothelial cells (data not shown), we have not yet determined to which receptor Wnt10b would bind in inducing such effects. Identifying the members of the Frizzled and other Wnt co-receptor family that interact with Wnt10b would be useful in screening for small molecule compounds that would mimic the ligand actions of Wnt10b.

We have not checked whether the pro-angiogenic and pro-growth effects of Wnt10b are universal to all types of endothelial cells. To test this, we will perform identical experiments using other types of endothelial cells, such as the aortic endothelial cells or the umbilical cord endothelial cells. If the other types of endothelial cells do not respond to Wnt10b as did the cardiac endothelial cells, this raises the possibility that different types of endothelial cells may express a different set of Fzd membrane receptors. We also know that endothelial cells are a heterogeneous population of cells. For example in the adult heart, we have identified a niche of mature endothelial cells that possess the potential to

differentiate into cardiomyocytes (Fioret *et al.,* 2014). It would be of interest then to determine whether only a specialized subset of cardiac endothelial cells respond to Wnt10b to possess the augmented angiogenic ability in the TG hearts after injury, or whether all endothelial cells are able to respond to Wnt10b in identical fashion.

In addition, we will perform the same set of endothelial cell experiments with drugs or compounds that activate canonical Wnt signaling. As we have determined that Wnt10b direct activates canonical Wnt signaling and induces Vegfr-2 expression in endothelial cells to promote growth and angiogenesis, we will test whether these phenotypes can be replicated using an independent Wnt activating molecule, such as BIO, a GSK-3β inhibitor that in turn activates canonical Wnt signaling (Sato *et al.,* 2004).

Regeneration of the microvasculature in the scar tissue observed in TG ventricles is significant (**Figure 15**). As previously mentioned, current interventional therapies that aim to restore blood flow fail to be effective in a substantial number of patients (Lavine and Ornitz, 2009). Development of noninvasive strategy to regenerate both the collateral vessels and the microvasculature is critical.

CHAPTER V

WNT10B ENHANCES BLOOD VESSEL STABILIZATION

INTRODUCTION

Wnt10b overexpression promotes the proliferative and angiogenic potential of cardiac endothelial cells by canonical Wnt activation and Vegfr-2 induction, leading to greater vascular density in the scar tissue. However, excessive angiogenic vessel formation without vessel stabilization is also not favorable in wound healing. Hyperpermeable neo-vessels lacking a mural cell-layered coat will extend the inflammatory response in the infarcted tissue, leading to prolonged extravasation of red blood cells and monocyte/macrophages (Frangogiannis, 2012). The mural cell coating of newly formed vessels is thus important in promoting resolution of inflammation, cell survival, and stabilization of the scar, and should be accompanied with neovascularization to form a functional scar tissue microenvironment.

Our results show that the scar tissue in TG mice contained large coronary vessels. Therefore we analyzed the phenotype of blood vessels formed after injury in TG scar tissue by investigating the molecular and cellular pathways that regulate vessel stability.

EXPERIMENTAL METHODS

Cell culture

Vascular aortic smooth muscle cells (MOVAS, ATCC# CRL-2797) isolated from C57Bl/6 mice were obtained from ATCC. Cells are cultured in DMEM supplemented with

10% FBS and 0.2 mg/ml G-418 (Afroze *et al.,* 2003). MCEC-1 cells were cultured as described in the previous chapter.

Endothelial cell-vascular smooth muscle cell co-culture assay

For endothelial cell-vascular smooth muscle cell co-culture experiment, MCEC-1 cells were incubated in empty DMEM (with no FBS) for 24 hours in absence or presence of 300 ng/ml Wnt10b. MCEC-1 cells were then labeled with 5 µM lipophilic DiD fluorescence dye (Life Technologies) for 1 hour at 37°C and 30,000 cells were plated per well (96-well plate) on GFR Matrigel for 18 hours in DMEM (with no FBS) in absence or present of 300 ng/ml Wnt10b. MOVAS cells were labeled with 5 µM DiO dye (Life Technologies) and plated on top of the MCEC-1 cells at 7,500 cells per well, as 4:1 EC : vSMC ratio, in presence or absence of 1 µM Tie2 Kinase Inhibitor (Calbiochem, 4-(6-Methoxy-2-naphthyl)-2-(4-methylsulfinylphenyl)-5-(4-pyridyl)-1H-imidazole). Cells were co-cultured for 6 hours and imaged using a fluorescence microscope.

Luciferase reporter assay

MCEC-1 and MOVAS cells were seeded in 12-well plates at concentration of 80,000 cells/well and cultured in complete medium for 12 hours. Cells were transiently transfected with 936 ng/well of pNF-κB-Luc (Stratagene) and 7.9 ng/well of pRL-SV40 for 24 hours using Fugene HD (Promega) following the manufacturer's instructions. Cells were treated with 300 ng/ml rmWnt10b, 300 ng/ml rhWnt11, 20 ng/ml rmTNF-α (R&D Systems), and/or 50 µg/ml NF-κB inhibitor SN-50 (Calbiochem) for 6 hours, then luciferase activity was measured as above. Firefly luciferase activity was normalized to

Renilla luciferase activity and reported as fold induction over basal levels.

Immunofluorescence

Immunofluorescence was performed as described in the previous chapter. $CD31^+/\alpha SMA^+$ vessels with diameter of 10 μm or greater were counted in the injury tissue. Four to six 0.4 mm^2 frames were randomly selected and analyzed per mouse (N=4 mice per group).

Flow cytometry

Flow cytometry was performed as described in the previous chapter.

Gene expression analysis

Gene expression analysis was performed as described in the previous chapter.

Statistical analysis

Statistical analysis was performed as previously described in Chapter III.

RESULTS

Wnt10b promotes formation of mature coronary-like blood vessels

In addition to greater density, the vasculature within injured tissue of TG hearts consisted of large diameter blood vessels, in contrast to micro-capillaries present in WT hearts (**Figure 15A**). Staining for endothelial cells and vSMCs with CD31 and αSMA antibodies respectively confirmed that the scar tissue in TG ventricles contained a higher

number of blood vessels that are surrounded by a prominent smooth muscle cell layer (**Figure 20**). Such vessels were large in diameter and often resembled coronary arteries.

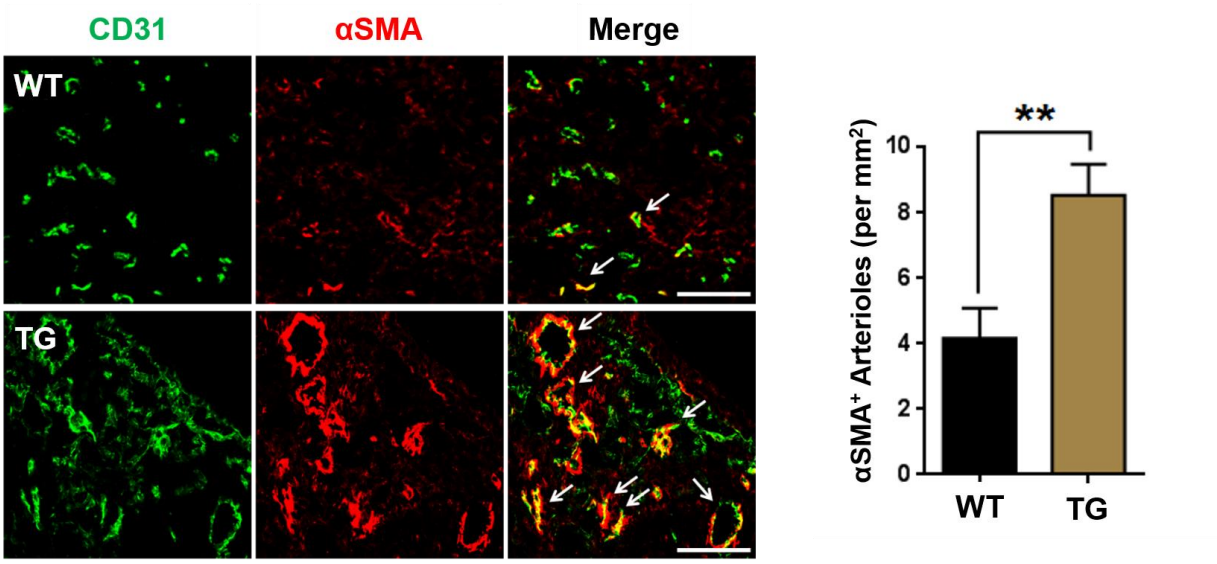

Figure 20. Wnt10b overexpression promotes coronary-like vessel formation. Immunofluorescence images of CD31 (green) and αSMA (red) antibody staining in the scar areas of WT and TG mouse hearts 3 weeks post cryoinjury show Wnt10b promotes formation of stable blood vessels with recruitment of αSMA$^+$ smooth muscle cells (left). Scale bar, 100 μm. Quantification of the number of αSMA$^+$ vessels shows that scar areas in TG hearts have twice more arterioles than WT controls. N=3 mice per group.

Wnt10b induces Ang-1 expression in vascular smooth muscle cells

To identify the molecular basis of the observed vascular phenotype, we measured expression of Angiopoietin-1 (Ang-1) and its receptor Tie2, which regulate vSMC recruitment and blood vessel stability (Thurston *et al.,* 2000; Fuxe *et al.,* 2011). Analysis of ventricular tissue RNA of uninjured WT and TG mouse hearts showed comparable baseline expression levels of Ang-1, Ang-2, and Tie2. However, we detected a strong induction of Ang-1 expression 1 week after injury in WT ventricular tissue, which was further increased by two-fold in TG ventricles (**Figure 21A**). In contrast, there were no

major differences in the expression of Tie2 and Ang-2, the antagonizing ligand to Ang-1, between WT and TG ventricles after injury (**Figure 21A**).

Histological analysis of transverse ventricular sections one week after injury also revealed higher Ang-1 levels in αSMA$^+$ cells that surround large diameter blood vessels within TG scar tissue, compared to those of WT counterparts (**Figure 21B**). We detected the expression of Ang-1 to be specific to vascular smooth muscle cell layer of the vessels (**Figure 21B**).

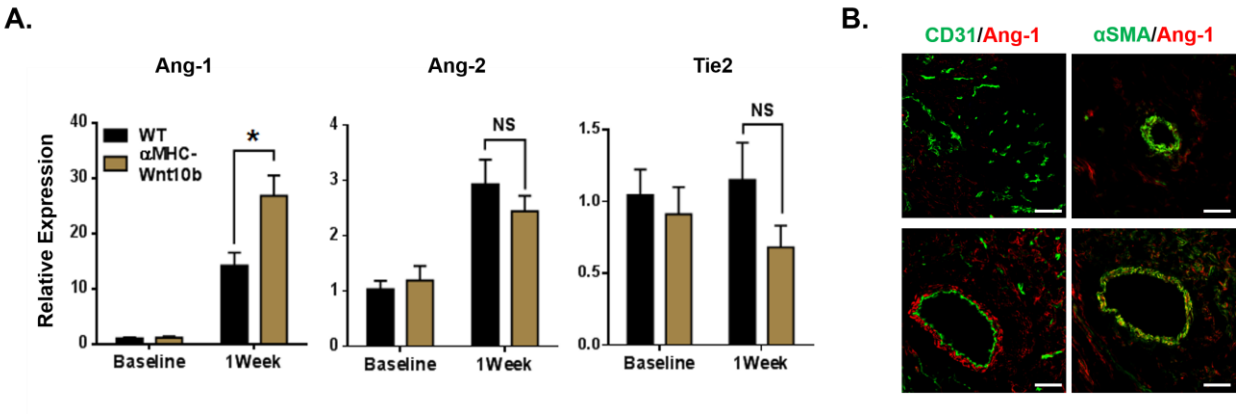

Figure 21. Wnt10b induces Ang-1 expression in vSMCs. A. qPCR analysis shows *Ang-1* expression 1 week after cryoinjury is enhanced by 2-fold in TG ventricles, as compared to WT controls. In contrast, Ang-2 induction levels are comparable between WT and TG, whereas Tie2 receptor expression remains unchanged after injury in both groups. N=3-4 mice per group. **B.** Immunofluorescence images of CD31 (green, left), αSMA (green, right), and Ang-1 (red) antibody staining in the injury areas of WT and TG mouse hearts one week after cryoinjury shows higher levels of Ang-1 expression in perivascular cells of TG cardiac tissue sections as compared to WT controls.

Induction of Ang-1 promotes endothelial cell recruitment to vascular smooth muscle cells

To test whether Wnt10b-induced arteriole formation is due to activation of the Ang-1/Tie2 signaling axis, we co-cultured endothelial cells and vSMCs with or without Wnt10b and a Tie2 kinase-specific inhibitor (Semones *et al.,* 2007). We found Wnt10b stimulated

the vSMCs to migrate toward the tube-like endothelial cells on GFR Matrigel after 6 hours of co-culture (**Figure 22**). Migrated vSMCs changed their morphology from a round shape to spindle-like shape when associating with the endothelial cells. This effect of Wnt10b was abolished when the Tie2 kinase inhibitor was added during the co-culture. This indicated that Wnt10b promotes vSMC recruitment to endothelial cells and consequently blood vessel stability in Ang-1/Tie2-dependent manner.

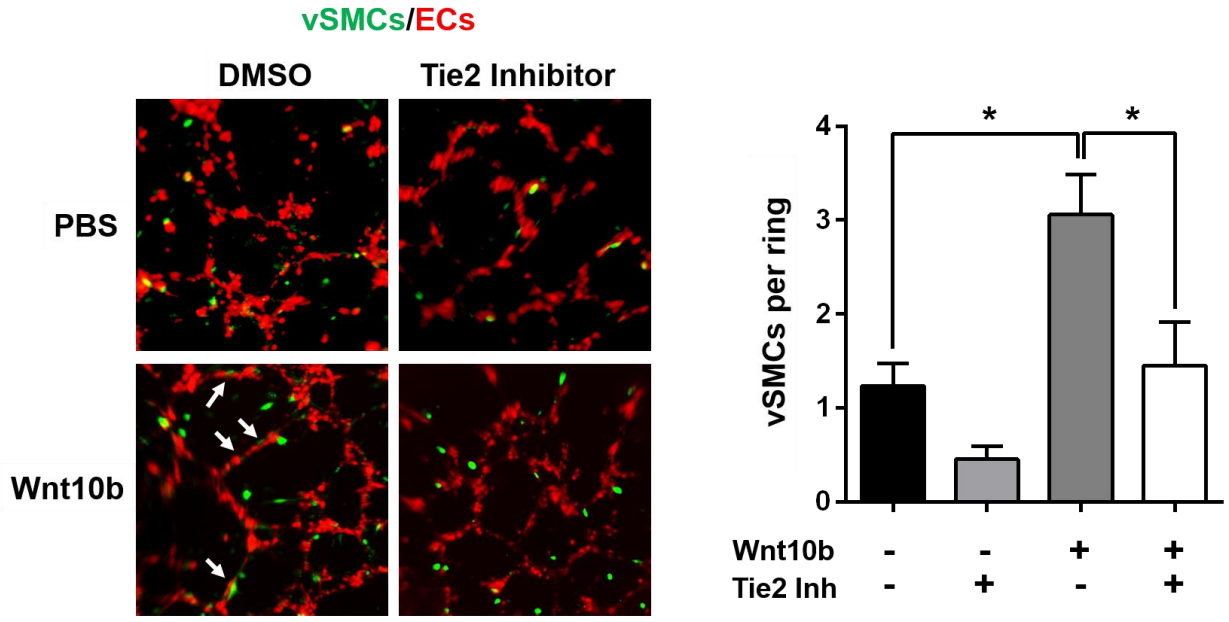

Figure 22. Enhanced vSMC recruitment by Wnt10b is mediated through Ang-1 induction. Co-culture assay of cardiac endothelial cells (ECs) stained with DiD (red) and vascular smooth muscle cells (vSMCs) stained with DiO (green) on GFR Matrigel to monitor migration and ensheathment of endothelial tubes by vSMCs in the absence of presence of Wnt10b (300 ng/ml) and/or Tie2 Kinase Inhibitor (1 μM). Number of vSMCs per ring counts are shown on the right. N=3-5 wells counted per group. * $P < 0.05$; ** $P < 0.01$; NS, not significant, unpaired *t* test. All data are means ± SEM.

Wnt10b induces vessel-stabilizing factors through activation of NF-κB signaling

Previous studies have identified NF-κB and Notch signaling as critical pathways for arteriogenesis, collateral vessel formation, and vascular network formation during development and in the adult tissue through coordinated stimulation of angiogenesis and vSMC recruitment (Tirziu *et al.,* 2012; Sweet *et al.,* 2013; Cristofaro *et al.,* 2013). To test whether Wnt10b acts upstream of NF-κB signaling pathway, we transfected endothelial cells and vSMCs with NF-κB luciferase reporter construct, treated the cells with Wnt10b for 6 hours, and measured the luciferase activity. The results showed Wnt10b robustly activated the pathway in both cell types, while the treatment with non-canonical Wnt ligand Wnt11 had only a moderate effect (**Figure 23A-B**). Wnt11 is another Wnt ligand that is strongly induced in the heart after injury (Aisagbonhi *et al.,* 2011).

No synergistic interaction was observed between Wnt10b and TNF-α on activation of NF-κB signaling in endothelial cells, even at low TNF-α concentrations (data not shown). Wnt10b treatment also did not alter expression levels of Notch signaling genes, such as Hes1, Hey1, Hey2, and Notch1, in endothelial cells (data not shown). Activation of Notch genes downstream of NF-κB signaling had previously been implicated in arteriogenesis (Tirziu *et al.,* 2012). This suggests that NF-κB-dependent formation of arterioles by Wnt10b is mediated through the Ang-1/Tie2 signaling axis, but not Notch.

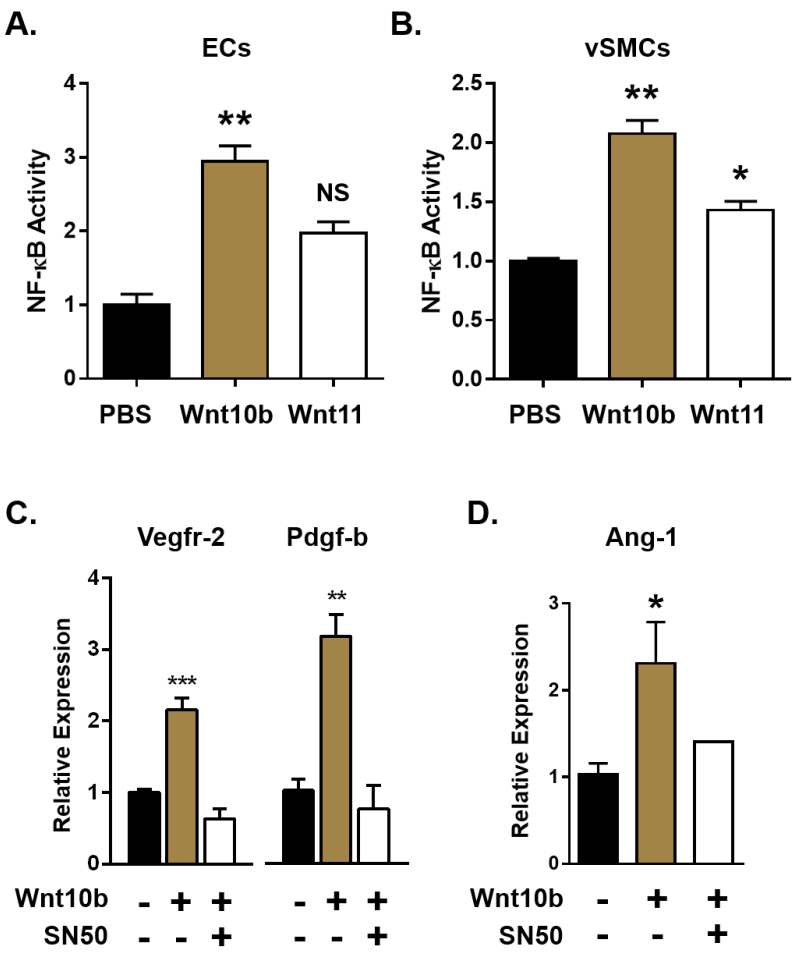

Figure 23. Wnt10b activates NF-κB signaling in vascular cells. A. Luciferase activity assay in pNF-κB-luc-plasmid-transfected endothelial cells MCEC-1 and **B.** smooth muscle cells MOVAS treated with vehicle (PBS), Wnt10b (300 ng/ml) or Wnt11 (300 ng/ml). Wnt10b activates NF-κB signaling in both cell types. **C.** Wnt10b induction of *Vegfr-2* and *Pdgf-b* in MCEC-1 and **D.** *Ang-1* in MOVAS is blocked by the NF-κB inhibitor SN-50 (50 µg/ml).

To assess whether the effect of Wnt10b on the induction of genes that regulate endothelial cell growth and vSMC was due to NF-κB signaling activation, we treated endothelial cells and vSMCs with Wnt10b in the presence or absence of NF-κB signaling inhibitor SN-50 (Lin *et al.,* 1995). The results show that Wnt10b-mediated induction of Vegfr-2 in endothelial cells and Ang-1 in vSMCs were abolished by SN-50 (**Figure 23C-**

D). Furthermore, Wnt10b induced Pdgf-b expression in NF-κB-dependent manner (**Figure 23C**). Pdgf-b is known to act on Pdgfr-β, expressed in vSMCs, to promote recruitment to newly formed blood vessels (Andrae *et al.,* 2008).

Consequently, our data indicate Wnt10b coordinates angiogenesis and blood vessel stabilization during the cardiac tissue repair process to form mature blood vessels in the scar tissue. In endothelial cells, Wnt10b activates canonical Wnt signaling to promote proliferation and NF-κB signaling to induce Vegfr-2 and Pdgf-b, growth factors that promote angiogenesis and vessel stabilization respectively. In vSMCs, Wnt10b activates NF-κB signaling to increase Ang-1 expression, which acts on Tie2 receptor of endothelial cells to stimulate vSMC recruitment (**Figure 24**).

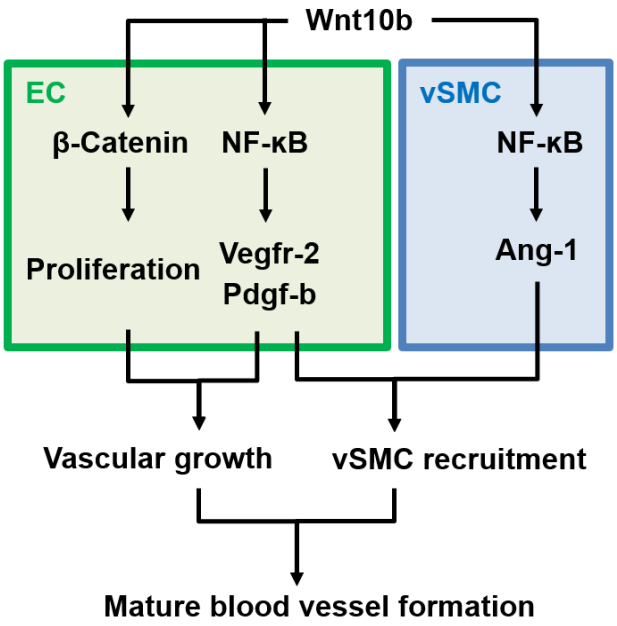

Figure 24. Model of Wnt10b gain-of-function effects on arteriole formation in the injured heart. Wnt10b coordinates blood vessel growth and stability by a) activation of canonical Wnt/β-catenin signaling to stimulate endothelial cell proliferation, and b) NF-κB-dependent induction of Vegfr-2 and Pdgf-b in endothelial cells (EC) and Ang-1 in vascular smooth muscle cells (vSMC) to further promote vascular growth, as well as vSMC recruitment.

Inflammatory cell infiltration in scar tissue is attenuated

Previous studies have shown that leaky blood vessels hindered tissue recovery because they allow infiltration of immune cells resulting in resolved inflammation, which in turn can further aggravate ventricular remodeling (Frangogiannis, 2014). This raised the possibility that Wnt10b-induced blood vessel stability attenuates inflammation. Consistent with this hypothesis, flow cytometry analysis 5 days after cryoinjury revealed lower levels of total immune cells ($CD45^+$) and neutrophils ($CD11b^+Ly6G^+$) within ventricular tissue of TG mice compared with WT counterparts (**Figure 25A-B**).

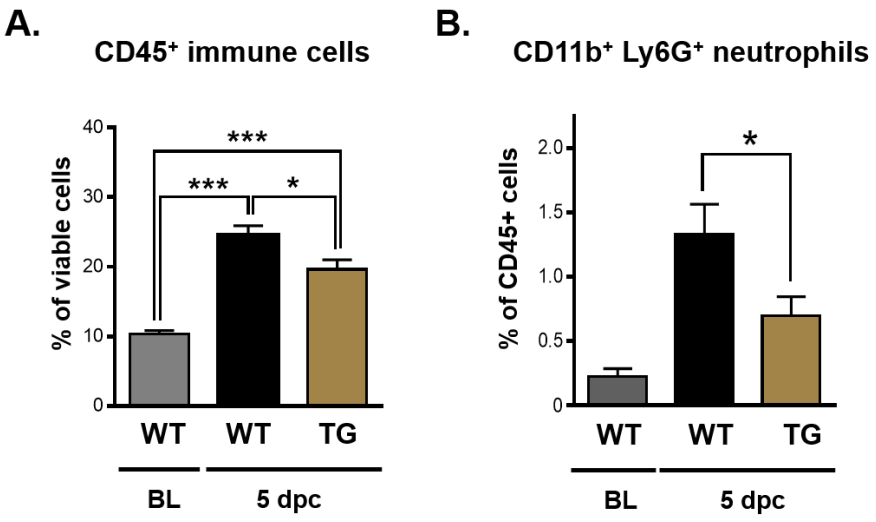

Figure 25. Less inflammatory cells infiltrate in TG scar tissue. Flow cytometry based quantification of **A.** $CD45^+$ immune cells among viable non-cardiomyocytes and **B.** $CD11b^+Ly6G^+$ neutrophils (F) among $CD45^+$ cells isolated from WT and TG ventricles 5 days post cryoinjury (dpc) shows immune cell infiltration is attenuated in TG hearts. Cell populations from WT ventricles at baseline used as reference. N=4-6 mice per group. * $P < 0.05$; ** $P < 0.01$; *** $P < 0.001$; NS, not significant, unpaired *t* test. All data are means ± SEM.

DISCUSSION

Formation of large diameter blood vessels with robust support structures involves endothelial cell growth, branching, and recruitment of smooth muscle cells (Augustin *et al.,* 2009). In support of our data on the role of Wnt10b in adult cardiac repair, it was recently shown that endothelial transcription factor ERG promotes vascular stability and growth through canonical Wnt activation during development (Birdsey *et al.,* 2015). Previous studies have also identified the NF-κB pathway, Notch signaling, RAF-1/ERK, and the adaptor protein Shc as intracellular components that coordinate arteriogenesis, collateral vessel formation, and vascular network size during development or in the adult tissue (36-38). While expression of Notch signaling components was unaltered in TG mouse hearts, we found Wnt10b activated NF-κB signaling in both cardiac endothelial and smooth muscle cells (**Figure 23A-B**). We believe coordinated activation of NF-κB signaling by Wnt10b in both cell types mediate the vessel growth and stability.

The molecular basis of the Wnt10b/NF-κB crosstalk is currently poorly understood. One study identified the NF-κB-binding site conserved in multiple mammalian WNT10B orthologs, suggesting that Wnt10b may directly activate NF-κB (Katoh and Katoh, 2007). It is also likely that stabilized β-catenin or GSK-3β inhibition in canonical Wnt activated state are able to interact with the intracellular NF-κB components to trigger NF-κB activation. Also, it has been shown by others that Wnt10b activates NF-κB signaling in non-cardiac cell types, such as in osteosarcoma cells (Mödder *et al.,* 2011). This study was revealing because it suggested the unique role of Wnt10b in activation of NF-κB signaling, as another classical canonical Wnt ligand Wnt3a did not yield the same effects. We have shown that the non-canonical Wnt ligand Wnt11 did not induce NF-κB signaling

in cardiac endothelial cells and vSMCs as effectively as Wnt10b did (**Figure 23A-B**). It will be important to test the effects of other canonical Wnt ligands, such as Wnt3a, on NF-κB activation in cardiac endothelial cells and vSMCs to determine whether the observed effects in TG mice are unique to Wnt10b.

Formation of stable vessels in tissue repair is critical, as previous studies have shown formation of excessively angiogenic vessels with high permeability can in fact be detrimental to tissue repair. Administration of VEGF alone generated leaky vessels and hemorrhages, while simultaneous supply of VEGF and Ang-1 in swine models led to superior functional neovascularization of ischemic tissues (Su *et al.,* 2007; Tao *et al.,* 2011; Taimeh *et al.,* 2013). Here we found that Wnt10b induces both growth factors, in endothelial cells and smooth muscle cells respectively, to increase the vascular density but also to promote vessel stabilization (**Figure 24**). We did not detect up-regulation of Tie2 expression in whole TG ventricular RNA samples after injury (**Figure 21A**), suggesting that Wnt10b regulates the Ang-1/Tie2 signaling axis by inducing the expression of the ligand and not the receptor. By flow cytometry, we counted a greater number of endothelial cells in TG ventricles after injury than in WT ventricles (**Figure 15C**), but the difference in the number of endothelial cells is likely large enough to detect significant changes in Tie2 expression.

Stable vessel formation by Wnt10b overexpression also led to attenuated infiltration of inflammatory cells (**Figure 25**). This is consistent with past studies that describe the importance of PDGF-BB/PDGFR-β signaling axis that promotes mural coating formation to reduce vascular permeability (Ren *et al.,* 2002; Zymek *et al.,* 2006).

CHAPTER VI

SUMMARY AND CONCLUSIONS

Perspective

Coronary heart disease such as MI is the leading cause of death in the United States. The adult heart suffers from irreversible loss of cardiac muscle cells and from excessive formation of fibrotic scar. Despite the considerable progress to restore circulation to infarcted tissue using thrombolytics and percutaneous interventions, we currently have no pharmaceutical agents to modulate endogenous cardiac repair processes with the goal of preserving left ventricular function and preventing HF. In particular, it has been a great challenge in the field to simultaneously restore both stabilized mature coronary vessels and the microvasculature in ischemic patient hearts (Lavine and Ornitz, 2009).

Understanding the molecular signaling pathways that govern the cellular process of tissue repair therefore remains a priority. One of the major developmental signaling pathways found to regulate the cellular events of cardiac repair is Wnt signaling, but the previous studies in rodent models have shown mixed results on whether activation of the signaling is beneficial or detrimental for heart function after injury. The vast majority of the studies have reported the effects of genetic gain- or loss-of-function models of intracellular Wnt targets such as Dvl or β-catenin, injection or administration of Wnt inhibiting molecules such as sFRP2, or implantation of bone marrow-derived or mesenchymal stem cells with altered level of Wnt activation to injured hearts (Hermans and Blankesteijn,

2015). No study to our knowledge, however, has investigated the gain-of-function effects of a canonical Wnt ligand induced naturally during the endogenous wound healing mechanisms in the adult heart (Paik *et al.,* 2015).

Among the Wnt ligands naturally induced in the heart after MI is the canonical Wnt ligand, Wnt10b (Aisagbonhi *et al.,* 2011; Paik *et al.,* 2015). Wnt10b has been found to be involved in signaling networks controlling stemness, pluripotency, and cell fate decisions in hematopoietic cells, skeletal myoblasts, MSC differentiation to osteoblasts and adipocytes, and in mammary gland (Wend *et al.,* 2012). Yet its role in cardiac development or in cardiac cell types is unknown to this date. To investigate the effects of Wnt10b gain-of-function in cellular and molecular responses to injury in mouse heart we created a transgenic mouse model that overexpresses Wnt10b at its natural location of expression.

Summary and Implications

Wnt10b expression in adult heart localizes to intercalated discs, the cellular junctions of cardiomyocytes, in human and mouse. It is strongly induced and accumulates in the cytoplasm of the myocytes after an ischemic injury, suggesting that it plays a role as an injury-responsive gene. In mouse hearts following MI, Wnt10b is induced transiently during the proliferative phase of wound healing, which consists of the cellular processes of neovascularization and fibrosis. These data indicate that Wnt10b is linked to canonical Wnt activation during this particular time window of the repair process and regulates the scar tissue formation phase of cardiac repair (Aisagbonhi *et al.,* 2011; Clevers and Nusse, 2012; Clevers *et al.,* 2014). The role of Wnt signaling in angiogenesis during embryonic

development and in adult tissue repair has also been established (Dejana, 2010). Therefore we hypothesized that gain-of-function of Wnt10b can modulate the cellular processes of granulation tissue formation to regulate cardiac function outcomes after injury.

To test this hypothesis, we created the transgenic (TG) αMHC-Wnt10b mouse that overexpresses Wnt10b in adult cardiomyocytes. First, Wnt10b overexpression was found to attenuate pathological fibrosis by reducing the number of myofibroblasts and by diminishing Collagen I deposition in the scar tissue. These phenotypes led to smaller-sized scar in TG ventricles 3 weeks after injury. Wnt10b overexpression also generated aggregates of immature cardiomyocytes in the scar tissue, a phenotype never observed in the WT counterparts.

Wnt10b was found to activate canonical Wnt signaling in cardiac endothelial cells. This canonical Wnt activation stimulated proliferation of endothelial cells in the scar tissue, leading to greater microvascular density. We found the activation of canonical Wnt signaling and the increased proliferative effects of endothelial cells were direct effects of Wnt10b. Wnt10b also increased the angiogenic potential of endothelial cells, by inducing Vegfr-2 expression. This allowed synergistic effects between Wnt10b and Vegf-a to take place in promoting neovascularization.

Another unique effect of Wnt10b-overexpressing mice was the formation of coronary-like arterioles. A greater number of large diameter coronary-like vessels with a prominent coat of mural cells was found in TG scar tissue. Through *in vitro* studies, we detected Wnt10b activates NF-κB signaling pathway in both cardiac endothelial cells and vSMCs, which regulate the expression induction of beneficial growth factors for vessel

formation such as Vegfr-2, Pdgf-b in endothelial cells and Ang-1 in vSMCs. Pdgf-b and Ang-1 are known molecules that promote vessel stabilization. Because of this, neo-vessels in the TG scar tissue likely had decreased permeability, which in turn may have led to diminished number of inflammatory cell infiltration to the repairing tissue.

Combined together, such changes in the cellular response to injury triggered by Wnt10b overexpression led to improved left ventricular function recovery. Echocardiogram suggested TG mice were able to preserve chamber size and contractility of the left ventricle 3 weeks after injury, when compared to the WT controls. Expression levels of prognostic HF markers such as the natriuretic peptides and MMP-9 were also diminished, suggesting that Wnt10b overexpression may be effective in preventing HF in long term. Most importantly, we found a large number of α-Actinin^{+} cells in the scar tissue of TG ventricles after cryoinjury. Such phenotype has not been reported elsewhere during mammalian cardiac repair process and requires further investigation.

In zebrafish ventricular resection model, activation of NF-κB in myocytes was shown to be necessary for myocyte regeneration after injury (Karra *et al.,* 2015). Because we have found Wnt10b directly activated NF-κB signaling pathway in cardiac endothelial cells and vascular smooth muscle cells, it is likely that Wnt10b-mediated activation of NF-κB signaling in cardiomyocytes regulates growth of cardiomyocytes in the scar tissue of TG hearts after injury.

Our findings add to understanding of the molecular and cellular responses of neovascularization, fibrosis, and myocyte formation during adult cardiac repair, and provide a foundation to translate the beneficial effects of canonical Wnt signaling in developing new tools for HF and post MI therapy.

Limitations

A limitation of the Wnt10b gain-of-function approach is that the observed phenotypes may not only recapitulate the endogenous role of Wnt10b but also reflect the collective overexpression effects of structurally related Wnt ligands in the heart. This problem is particularly acute in the Wnt signaling pathway, which consists of 19 ligands and 10 Frizzled receptors with overlapping, often redundant expression and function (Clevers *et al.,* 2014; Paik and Hatzopoulos, 2014). It is noteworthy, however, that the observed phenotypes are distinct from those described in αMHC-Wnt11 transgenic mice, which displayed ventricular hypertrophy without pathological fibrosis or calcium deposition (Abdul-Ghani *et al.,* 2011). Wnt11 stimulation was shown to activate caspase 3 signaling cascade to inhibit stabilization of β-catenin, which was reported to promote myocyte maturation (Abdul-Ghani *et al.,* 2011). This suggests that the observations from αMHC-Wnt10b mice are specific to canonical Wnt activation by Wnt10b overexpression.

While the αMHC-Wnt10b mouse hearts overexpress the Wnt10b gene in adult cardiomyocytes without turning on the gene during embryonic development, they are not an inducible model. To most effectively mirror the innate response to ischemic injury of canonical Wnt activation in the heart tissue, it will be informative to use an inducible model to control the timing of Wnt10b overexpression. There are available cardiomyocyte-specific, Cre-loxP/tamoxifen-mediated inducible mouse models, such as cTnT-Cre^{ERT}. We can create a ROSA-Wnt10b mouse, which contains a stop codon sequence between two loxP sites followed by the Wnt10b gene under the ubiquitous promoter of ROSA. By mating the two mice, we can selectively induce cardiomyocyte-specific overexpression of

Wnt10b at the start of the proliferative phase of repair, but not during homeostasis or during inflammatory phase of repair. The limitation of Cre-loxP/tamoxifen-mediated inducible model is that it is not reversible. Once tamoxifen is administered to activate the Cre protein and initiate the Wnt10b overexpression, it cannot be undone. To limit the Wnt10b overexpression to a defined time window, we would instead consider the Flp-Flt inducible system. Alternative to inducing Wnt10b overexpression, we can consider doxycycline-mediated ablation of Wnt10b expression in WT mice, during the phases of repair when Wnt10b expression is not desired.

To determine whether Wnt10b is necessary in cardiac tissue repair, further studies would address the Wnt10b loss-of-function phenotype. If the observed phenotypes from αMHC-Wnt10b mice are abolished in Wnt10b knockout mice, it would indicate the phenotypes are specific to Wnt10b and not to the three other Wnt ligands, Wnt2, Wnt4, and Wnt11 that are up-regulated during the endogenous cardiac repair process (Aisagbonhi *et al.,* 2011).

We elucidated the effects of Wnt10b on NF-κB activation in endothelial cells and vSMCs *in vitro*. These findings would need to be confirmed *in vivo*. To test whether endothelial cells and vSMCs in the scar tissue of Wnt10b-overexpressing mouse hearts are NF-κB-activated. An alternative strategy would be to isolate and culture these cell types from the TG scar tissue and perform NF-κB-luc reporter assay to measure the level of NF-κB activation as described above for the canonical Wnt signaling reporter TOPFlash assay (**Figure 16B-C**).

Future Directions

We showed canonical Wnt activation by Wnt10b overexpression led to attenuated fibrosis and regeneration of myocytes in the scar tissue. Recent studies have revealed the potential of Wnt signaling on stimulation of cardiomyocyte proliferation (Heallen *et al.,* 2011; Rai *et al.,* 2012), yet the molecular mechanisms of these effects have not been investigated. Understanding these new discovered mechanisms of cardiac cell growth can thereof lead to approaches to reverse fibrosis or promote cardiogenesis after injury or during aging. We will thus test whether the effects of attenuated fibrosis and myocyte regeneration are indeed direct effects of Wnt10b. In zebrafish, NF-κB activation in cardiomyocytes has shown to be essential for myocyte regeneration (Karra *et al.,* 2015). While we found Wnt10b to activate NF-κB signaling in the vascular cell types, we will test whether Wnt10b also activates NF-κB signaling in cardiomyocytes of the adult heart. In this case, it will likely be informative to administer a cell-permeable inhibitor peptide for NF-κB, such as SN-50 (Lin *et al.,* 1995) to the TG mice before and after injury, to test the *in vivo* effects of NF-κB inhibition in Wnt10b-overexpressing hearts. This experiment will not only confirm whether 1) NF-κB activation by Wnt10b is necessary to create stabilized vessels observed in TG scar tissue, but also determine 2) if the regenerating myocytes observed in TG scar tissue are mediated through NF-κB activation, as reported in the zebrafish ventricular model (Karra *et al.,* 2015).

Because it is not currently feasible to deliver Wnt molecules therapeutically, it is necessary to find agents or small molecule compounds that would mimic the effects of Wnt10b. We would like to identify the receptors that interact with Wnt10b in the cell types of interest, such as the cardiac endothelial cells and vSMCs. Because all ten Frizzled

receptors are expressed in both cell types, further studies will elucidate which member(s) of the receptor family Wnt10b has the highest affinity to. This could be achieved by inactivating or inhibiting individual receptor proteins. Once the receptor(s) are identified, we can create inducible knockout mice for such genes and test whether the observed effects of Wnt10b overexpression are abolished. We can also screen for small molecule compounds that would bind to and activate the Wnt10b-binding receptors. Such chemicals can be used to test its efficacy in replicating the beneficial effects of cardiac repair we observed from the TG mice.

Similarly, it would be of interest to identify the factors that regulate Wnt10b induction observed during the proliferative phase of cardiac tissue repair. We speculate the signaling pathways involved in inflammation, cell death, and cell survival during the early inflammatory phase of wound healing would be the likely candidates. In particular, we will explore whether BMP signaling activation during the inflammatory phase would mediate the canonical Wnt activation during the proliferative phase. We will use a mouse model that overexpresses an endogenous BMP antagonist in the heart, which effectively blocks BMP activation during all phases of cardiac repair. If the induction of Wnt10b curtails in these mouse hearts after myocardial injury, it would prove that BMP activation during early phase of the repair triggers canonical Wnt activation in the ensuing phase. We can then mate the BMP antagonist-overexpressing mouse with αMHC-Wnt10b mouse to see if canonical Wnt activation is restored. The BMP antagonist-overexpressing mouse model is currently available to us and at our disposal. Alternatively, we can administer known BMP antagonizing chemical compounds such as DMH1 (Hao *et al.,* 2010) to WT mice, and determine whether Wnt10b expression induction is abolished 5 to

7 days after experimental MI.

In addition, we will explore the effects of Wnt activation on the cardiogenic potential of endogenous progenitor cells with endothelial characteristics (Fioret *et al.,* 2014), as we know canonical Wnt signaling likely plays a role in EndMT during cardiac tissue repair (Aisagbonhi *et al.,* 2011). EndMT has been proposed as a model to which mature endothelial cells in the adult heart can give rise to ventricular cardiomyocytes (Fioret *et al.,* 2014), and modulating this process by Wnt activation can augment the cardiogenic potential of endothelial cells.

APPENDIX A

Gene	Primer Direction	Primer Sequence
Ang-1	5'	CCACCATGCTTGAGATAGGAACC
	3'	CTGTGAGTAGGCTCGGTTCCC
Ang-2	5'	GTGGTGCAGAACCAGACAGCTG
	3'	CACTTCCTGGTTGGCTGATGC
Axin2	5'	CCAGAAGATCACAAAGAGCCAAAGA
	3'	CTCAGTCGATCCTCTCCACTTTGC
β-actin	5'	CTACGAGGGCTATGCTCTCCC
	3'	CCGGACTCATCGTACTCCTGC
Gapdh	5'	CTCACTCAAGATTGTCAGCAATG
	3'	GAGGGAGATGCTCAGTGTTGG
Lef1	5'	ATCCACCACAGGAGGAAAAAGAAAT
	3'	GTTAGGCTGCCTGTCTCTGAGATTC
Mmp-9	5'	CAGGAGTCTGGATAAGTTGGGTC
	3'	GGTACTGGAAGATGTCGTGTGAG
Nppa	5'	TTTCAAGAACCTCGTAGACCACCTG
	3'	AAGCTGTTGCAGCCTAGTCCACTCT
Nppb	5'	ATGGATCTCCTGAAGGTGCTG
	3'	GTGCTGCCTTGAGACCGAA
Pdgf-b	5'	GCCAACTTCCTGGTGTGGCC
	3'	CCACAGGACTGCAAGGGACC
Tcf7	5'	GCATCCCTCATCCAGCTATTGTAAC
	3'	GCTGTCTCTCTTTCCGTGCTAGTTC
Tie2	5'	CAACAGCGTCTATCGGACTCC
	3'	GAAAAGGCTGGGTTGCTTGATC
Tgf-β1	5'	AGATTAAAATCAAGTGTGGAGCAAC
	3'	GTCCTTCCTAAAGTCAATGTACAGC
Vegf-a	5'	CAAGTGGTCCCAGGCTGCACCC
	3'	CCCTGAGGAGGCTCCTTCCTGCC
Vegfr-1	5'	GGAAACCACAGCAGGAAGACG
	3'	GTCAGCCACCACCAATGTGC
Vegfr-2	5'	CTCTGTCAGTGACCAGCATGG
	3'	GACTTGACTGCCCACTGTGG
Wnt10b	5'	AGAAGTTCTCTCGGGATTTCTTG
	3'	CAAAGTAAACCAGCTCTCCAG

Table 2. Primer sequences for RT-qPCR. Forward and reverse primers used to measure gene expression by real-time quantitative PCR.

REFERENCES

Abdul-Ghani M, Dufort D, Stiles R, De Repentigny Y, Kothary R, Megeney LA. Wnt11 promotes cardiomyocyte development by caspase-mediated suppression of canonical Wnt signals. *Mol Cell Biol.* 2011; 31:163–178.

Afouda BA, Martin J, Liu F, Ciau-Uitz A, Patient R, Hoppler S. GATA transcription factors integrate Wnt signalling during heart development. Development. 2008;135:3185–3190.

Afroze T, Yang LL, Wang C, Gros R, Kalair W, Hoque AN, Mungrue IN, Zhu Z, Husain M. Calcineurin-independent regulation of plasma membrane Ca2+ ATPase-4 in the vascular smooth muscle cell cycle. *Am J Physiol., Cell Physiol.* 2003; 285:C88–C95.

Ai D, Fu X, Wang J, Lu MF, Chen L, Baldini A, Klein WH, Martin JF. Canonical Wnt signaling functions in second heart field to promote right ventricular growth. *Proc Natl Acad Sci U S A.* 2007; 104:9319 –9324.

Aisagbonhi O, Rai M, Ryzhov S, Atria N, Feoktistov I, Hatzopoulos AK. Experimental myocardial infarction triggers canonical Wnt signaling and endothelial-to-mesenchymal transition. *Dis Model Mech*. 2011; 4:469–483.

Alfaro MP, Pagni M, Vincent A, Atkinson J, Hill MF, Cates J, Davidson JM, Rottman J, Lee E, Young PP. The Wnt modulator sFRP2 enhances mesenchymal stem cell engraftment, granulation tissue formation and myocardial repair. *Proc Natl Acad Sci U S A.* 2008; 105:18366-18371.

Andrae J, Gallini R, Betsholtz C. Role of platelet-derived growth factors in physiology and medicine. *Genes Dev.* 2008; 22:1276–1312.

Armstrong DD, Esser KA. Wnt/beta-catenin signaling activates growth-control genes during overload-induced skeletal muscle hypertrophy. *Am J Physiol Cell Physiol.* 2005; 289:C853-C859.

Augustin HG, Koh GY, Thurston G, Alitalo K. Control of vascular morphogenesis and homeostasis through the angiopoietin-Tie system. *Nat Rev Mol Cell Biol.* 2009; 10:165–177.

Barandon L, Couffinhal T, Ezan J, Dufourcq P, Costet P, Alzieu P, Leroux L, Moreau C, Dare D, Duplaa C. Reduction of infarct size and prevention of cardiac rupture in transgenic mice overexpressing FrzA. *Circulation* 2003; 108:2282-2289.

Barandon L, Casassus F, Leroux L, Moreau C, Allieres C, Lamaziere JM, Dufourcq P, Couffinhal T, Duplaa C. Secreted frizzled-related protein-1 improves postinfarction scar formation through a modulation of inflammatory response. *Arterioscler Thromb Vasc Biol.*

2011; 31:e80-e87.

Birdsey GM, Shah AV, Dufton N, Reynolds LE, Osuna Almagro L, Yang Y, Aspalter IM, Khan ST, Mason JC, Dejana E, Gottgens B, Hodivala-Dilke K, Gerhardt H, Adams RH, Randi AM. The endothelial transcription factor ERG promotes vascular stability and growth through Wnt/β-catenin signaling. *Dev Cell.* 2015; 32:82-96.

Blankesteijn WM, Van Gijn ME, Essers-Janssen YP, Daemen MJ, Smits JF. Beta-catenin, an inducer of uncontrolled cell proliferation and migration in malignancies, is localized in the cytoplasm of vascular endothelium during neovascularization after myocardial infarction. *Am J Pathol.* 2000; 157:877–883.

Bombelli M, Facchetti R, Cuspidi C, Villa P, Dozio D, Brambilla G, Grassi G, Mancia G. Prognostic significance of left atrial enlargement in a general population: results of the PAMELA study. *Hypertension.* 2014; 64:1205-12011.

Boudoulas KD, Hatzopoulos AK. Cardiac repair and regeneration: the Rubik's cube of cell therapy for heart disease. *Dis Model Mech.* 2009; 2:344–358.

Brade T, Männer J, Kühl M. The role of Wnt signaling in cardiac development and tissue remodeling in the mature heart. *Cardiovasc Res.* 2006; 72:198-209.

Braunwald E. The war against heart failure: the Lancet lecture. *Lancet.* 2015; 385:812-824.

Caines AE, Massad MG, Kpodonu J, Rebeiz AG, Evans A, Geha AS. Outcomes of coronary artery bypass grafting versus percutaneous coronary intervention and medical therapy for multivessel disease with and without left ventricular dysfunction. *Cardiology.* 2004; 101: 21–28.

Caneparo L, Huang YL, Staudt N, Tada M, Ahrendt R, Kazanskaya O, Niehrs C, Houart C. Dickkopf-1 regulates gastrulation movements by coordinated modulation of Wnt/beta catenin and Wnt/PCP activities, through interaction with the Dally-like homolog Knypek. *Genes Dev.* 2007; 21:465– 480.

Chan D, Ng LL. Biomarkers in acute myocardial infarction. *BMC Med.* 2010; 8:34.

Chen B, Dodge ME, Tang W, Lu J, Ma Z, Fan C-W, Wei S, Hao W, Kilgore J, Williams NS, Roth MG, Amatruda JF, Chen C, Lum L. Small molecule-mediated disruption of Wnt-dependent signaling in tissue regeneration and cancer. *Nat Chem Biol.* 2009;5:100–107.

Chen K, Fallen S, Abaan HO, Hayran M, Gonzalez C, Wodajo F, MacDonald T, Toretsky JA, Uren A. Wnt10b induces chemotaxis of osteosarcoma and correlates with reduced survival. *Pediatr Bood Cancer.* 2008; 51:349-355.

Clevers H, Loh KM, Nusse R. An integral program for tissue renewal and regeneration:

Wnt signaling and stem cell control. *Science.* 2014; 346:1248012.

Chen VC, Stull R, Joo D, Cheng X, Keller G. Notch signaling respecifies the hemangioblast to a cardiac fate. *Nat Biotechnol.* 2008; 26:1169 –1178.

Clevers H, Nusse R. Wnt/β-catenin signaling and disease. *Cell.* 2012; 149:1192–205.

Cohen ED, Wang Z, Lepore JJ, Lu MM, Taketo MM, Epstein DJ, Morrisey EE. Wnt/beta-catenin signaling promotes expansion of Isl-1- positive cardiac progenitor cells through regulation of FGF signaling. *J Clin Invest.* 2007; 117:1794 –1804.

Cohen ED, Tian Y, Morrisey EE. Wnt signaling: an essential regulator of cardiovascular differentiation, morphogenesis and progenitor self-renewal. *Development.* 2008; 135:789–98.

Cristofaro B, Shi Y, Faria M et al. Dll4-Notch signaling determines the formation of native arterial collateral networks and arterial function in mouse ischemia models. *Development.* 2013; 140:1720–1729.

Cuspidi C, Negri F, Tadic MV, Sala C, Parati G. Association of left atrial enlargement with left ventricular hypertrophy and diastolic dysfunction: a tissue Doppler study in echocardiographic practice. *Blood Press.* 2012; 21:24-30.

David R, Brenner C, Stieber J, Schwarz F, Brunner S, Vollmer M, Mentele E, Muller-Hocker J, Kitajima S, Lickert H, Rupp R, Franz WM. MesP1 drives vertebrate cardiovascular differentiation through Dkk-1- mediated blockade of Wnt-signalling. *Nat Cell Biol.* 2008;10:338 –345.

de Vries C, Escobedo JA, Ueno H, Houck K, Ferrara N, Williams LT. The fms-like tyrosine kinase, a receptor for vascular endothelial growth factor. *Science.* 1992; 255:989–991.

Dejana E. The role of wnt signaling in physiological and pathological angiogenesis. *Circ Res.* 2010; 107:943-952.

Duan J, Gherghe C, Liu D, Hamlett E, Srikantha L, Rodgers L, Regan JN, Rojas M,Willis M, Leask A,Majesky M, Deb A.Wnt1/betacatenin injury response activates the epicardium and cardiac fibroblasts to promote cardiac repair. *EMBO J.* 2012; 31:429-442.

Ellison GM, Vicinanza C, Smith AJ, Aquila I, Leone A, Waring CD, Henning BJ, Stirparo GG, Papait R, Scarfò M, Agosti V, Viglietto G, Condorelli G, Indolfi C, Ottolenghi S, Torella D, Nadal-Ginard B. Adult c-kit positive cardiac stem cells are necessary and sufficient for functional cardiac regeneration and repair. *Cell.* 2013; 154:827–42.

Estigoy CB, Ponten F, Odeberg J, Herbert B, Guilhaus M, Charleston M, Ho JWK, Cameron D, dos Remedios CG. Intercalated discs: multiple proteins perform multiple functions in non-failing and failing human hearts. *Biophys Rev.* 2009; 1:43-49.

Fioret BA, Heimfeld JD, Paik DT, Hatzopoulos AK. Endothelial cells contribute to generation of adult ventricular myocytes during cardiac homeostasis. *Cell Rep.* 2014; 8:229-241.

Frangogiannis NG. Regulation of the inflammatory response in cardiac repair. *Circ Res.* 2012; 110:159-173.

Frangogiannis NG. The inflammatory response in myocardial injury, repair, and remodelling. *Nat Rev Cardiol.* 2014; 11:255–265.

Fuxe J, Tabruyn S, Colton K, Zaid H, Adams A, Baluk P, Lashnits E, Morisada T, Le T, O'Brien S, Epstein DM, Koh GY, McDonald DM. Pericyte requirement for anti-leak action of angiopoietin-1 and vascular remodeling in sustained inflammation. *Am J Pathol.* 2011; 178:2897-2909.

Garriock RJ, D'Agostino SL, Pilcher KC, Krieg PA. Wnt11-R, a protein closely related to mammalian Wnt11, is required for heart morphogenesis in Xenopus. *Dev Biol*. 2005; 279:179 –192.

Gessert S, Maurus D, Brade T, Walther P, Pandur P, Kühl M. DM-GRASP/ALCAM/CD166 is required for cardiac morphogenesis and maintenance of cardiac identity in first heart field derived cells*. Dev Biol.* 2008; 321:150 –161.

Gessert S, Kühl M. The Multiple Phases and Faces of Wnt Signaling During Cardiac Differentiation and Development. *Circ Res.* 2010; 107:186–199.

Gitler AD, Lu MM, Jiang YQ, Epstein JA, Gruber PJ. Molecular markers of cardiac endocardial cushion development. *Dev Dyn.* 2003; 228:643– 650.

Gustafson B, Smith U. Cytokines promote Wnt signaling and inflammation and impair the normal differentiation and lipid accumulation in 3T3-L1 preadipocytes. *J Biol Chem.* 2006; 281:9507-9516.

Hahn JY, Cho HJ, Bae JW, Yuk HS, Kim KI, Park KW, Koo BK, Chae IH, Shin CS, Oh BH, Choi YS, Park YB, Kim HS. Beta-catenin overexpression reduces myocardial infarct size through differential effects on cardiomyocytes and cardiac fibroblasts. *J Biol Chem.* 2006; 281:30979-30989.

Hao J, Ho JN, Lewis JA, Karim KA, Daniels RN, Gentry PR, Hopkins CR, Lindsley CW, Hong CC. In vivo structure-activity relationship study of dorsomorphin analogues identifies selective VEGF and BMP inhibitors. *ACS Chem Biol.* 2010; 5:245-253.

He TC, Sparks AB, Rago C, Hermeking H, Zawel L, da Costa LT, et al. Identification of c-

MYC as a target of the APC pathway. *Science.* 1998; 281:1509–1512.

He W, Zhang L, Ni A, Zhang Z, Mirotsou M, Mao L, Pratt RE, Dzau VJ. Exogenously administered secreted frizzled related protein 2 (Sfrp2) reduces fibrosis and improves cardiac function in a rat model of myocardial infarction. *Proc Natl Acad Sci U S A.* 2010;107: 21110-21115.

Heallen T, Zhang M, Wang J, Bonilla-Claudio M, Klysik E, Johnson RL, Martin JF. Hippo pathway inhibits Wnt signaling to restrain cardiomyocyte proliferation and heart size. *Science.* 2011; 332:458-461.

Henry GD, Byrne R, Hunyh TT, Abraham V, Annex BH, Hagen PO, Donatucci CF. Intracavernosal injections of vascular endothelial growth factor protects endothelial dependent corpora cavernosal smooth muscle relaxation in the hypercholesterolemic rabbit: a preliminary study. *Int J Impot Res.* 2000; 12:334–339.

Hermans KC, Blankesteijn WM. Wnt signaling in cardiac disease. *Compr Physiol.* 2015; 5:1193-1209.

Huelsken J, Vogel R, Brinkmann V, Erdmann B, Birchmeier C, Birchmeier W. Requirement for beta-catenin in anterior-posterior axis formation in mice. *J Cell Biol.* 2000; 148:567–578.

Hunt SA, Abraham WT, Chin MH, Feldman AM, Francis GS, Ganiats TG, *et al*. 2009 Focused Update Incorporated Into the ACC/AHA 2005 Guidelines for the Diagnosis and Management of Heart Failure in Adults: A Report of the American College of Cardiology Foundation/American Heart Association Task Force on Practice Guidelines Developed in Collaboration With the International Society for Heart and Lung Transplantation. *J Am Coll Cardiol.* 2009; 53:e1–e90.

Hurlstone AF, Haramis AP, Wienholds E, Begthel H, Korving J, Van Eeden F, Cuppen E, Zivkovic D, Plasterk RH, Clevers H. The Wnt/ beta-catenin pathway regulates cardiac valve formation. *Nature.* 2003; 425:633– 637.

Jain R, Li D, Gupta M, Manderfield LJ, Ifkovits JL, Wang Q, Liu F, Liu Y, Poleshko A, Padmanabhan A, Raum JC, Li L, Morrisey EE, Lu MM, Won K-J, Epstein JA. Integration of Bmp and Wnt signaling by Hopx specifies commitment of cardiomyoblasts. *Science.* 2015; 348:aaa6071.

Kaplan SR, Gard JJ, Protonotarios N, Tsatsopoulou A, Spiliopoulou C, Anastasakis A, Squaarcioni CP, McKenna WJ, Thiene G, Basso C, Brousse N, Fontaine G, Saffitz JE. Remodeling of myocyte gap junctions in arrhythmogenic right ventricular cardiomyopathy due to a deletion in plakoglobin (Naxos disease). *Heart Rhythm.* 2004; 1:3-11.

Karra R, Knecht AK, Kikuchi K, Poss KD. Myocardial NF-κB activation is essential for zebrafish heart regeneration. *Proc Natl Acad Sci U S A.* 2015; 112;13255-13260.

Katayama T, Fujiwara N, Tsuruya Y. Factors contributing to left atrial enlargement in adults with normal left ventricular systolic function. *J Cardiol.* 2010; 55:196-204.

Katoh M, Katoh M. AP1- and NF-kappaB-binding sites conserved among mammalian WNT10B orthologs elucidate the TNFalpha-WNT10B signaling loop implicated in carcinogenesis and adipogenesis. *Int J Mol Med.* 2007; 19:699-703.

Klaus A, Saga Y, Taketo MM, Tzahor E, Birchmeier W. Distinct roles of Wnt/beta-catenin and Bmp signaling during early cardiogenesis. *Proc Natl Acad Sci U S A*. 2007; 104:18531–18536.

Kobayashi K, Luo M, Zhang Y, Wilkes DC, Ge G, Grieskamp T, Yamada C, Liu TC, Huang G, Basson CT, Kispert A, Greenspan DS, Sato TN. Secreted Frizzled-related protein 2 is a procollagen C proteinase enhancer with a role in fibrosis associated with myocardial infarction. *Nat Cell Biol.* 2009; 11:46-55.

Konstantinidis K, Whelan RS, Kitsis RN. Mechanisms of Cell Death in Heart Disease. *Arterioscler Thromb Vasc Biol*. 2012;32: 1552–1562.

Kusserow A, Pang K, Sturm C, Hrouda M, Lentfer J, Schmidt HA, et al. Unexpected complexity of the Wnt gene family in a sea anemone. *Nature.* 2005; 433:156–60.

Kwon C, Arnold J, Hsiao EC, Taketo MM, Conklin BR, Srivastava D. Canonical Wnt signaling is a positive regulator of mammalian cardiac progenitors. *Proc Natl Acad Sci U S A.* 2007; 104:10894 –10899.

Kwon C, Qian L, Cheng P, Nigam V, Arnold J, Srivastava D. A regulatory pathway involving Notch1/beta-catenin/Isl1 determines cardiac progenitor cell fate. *Nat Cell Biol.* 2009; 11:951–957.

Laeremans H, Hackeng TM, van Zandvoort MA, Thijssen VL, Janssen BJ, Ottenheijm HC, Smits JF, Blankesteijn WM. Blocking of frizzled signaling with a homologous peptide fragment of wnt3a/wnt5a reduces infarct expansion and prevents the development of heart failure after myocardial infarction. *Circulation.* 2011; 124:1626-1635.

Lavine KJ, Ornitz DM. Developmental signaling cascades regulate both embryonic and adult coronary vasculature. *Circ Res.* 2009; 104:159-169.

Liebner S, Cattelino A, Gallini R, Rudini N, Iurlaro M, Piccolo S, Dejana E. Beta-catenin is required for endothelial-mesenchymal transformation during heart cushion development in the mouse. *J Cell Biol.* 2004; 166:359 –367.

Lidington EA, Rao RM, Marelli-Berg FM, Jat PS, Haskard DO, Mason JC. Conditional

immortalization of growth factor-responsive cardiac endothelial cells from H-2K(b)-tsA58 mice. *Am J Physiol Cell Physiol*. 2002; 282:C67–C74.

Lin YZ, Yao SY, Veach RA, Torgerson TR, Hawinger J. Inhibition of nuclear translocation of transcription factor NF-kappa B by a synthetic peptide containing a cell membrane-permeable motif and nuclear localization sequence. *J Biol Chem.* 1995; 270:14255-14258.

Lin L, Cui L, Zhou W, Dufort D, Zhang X, Cai CL, Bu L, Yang L, Martin J, Kemler R, Rosenfeld MG, Chen J, Evans SM. Beta-catenin directly regulates Islet1 expression in cardiovascular progenitors and is required for multiple aspects of cardiogenesis. *Proc Natl Acad Sci U S A.* 2007; 104:9313–9318.

Lindsley RC, Gill JG, Murphy TL, Langer EM, Cai M, Mashayekhi M, Wang W, Niwa N, Nerbonne JM, Kyba M, Murphy KM. Mesp1 coordinately regulates cardiovascular fate restriction and epithelialmesenchymal transition in differentiating ESCs. *Cell Stem Cell*. 2008; 3:55– 68.

Liu C, Li Y, Semenov M, Han C, Baeg GH, Tan Y, et al. Control of beta-catenin phosphorylation/degradation by a dual-kinase mechanism. *Cell.* 2002; 108:837–847.

Liu P, Wakamiya M, Shea MJ, Albrecht U, Behringer RR, Bradley A. Requirement for Wnt3 in vertebrate axis formation. *Nat Genet.* 1999; 22:361–365.

Livak, K, Schmittgen T. Analysis of relative gene expression data using real-time quantitative PCR and the 2(-Delta Delta C(T)) Method. *Methods.* 2001; 25:402-408.

Losordo DW, Vale PR, Hendel RC, Milliken CE, Fortuin FD, Cummings N, Schatz RA, Asahara T, Isner JM, Kuntz RE. Phase 1/2 placebo-controlled, double-blind, dose-escalating trial of myocardial vascular endothelial growth factor 2 gene transfer by catheter delivery in patients with chronic myocardial ischemia. *Circulation.* 2002; 105:2012–2018.

MacDonald BT, Tamai K, He X. Wnt/beta-catenin signaling: components, mechanisms, and diseases. *Dev Cell*. 2009; 17:9–26.

Macián F, López-Rodríguez C, Rao A. Partners in transcription: NFAT and AP-1. *Oncogene.* 2001; 30:2476-2489.

Matsushima K, Suyama T, Takenaka C, Nishishita N, Ikeda K, Ikada Y, Sawa Y, Jakt LM, Mori H, Kawamata S. Secreted frizzled related protein 4 reduces fibrosis scar size and ameliorates cardiac function after ischemic injury. *Tissue Eng Part A.* 2010; 16:3329-3341.

Maye P, Zheng J, Li L, Wu D. Multiple mechanisms for Wnt11-mediated repression of the canonical Wnt signaling pathway. *J Biol Chem*. 2004; 279:24659–24665.

McAlister FA, Ezekowitz J, Hooton N, Vandermeer B, Spooner C, Dryden DM, et al. Cardiac resynchronization therapy for patients with left ventricular systolic dysfunction: a systematic review. *J. Am. Med. Assoc.* 2007; 297:2502–2514.

Merlo M, Pyxaras SA, Pinamonti B, Barbati G, Di Lenarda A, Sinagra G. Prevalence and Prognostic Significance of Left Ventricular Reverse Remodeling in Dilated Cardiomyopathy Receiving Tailored Medical Treatment. *J Am Coll Cardiol.* 2011; 57:1468–1476.

Min JK, Park H, Choi HJ, Kim Y, Pyun BJ, Agrawal V, Song BW, Jeon J, Maeng YS, Rho SS, Shim S, Chai JH, Koo BK, Hong HJ, Yun CO, Choi C, Kim YM, Hwang KC, Kwon YG. The WNT antagonist Dickkopf2 promotes angiogenesis in rodent and human endothelial cells. *J Clin Invest.* 2011; 121:1882-1893.

Mirotsou M, Zhang Z, Deb A, Zhang L, Gnecchi M, Noiseux N, Mu H, Pachori A, Dzau V. Secreted frizzled related protein 2 (Sfrp2) is the key Akt-mesenchymal stem cell-released paracrine factor mediating myocardial survival and repair. *Proc Natl Acad Sci U S A.* 2007; 104:1643-1648.

Mödder UI, Oursler MJ, Khosla S, Monroe DG. Wnt10b activates the Wnt, notch, and NFκB pathways in U2OS osteosarcoma cells. *J Cell Biochem.* 2011; 112:1392-1402.

Mozaffarian D, Benjamin EJ, Go AS, et al. Heart disease and stroke statistics—2015 update: a report from the American Heart Association. *Circulation.* 2015; 27:e29-322.

Nakamura T, Sano M, Songyang Z, Schneider MD. A Wnt- and betacatenin-dependent pathway for mammalian cardiac myogenesis. *Proc Natl Acad Sci U S A*. 2003; 100:5834–5839.

Nusse R. Wnt signaling and stem cell control. *Cell Res.* 2008; 18:523–527.

Oikonomopoulos A, Sereti KI, Conyers F, Bauer M, Liao A, Guan J, Crapps D, Han JK, Dong H, Bayomy AF, Fine GC, Westerman K, Biechele TL, Moon RT, Force T, Liao R. Wnt signaling exerts an antiproliferative effect on adult cardiac progenitor cells through IGFBP3. *Circ Res.* 2011; 109:1363-1374.

Omland T, Aakvaag A, Bonarjee VV, Caidahl K, Lie RT, Nilsen DW, Sundsfjord JA, Dickstein K. Plasma brain natriuretic peptide as an indicator of left ventricular systolic function and long-term survival after acute myocardial infarction. Comparison with plasma atrial natriuretic peptide and N-terminal proatrial natriuretic peptide. *Circulation.* 1996; 93:1963-1969.

Paik DT, Hatzopoulos AK. Wnt signaling in regulation of stem cells. In: Ao A, Hao J, Hong CC, eds. *Chemical Biology in Regenerative Medicine: Bridging Stem Cells and Future*

Therapies. 2014. John Wiley & Sons, Ltd. Chichester, UK.

Paik DT, Rai M, Ryzhov S, Sanders LN, Aisagbonhi O, Funke MJ, Feoktistov I, Hatzopoulos AK. Wnt10b gain-of-function improves cardiac repair by arteriole formation and attenuation of fibrosis. *Circ Res.* 2015; 117:804-816.

Pandur P, Lasche M, Eisenberg LM, Kühl M. Wnt-11 activation of a non-canonical Wnt signalling pathway is required for cardiogenesis. *Nature.* 2002; 418:636–641.

Perriard JC, Hirschy A, Ehler E. Dilated cardiomyopathy: a disease of the intercalated disc? *Trends Cardiovasc Med.* 2003; 13:30-38.

Person AD, Garriock RJ, Krieg PA, Runyan RB, Klewer SE. Frzb modulates Wnt-9a-mediated beta-catenin signaling during avian atrioventricular cardiac cushion development. *Dev Biol.* 2005; 278:35– 48.

Qyang Y, Martin-Puig S, Chiravuri M, Chen S, Xu H, Bu L, Jiang X, Lin L, Granger A, Moretti A, Caron L, Wu X, Clarke J, Taketo MM, Laugwitz KL, Moon RT, Gruber P, Evans SM, Ding S, Chien KR. The renewal and differentiation of Isl1 cardiovascular progenitors are controlled by a Wnt/beta-catenin pathway. *Cell Stem Cell*. 2007; 1: 165–179.

Rai M, Walthall JM, Hu J, Hatzopoulos AK. Continuous antagonism by Dkk1 counter activates canonical Wnt signaling and promotes cardiomyocyte differentiation of embryonic stem cells. *Stem Cells Dev.* 2012; 21:54-66.

Rao TP, Kühl M. An updated overview on Wnt signaling pathways: a prelude for more. *Circ Res.* 2010; 106:1798–1806.

Ren G, Michael LH, Entman ML, Frangogiannis NG. Morphological characteristics of the microvasculature in healing myocardial infarcts. *J Histochem Cytochem.* 2002; 50:71–79.

Ryzhov S, Goldstein AE, Novitskiy SV, Blackburn MR, Biaggioni I, Feoktistov I. Role of A2B adenosine receptors in regulation of paracrine functions of stem cell antigen 1-positive cardiac stromal cells. *J Pharmacol Exp Ther*. 2012; 341:764–774.

Ryzhov S, Zaynagetdinov R, Goldstein AE, Novitskiy SV, Dikov MM, Blackburn MR, Biaggioni I, Feoktistov I. Adenosine receptor-mediated adhesion of endothelial progenitors to cardiac microvascular endothelial cells. *Circ Res.* 2008; 102:356-363.

Saga Y, Miyagawa-Tomita S, Takagi A, Kitajima S, Miyazaki J, Inoue T. MesP1 is expressed in the heart precursor cells and required for the formation of a single heart tube. *Development.* 1999; 126:3437–3447.

Saga Y, Kitajima S, Miyagawa-Tomita S. Mesp1 expression is the earliest sign of cardiovascular development. *Trends Cardiovasc Med.* 2000; 10:345–352.

Saraste A, Nekolla S, Schwaiger M. Contrast-enhanced magnetic resonance imaging in the assessment of myocardial infarction and viability. *J Nucl Cardiol.* 2008; 15:105–117.

Sato N, Meijer L, Skaltsounis L, Greengard P, Brivanlou AH. Maintenance of pluripotency in human and mouse embryonic stem cells through activation of Wnt signaling by a pharmacological GSK-3-specific inhibitor. *Nat. Med.* 2004; 10:55-63.

Semones M, Feng Y. Johnson N, Adams JL, Winkler J, Hansbury M. Pyridinylimidazole inhibitors of Tie2 kiase. *Bioorg Med Chem Lett.* 2007; 17:4756-5760.

Senyo SE, Steinhauser ML, Pizzimenti CL, Yang VK, Cai L, Wang M, Wu TD, Guerquin-Kern JL, Lechene CP, Lee RT. Mammalian heart renewal by pre-existing cardiomyocytes. *Nature.* 2013; 493:433-496.

Simons M, Annex BH, Laham RJ, Kleiman N, Henry T, Dauerman H, Udelson JE, Gervino EV, Pike M, Whitehouse MJ, Moon T, Chronos NA. Pharmacological treatment of coronary artery disease with recombinant fibroblast growth factor-2: double-blind, randomized, controlled clinical trial. *Circulation.* 2002; 105:788–793.

Smith RR, Barile L, Cho HC, Leppo MK, Hare JM, Messina E, Giacomello A, Abraham MR, Marbán E. Regenerative potential of cardiosphere-derived cells expanded from percutaneous endomyocardial biopsy specimens. *Circulation.* 2007; 115:896–908.

Spinale FG, Coker ML, Heung LJ, Bond BR, Gunasinghe HR, Etoh T, Goldberg AT, Zellner JL, Crumbley AJ. A matrix metalloproteinase induction/activation system exists in the human left ventricular myocardium and is upregulated in heart failure. *Circulation.* 2000;102: 1944–1949.

Su H, Takagawa J, Huang Y, Arakawa-Hoyt J, Pons J, Grossman W, Kan YW. Additive effect of AAV-mediated angiopoietin-1 and VEGF expression on the therapy of infarcted heart. *Int J Cardiol.* 2009; 133:191–197.

Subramaniam A, Jones WK, Gulick J, Wert S, Neumann J, Robbins J. Tissue-specific regulation of the alpha-myosin heavy chain gene promoter in transgenic mice. *J Biol Chem.* 1991; 266:24613–24620.

Sweet DT, Chen Z, Givens CS, Owens AP 3rd, Rojas M, Tzima E. Endothelial Shc Regulates Arteriogenesis Through Dual Control of Arterial Specification and Inflammation via the Notch and NF-κB Pathways. *Circ Res.* 2013; 113:32-39.

Syed IS, Sanborn TA, Rosengart TK. Therapeutic angiogenesis: a biologic bypass. *Cardiology.* 2004; 101:131–143.

Taimeh Z, Loughran J, Birks EJ, Bolli R. Vascular endothelial growth factor in heart failure.

Nat Rev Cardiol. 2013;10:519-30.

Tao Z, Chen B, Tan X, Zhao Y, Wang L, Zhu T, Cao K, Yang Z, Kan YW, Su H. Coexpression of VEGF and angiopoietin-1 promotes angiogenesis and cardiomyocyte proliferation reduces apoptosis in porcine myocardial infarction (MI) heart. *Proc. Natl. Acad. Sci. U.S.A.* 2011; 108:2064–2069.

ten Berge D, Kurek D, Blauwkamp T, Koole W, Maas A, Eroglu E, et al. Embryonic stem cells require Wnt proteins to prevent differentiation to epiblast stem cells. *Nat Cell Biol*. 2011; 13:1070–5.

Thurston G, Rudge JS, Ioffe E, Zhou H, Ross L, Croll SD, Glazer N, Holash J, McDonald DM, Yancopoulos GD. Angiopoietin-1 protects the adult vasculature against plasma leakage. *Nat Med*. 2000; 6:460–463.

Timmers L, Pasterkamp G, Hoog VC de, Arslan F, Appelman Y, Kleijn DPV de. The innate immune response in reperfused myocardium. *Cardiovasc Res.* 2012; 94:276-283.

Tirziu D, Jaba IM, Yu P, Larrivée B, Coon BG, Cristofaro B, Zhuang ZW, Lanahan AA, Schwartz MA, Eichmann A, Simons M. Endothelial Nuclear Factor-κB–Dependent Regulation of Arteriogenesis and Branching. *Circulation.* 2012; 126:2589–2600.

Ubil E, Duan J, Pillai ICL, Rosa-Garrido M, Wu Y, Bargiacchi F, Lu Y, Stanbouly S, Huang J, Rojas M, Vondriska TM, Stefani E, Deb A. Mesenchymal-endothelial transition contributes to cardiac neovascularization. *Nature.* 2014; 514:585-590.

Ueno S, Weidinger G, Osugi T, Kohn AD, Golob JL, Pabon L, Reinecke H, Moon RT, Murry CE. Biphasic role for Wnt/beta-catenin signaling in cardiac specification in zebrafish and embryonic stem cells. *Proc Natl Acad Sci U S A.* 2007; 104:9685–9690.

van Amerongen MJ, Harmsen MC, Petersen AH, Popa ER, van Luyn MJA. Cryoinjury: a model of myocardial regeneration. *Cardiovasc Pathol.* 2008; 17:23-31.

van Amerongen R, Nusse R. Towards an integrated view of Wnt signaling in development. *Development.* 2009; 136:3205–3214.

van den Bos EJ, Mees BME, De Waard MC, De Crom R, Duncker DJ. A novel model of cryoinjury-induced myocardial infarction in the mouse: a comparison with coronary artery ligation. *Am J Physiol Heart Circ Physiol.* 2005; 289:H1291–H1300.

Veeman MT, Axelrod JD, Moon RT. A Second Canon: Functions and Mechanisms of β-Catenin-Independent Wnt Signaling. *Dev Cell.* 2003; 5:367–377.

Virag JI, Murry CE. Myofibroblast and endothelial cell proliferation during murine myocardial infarct repair. *Am. J. Pathol.* 2003; 163:2433–2440.

Vonica A, Gumbiner BM. Zygotic Wnt activity is required for Brachyury expression in the early Xenopus laevis embryo. *Dev Biol.* 2002; 250:112–127.

Wend P, Wend K, Krum SA, Miranda-Carboni GA. The role of WNT10B in physiology and disease. *Acta Physiol.* 2012; 204:34-51.

Yamaguchi TP, Takada S, Yoshikawa Y, Wu N, McMahon AP. T (Brachyury) is a direct target of Wnt3a during paraxial mesoderm specification. *Genes Dev.* 1999; 13:3185–3190.

Zelarayan LC, Noack C, Sekkali B, Kmecova J, Gehrke C, Renger A, Zafiriou MP, van der Nagel R, Dietz R, de Windt LJ, Balligand JL, Bergmann MW. Beta-catenin downregulation attenuates ischemic cardiac remodeling through enhanced resident precursor cell differentiation. *Proc Natl Acad Sci U S A.* 2008; 105:19762-19767.

Zhang X, Gaspard JP, Chung DC. Regulation of vascular endothelial growth factor by the Wnt and K-ras pathways in colonic neoplasia. *Cancer Res.* 2001; 61:6050.

Zymek P, Bujak M, Chatila K, Cieslak A, Thakker G, Entman ML, Frangogiannis NG. The role of platelet-derived growth factor signaling in healing myocardial infarcts. *J Am Coll Cardiol.* 2006; 48:2315–2323.